

Cell-Biology of Interferon Inducible GTPases

Inaugural-Dissertation

zur

Erlangung des Doktorgrades

der Mathematisch-Naturwissenschaftlichen Fakultät

der Universität zu Köln

vorgelegt von

Sascha Martens

aus Berlin

Copy Team GmbH, Köln

2004

Berichtersteller: Prof. Dr. Jonathan C. Howard
Prof. Dr. Thomas Langer

Tag der mündlichen Prüfung: 9.7.2004

Für meine Familie und Anne

TABLE OF CONTENTS

1. INTRODUCTION.....	1
1.1 RESISTANCE AND IMMUNITY.....	1
1.2 CYTOKINES AND INTERFERONS.....	2
1.3 THE INTERFERON SIGNAL TRANSDUCTION PATHWAY.....	3
1.4 CELL-AUTONOMOUS IMMUNITY.....	4
1.5 GTP BINDING PROTEINS AND MEMBRANE DYNAMICS.....	6
1.6 DYNAMIN.....	8
1.7 THE ANTIVIRAL MX PROTEINS.....	9
1.8 OTHER INTERFERON INDUCIBLE GTPASES.....	10
1.9 THE p47 GTPASES.....	11
1.10 PHAGOCYTOSIS OF MICROBES.....	15
1.11 THE AIM OF THIS STUDY.....	16
2. MATERIAL AND METHODS.....	18
2.1 REAGENTS AND CELLS.....	18
2.1.1 <i>Chemicals, Reagents and Accessories</i>	18
2.1.2 <i>Equipment</i>	18
2.1.3 <i>Materials</i>	18
2.1.4 <i>Enzymes/Proteins</i>	19
2.1.5 <i>Kits</i>	19
2.1.6 <i>Vectors</i>	19
2.1.7 <i>Cell lines</i>	19
2.1.8 <i>Media</i>	20
2.1.9 <i>Bacterial strains</i>	20
2.1.10 <i>Serological reagents</i>	21
2.2 MOLECULAR BIOLOGY.....	22
2.2.1 <i>Agarose gel electrophoresis</i>	22
2.2.2 <i>Generation of p47 GTPase expression constructs</i>	23
2.2.3 <i>Cloning of PCR amplification products</i>	25

2.2.4 Purification of DNA fragments from agarose gels.....	25
2.2.5 Ligation	25
2.2.6 Preparation of competent cells.....	26
2.2.7 Transformation of competent bacteria	26
2.2.8 Plasmid isolation.....	27
2.2.9 Determination of the concentration of DNA.....	27
2.2.10 Site directed mutagenesis	27
2.2.11 DNA Sequencing.....	28
2.3 CELL BIOLOGY	28
2.3.1 Transfections	28
2.3.2 Bead uptake experiments.....	29
2.3.3 Transferrin uptake experiments.....	29
2.3.4 Indirect immunofluorescence	29
2.3.5 Image acquisition and processing	30
2.3.6 Triton X-114 partitioning assay.....	30
2.3.7 Membrane extraction experiments	31
2.3.8 Preparation of artificial lipid vesicles.....	32
2.3.9 Western Blotting	32
2.3.10 Isolation of phagosomes.....	32
2.3.11 Nucleotide agarose binding assay.....	34
2.3.12 Preparation of infectious <i>Salmonella typhimurium</i>	34
2.3.13 Infection of B6m26 cells with <i>Salmonella typhimurium</i>	34
2.3.14 In vitro passage of <i>Toxoplasma gondii</i>	35
2.3.15 Preparation and culture of murine primary astrocytes	35
2.3.16 In vitro infection experiments and inoculation of primary astrocytes with <i>Toxoplasma gondii</i>	36

3. RESULTS	27
3.1 THE P47 GTPASES ARE INDUCED BY IFN- γ IN L929 AND TIB-75 CELLS.	37
3.2 THE P47 GTPASES SHOW DIFFERENT LEVELS OF MEMBRANE ASSOCIATION.	37
3.3 LRG-47 BINDS GDP AND LOCALIZES TO THE GOLGI APPARATUS AND THE ER.	38
3.4 LRG-47 DOES NOT ASSOCIATE WITH THE ENDOSOMAL OR LYSOSOMAL COMPARTMENT.	43
3.5 LRG-47 IS RECRUITED TO THE PLASMA MEMBRANE UPON PHAGOCYTOSIS AND REMAINS ASSOCIATED WITH MATURING PHAGOSOMES.	45
3.6 MEMBRANE BINDING OF LRG-47 IS IFN- γ AND NUCLEOTIDE INDEPENDENT.	48
3.7 LRG-47 IS TARGETED TO THE GOLGI APPARATUS AND PLASMA MEMBRANE BY DIFFERENT DOMAINS. .	51
3.8 THE α K REGION OF LRG-47 IS SUFFICIENT FOR GOLGI TARGETING.	52
3.9 THE GOLGI TARGETING ACTIVITY OF THE LRG-47 α K REGION REQUIRES AN AMPHIPATHIC HELIX.	54
3.10 THE α K REGIONS OF GTPI AND IGTP ALSO SHOW MEMBRANE TARGETING ACTIVITY.	56
3.11 THE α K PEPTIDES OF GTPI AND IGTP SHOW HOMOLGY TO TWO DIFFERENT REGIONS OF PHOSPHOLIPASE C.	57
3.12 THE α I, J REGION LRG-47 SHOWS HOMOLGY TO HUMAN PHOSPHOLIPASE C LIKE PROTEIN.	59
3.13 IIGP1 IS ASSOCIATED WITH THE ER.	60
3.14 IIGP1 FORMS NUCLEOTIDE AND C-TERMINAL DOMAIN DEPENDENT AGGREGATES AFTER TRANSFECTION.	60
3.15 IIGP1 IS N-TERMINALLY MYRISTOYLATED.	63
3.16 IIGP1 IS TARGETED TO ENDOMEMBRANES BY THE N-TERMINAL DOMAIN AND TO THE PLASMA MEMBRANE BY THE G-DOMAIN.	65
3.17 THE P47 GTPASES BIND TO MEMBRANE WITH DIFFERENT STRENGTH.	68
3.18 THE MYRISTOYL-GROUP OF IIGP1 DOES NOT CONTRIBUTE TO THE STRENGTH OF MEMBRANE ASSOCIATION.	68
3.19 LOCALIZATION OF TAGGED GMS GTPASES IN L929 CELLS	69
3.20 EXPRESSION OF TGTP IN CELLS	71
3.21 EXPRESSION OF IIGP1-HIS IN CELLS	74
3.22 IIGP1 ACCUMULATES AT <i>TOXOPLASMA GONDII</i> CONTAINING PARASITOPHOUS VACUOLES.	76
3.23 IGTP LOCALIZES TO <i>TOXOPLASMA GONDII</i> CONTAINING PARASITOPHOUS VACUOLES.	78

4. DISCUSSION	81
4.1 THE INTERFERON INDUCIBLE P47 GTPASES ARE REMARKABLY DIVERSE REGARDING THEIR MEMBRANE ASSOCIATION PROPERTIES.	81
4.2 LRG-47 BINDS GDP AND IS A GOLGI ASSOCIATED PROTEIN	82
4.3 LRG-47 IS RECRUITED TO PHAGOSOMAL ENVIRONMENT AND PLASMA MEMBRANE EARLY UPON PHAGOCYTOSIS.....	84
4.4 DOMAINS RESPONSIBLE FOR THE DYNAMIC INTRACELLULAR BEHAVIOUR OF LRG-47	86
4.5 LRG-47 IS TARGETED TO GOLGI BY A C-TERMINAL AMPHIPATHIC HELIX.	87
4.6 THE αK REGIONS OF ALL MOUSE GMS GTPASES MEDIATE MEMBRANE ASSOCIATION.	89
4.7 THE ER PROTEIN IIGP1 SHOWS STRIKING DIFFERENCES TO LRG-47	91
4.8 TRANSFECTION AND EXPRESSION OF P47 GTPASES IN CELLS	95
4.9 THE DYNAMICS OF P47 GTPASES IN INFECTED CELLS	97
4.10 MODELS FOR P47 GTPASE FUNCTION.....	100
5. REFERENCES	105
6. SUMMARY.....	123
7. ZUSAMMENFASSUNG	124
8. DANKSAGUNGEN	126
9. ERKLÄRUNG.....	127
10. LEBENSLAUF	128

ABBREVIATIONS

2'-5'-OAS	2'-5'-oligoadenylate synthetase
ADAR	adenosine deaminases that act on double-stranded RNA
APC	antigen presenting cell
APOBEC3G	apolipoprotein B mRNA-editing, enzyme-catalytic, polypeptide-like 3G
APS	ammoniumpersulfate
ATP	adenosine triphosphate
BAC	bacterial artificial chromosome
bp	base pair
BSA	bovine serum albumine
CI-MP6R	cation-independent mannose 6-phosphate receptor
C-terminal	carboxy terminal
DMEM	Dulbecco Modified Eagles Medium
DMSO	dimethylsulfoxid
DNA	desoxyribonucleicacid
<i>E. coli</i>	<i>Escherichia coli</i>
EDTA	ethylendiamintetraacetic acid
ER	endoplasmatic reticulum
EtBr	ethidium bromide
EtOH	ethanol
FCS	foetal calf serum
GAP	GTPase activating protein
GBP	guanylate binding protein
GEF	guanine nucleotide exchange factor
GDI	guanine nucleotide dissociation inhibitor
GDP	guanosine diphosphate
GMP	guanosine monophosphate
GTP	guanosine triphosphate
IB	immuno blot
IDO	indoleamine 2,3-dioxygenase
IF	immunofluorescence
IFN- γ	Interferon- γ
IFN- α/β	Interferon- α/β
IFNGR	IFN- γ receptor
IFNAR	IFN- α receptor
iNOS	inducible nitric oxide synthetase
NRAMP1	natural resistance associated membrane protein 1
IRF-1	Interferon regulatory factor 1
IP ₃	inositol-1,4,5-trisphosphate
ISG20	interferon stimulated gene 20
JAK	janus kinase
kb	kilobase
kDa	kilodalton
LAMP-1	lysosome associated membrane protein 1
LPS	lipopolysaccharide
M	molar
MEF	mouse embryonic fibroblats
MOPS	3-[Morpholino]propansulfonsäure
N-terminal	amino-terminal
OD	optical density
ON	over night
ORF	open reading frame
PBS	phosphate buffered saline
PCR	polymerase chain reaction
PFA	paraformaldehyde
PH	pleckstrin homology domain
PLC	phospholipase C
phox	phagosome oxidase
PIK	phosphatidyl inositol kinase
PIP	phosphatidyl inositol phosphate

PKR	protein kinase R
PML	promyelocytic leukaemia
PtdInsP	phosphatidyl inositol phosphates
RNAse	ribonuclease
rpm	rounds per minute
RT	room temperature
RNAi	RNA interference
<i>S. typhimurium</i>	<i>Salmonella typhimurium</i>
SDS	sodium dodecylsulfate
SDS-PAGE	SDS polyacrylamide gel electrophoresis
SSH	suppressive subtractive hybridization
STAT	signal transducer and activator of transcription
TEMED	N,N,N',N' -Tetramethyldiamine
<i>T. gondii</i>	<i>Toxoplasma gondii</i>
TGN	trans-Golgi network
Tris/HCl	Tris[hydroxymethyl]aminoethane
TRITC	tetramethylrhodamine isothiozyanate
TNF- α	tumor necrosis factor α
TRIM5 α	tripartite motif 5 α
U	unit
UV	ultraviolet
VOL	volume
WT	wild type
ZAP	Zinc-finger Antiviral Protein

Units

'	minute
"	second
Ø	diameter
%	percent
% solution	grams in 100ml solution
°C	degree Celsius
aa	amino acids
bp	base pair
Ci	Curie (1 Ci = 3.7x10 ⁷ cpm)
cpm	counts per minute
g	G force
g	gram
h	hour
kb	kilo bases
l	Litre
LD	lethal doses
m	meter
M	molar
m ²	square meter
nt	nucleotide
OD	optical density
rpm	rounds per minute
t	time
U	unit
v/v	weight pro volume
c	centi, 10 ⁻²
m	milli, 10 ⁻³
µ	micro, 10 ⁻⁶
n	nano, 10 ⁻⁹
p	pico, 10 ⁻¹²

1. Introduction

1.1 Resistance and Immunity

Resistance to infectious agents is a common property of all living things in order to maintain their structural integrity. Pathogens try to invade the host, disseminate and establish infection to exploit the organism for its own advantage. The host in contrast attempts to intervene in the pathogens actions at every possible step vulnerable to attack. Hundreds of million years of reciprocal adaptation have led to a complex many layered and interconnected system of interactions between host and pathogen. These interactions often led to a relationship in which action and counteraction are well balanced and infections become only visible, or even possible, upon impairment of host resistance. A remarkable proportion of the genome of both players is devoted to these interactions (1-5).

Central to prevention and containment of infectious agents is their recognition. This is achieved by receptors sensing molecules invariably associated with pathogens and/or their actions (6, 7). The list of receptors recognizing pathogen associated patterns (PAMPs) is long and ever growing including the Toll-like receptors (6), Nod receptors (8, 9), lectins (10) and double-stranded RNA recognizing molecules (11, 12). These receptors are found throughout life including plants and mammals. The activation of these receptors elicits the induction or activation of defence programs counteracting infections in a diverse manner (13, 14). The expression of pattern recognition receptors (PRRs) is in principle not restricted to special cell types but is particularly eminent on phagocytic cells such as macrophages (10).

In vertebrates, the adaptive immune system builds a second, highly sophisticated resistance system. In contrast to the innate immune system which utilizes the aforementioned receptors, adaptive immunity is based on receptors which are clonally rearranged in the soma. In their entirety they are potentially able to recognize virtually every chemical component in the appropriate context. B-cells carry special receptors (BCR) which induce, upon their activation, clonal expansion and production of antibodies targeting extracellular pathogens. T-cells, and in particular CD8 positive T-cells, recognize intracellular pathogens by means of their T-cell receptor (TCR). Upon activation T-cells kill the infected cell or secrete factors inducing the infected cell to neutralize the pathogen by itself in a non-cytolytic manner (15, 16).

Upon the first encounter of a pathogen it takes several days for the adaptive immune system to mount an effective and robust immune response. The innate immune system in contrast is able to respond to invading microbes within minutes and most infections are therefore contained within a short time. However in many cases the response to infections involves cells of both systems and is orchestrated by small soluble molecules called cytokines.

1.2 Cytokines and Interferons

Cytokines are small soluble proteins which belong to four, structurally distinct, classes namely the haematopins, the chemokines, members of the TNF (tumor necrosis factor) family and the interferons (IFN). Although the secretion is not limited to them, major producers of cytokines are professional immune cells. Numerous cellular responses such as proliferation, chemotaxis but also angiogenesis and embryogenesis are regulated by cytokines (17). Some cytokines, and in particular interferons, have the remarkable ability to elicit extraordinarily complex cellular responses virtually changing the whole physiology of the responding cell (18-20).

Interferons are subdivided into three types. Type I interferons include IFN- α with 10 members and IFN- β (21), IFN- ω (22), IFN- κ (23), IFN- δ (24) with a single member each. Type II interferon has only one member, IFN- γ and finally the recently discovered IFN- λ (25, 26) having three members.

Type I interferons are secreted by many cell-types including fibroblasts and dendritic cells (DCs) (27, 28). The main stimulus of type I interferon production is virus infection and consequently its main function is the induction of an antiviral state in the responding cell (12). However the action of type I interferons is not restricted to viral purging (19).

IFN- γ is secreted by activated T-cells (29, 30), NK-cells (31) and macrophages (32). The cellular response to IFN- γ is enormously complex (18-20) regulating a considerable percentage of the genome (1). Thus it is not surprising that the actions of IFN- γ are diverse and play an important role in innate and adaptive immunity.

1.3 The interferon signal transduction pathway

Type I and type II interferons are recognized by different receptors (Figure 11). Biologically active IFN- γ is a homodimer and binds to the heterodimeric IFN- γ receptor (IFNGR1 and IFNGR2) expressed on all nucleated cells. Binding of IFN- γ to its receptor induces receptor dimerization and thereby a cascade of intracellular tyrosine phosphorylation events involving JAK1 and JAK2 ultimately leading to the activation and nuclear translocation of a STAT1 transcription factor homodimer called GAF (gamma activated factor) (33). In the nucleus GAF binds to gamma-interferon activated sequence (GAS) elements found at the promoter of many interferon responsive genes leading to their activation.

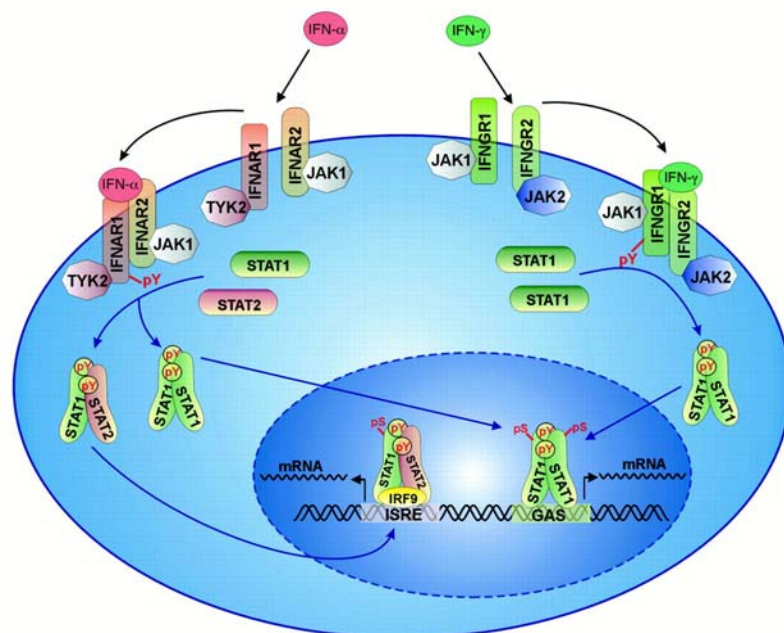


Figure 11: Simplified scheme of the type I and Type II signal transduction pathways taken from (34). Binding of type I interferon (IFN- α) to its receptor induces dimerization of the IFNAR1 and IFNAR2 receptor subunits, activation of the associated JAK1 and TYK2 proteins subsequent phosphorylation of STAT1 and STAT2 and thereby their dimerization. The STAT1/STAT2 dimer translocates into the nucleus and forms a trimeric complex with IRF9 which binds to ISRE elements at the promoter of IFN stimulated genes and promotes their transcription. Binding of type II IFN (IFN- γ) to its receptor induces its dimerization, activation of JAK1 and JAK2 which is followed by phosphorylation of STAT1 and its homodimerization. The STAT1 homodimer binds to GAS elements at the promoter of IFN- γ stimulated genes after translocation into the nucleus.

Among the primary response genes are further transcription factors such as IRF-1 leading to a second wave of gene expression (18).

The signal transduction pathway of type I IFN is very similar to that of IFN- γ . Binding of IFN- α or IFN- β to its heterodimeric receptor (IFNAR1 and IFNAR2) induces receptor dimerization, activation of JAK1 and TYK2 and subsequent phosphorylation of

STAT1 and STAT2. The STAT1/STAT2 heterodimer associates with IRF-9 to form a heterotrimeric complex called ISGF3. ISGF3 binds to ISRE (interferon stimulated response elements) near the promoter of IFN activated genes. Type I and type II IFNs activate distinct but overlapping sets of genes (19, 35-37).

Experiments with mice carrying targeted deletions of components of the IFN- γ and IFN- α/β signal transduction pathways respectively have shown that IFN- γ is essential for resistance against bacterial and protozoan pathogens having a rather mild effect on certain viral infections. The opposite effect was observed for IFN- α/β which is central to combat viral infections but has a comparably moderate effect on bacterial and protozoan infections (38, 39).

Due to its complexity the function of IFN regulated genes is hard to assess not least because the function of many inducible genes is unknown. However, in general IFN inducible genes play a role in one or more of the following cellular programs (18, 19). This includes the regulation of immune cell function, regulation of proliferation, enhancement and modulation of antigen-presentation and direct anti-microbial effects. Many of the direct anti-microbial effects are mediated in a cell-autonomous manner.

1.4 Cell-autonomous immunity

It is becoming increasingly clear that cell-autonomous immunity plays a major role in resistance to intracellular pathogens of all classes. Many of the molecular players of intracellular resistance are inducible by interferons. The main focus has been on factors restricting viral growth (12) but it is now appreciated that also bacteria and protozoa are restricted by cell-autonomous resistance mechanisms (40). By definition cell-autonomous immunity is mediated by a cell for itself without the requirement for other specialized cell types. However, the induction of cell-autonomous resistance in a particular cell might be dependent on specialized cells as exemplified by the production of IFN- γ . Indeed it turned out that production of IFN- γ is used by activated T-cells to induce cell-autonomous immunity in the target cell and thereby to clear viral infections (16, 15).

The list of proteins implicated in cell-autonomous immunity is long and still growing (41). The following table includes an incomplete overview of factors known to play an important role in cell-autonomous immunity (Table 1). Many of the listed proteins have in addition functions different from direct anti-microbial effects. PKR for example has

been shown to be central for signal transduction in a variety of cellular pathways (11) (42) or to mediate general functions in membrane traffic like Rab5a (43, 44). However many of the included proteins have no known function besides pathogen resistance.

Table 1

NAME	SPECIES	TARGET	LOCATION	REFERENCE
Mx	vertebrates	<i>Bunyaviridae</i> , <i>Orthomyxoviridae</i>	nucleus, cytoplasm (smooth ER)	(45-48)
2'-5' OAS, RNaseL	mouse, human	<i>Picornaviridae</i>	nucleus, cytoplasm	(12, 49)
PKR	mouse, human	EMCV, <i>Vaccinia</i> <i>Virus</i> , VSV	cytoplasm	(50-53)
ADAR1	human	<i>Hepatitis delta virus</i>	nucleus, cytoplasm	(54, 55)
ISG20	human	VSV, <i>Influenza virus</i> , EMCV	nucleus	(56, 57)
p65 GTPases	vertebrates	VSV, EMCV	cytoplasm	(58-60)
PML	mouse, human	VSV, <i>influenza virus</i> , <i>human foamy virus</i> , HSV1	nucleus	(61-63)
ZAP	rat	<i>Murine leukaemia</i> <i>virus</i> (MLV)	ND	(64)
CEM15/APOBEC3G	mammals	<i>Hepatitis B Virus</i> and retroviruses including HIV, SIV, MLV, EIAV	cytoplasm	(65-70)
TRIM5 α	primates	HIV, SIV	cytoplasmic bodies	(41)
RNAi machinery	eukaryotes	dsRNA viruses including HIV-1, HCV, <i>Poliovirus</i> , <i>Hepatitis delta virus</i>	cytoplasm	(71-75)
FV1, Ref1, Lv1	rodents, primates	retroviruses including FV1, MLV, HIV-1, HIV-2, EIAV	Golgi, ER	(76-79),
IDO	mouse, human	viruses, bacteria and protozoa including cytomegalovirus, <i>Clamydia</i> , <i>Toxoplasma</i> <i>gondii</i>	cytosol	(80-83)
iNOS	vertebrates	over 80 pathogens of all classes	cytoplasm	(84-87)
phox complex	vertebrates	pathogens of viral, bacterial and protozoan origin	phagosomal membrane	(88)
NRAMP1	mouse, human	<i>Salmonella</i> , <i>Leishmania</i> , <i>Mycobacterium</i>	phagosomal membrane	(89-91)
p47 GTPases	mouse	bacterial and protozoan pathogens	ER, Golgi, cytosol	(40, 92-96), this study
Rab5a	eukaryotes	<i>Listeria</i>	early endosomes	(43)

The diversity of factors included in the table (Table 1) reflects the diverse and complex intracellular behaviours of the respective pathogens.

It is conspicuous that many of the proteins targeting bacterial and protozoan pathogens are membrane-bound. Intracellular membranes are central for the survival of many pathogens and therefore it is not surprising that pathogen and host attempt to take over control of cellular membrane dynamics (97). In eukaryotic cells many of the essential steps involving membrane dynamics are mediated by GTP binding proteins (10, 44, 98).

1.5 GTP binding proteins and membrane dynamics

GTP binding proteins are central to a plethora of cellular functions including protein biosynthesis, transport across the nuclear envelope, signal transduction and membrane traffic. Despite such diverse functions the underlying mechanism is the same for all GTPases involving a conformational change upon binding of GTP and subsequent hydrolysis of the nucleotide to GDP and/or GMP (99-102). The energetically favourable reaction is able to create order or force. Guanine nucleotide binding is essential for the function of GTPases and involves 5 motifs called G1-G5 among which G1, G3 and G4 are universally conserved. The consensus sequence of the G1 motif is GX₄GKS contacting the α -, β - and γ -phosphate of the bound nucleotide. The G3 motif makes contact to the γ -phosphate and the G4 motif confers specificity by contacting the base of the guanine nucleotide (99-101).

For the switch GTPases the GTP bound form is considered active and interacts with other molecules termed GTPase effectors. This interaction is responsible for the downstream effects of the GTP bound GTPase. Inactivation is achieved by hydrolysis of GTP and dissociation of the γ phosphate. Many GTPases have a low intrinsic activity and inactivation is mediated by the action of GTPase activating proteins (GAPs) which accelerate hydrolysis. The resulting GDP bound form is considered inactive. In many cases GTPases become activated upon interaction with guanine nucleotide exchange factors (GEFs). GEFs mediate dissociation of GDP from the GTPase. Due to the 3 fold higher concentration of GTP within the cell (103) GTPases become thereby activated despite often similar affinities for GTP and GDP (100). Some GTPases like the Rab and Rho are additionally regulated by guanine nucleotide dissociation inhibitors (GDIs)

which bind to the GDP bound form and prevent nucleotide dissociation (104). A simplified cartoon summarizing the GTPase cycle is shown in Figure I2.

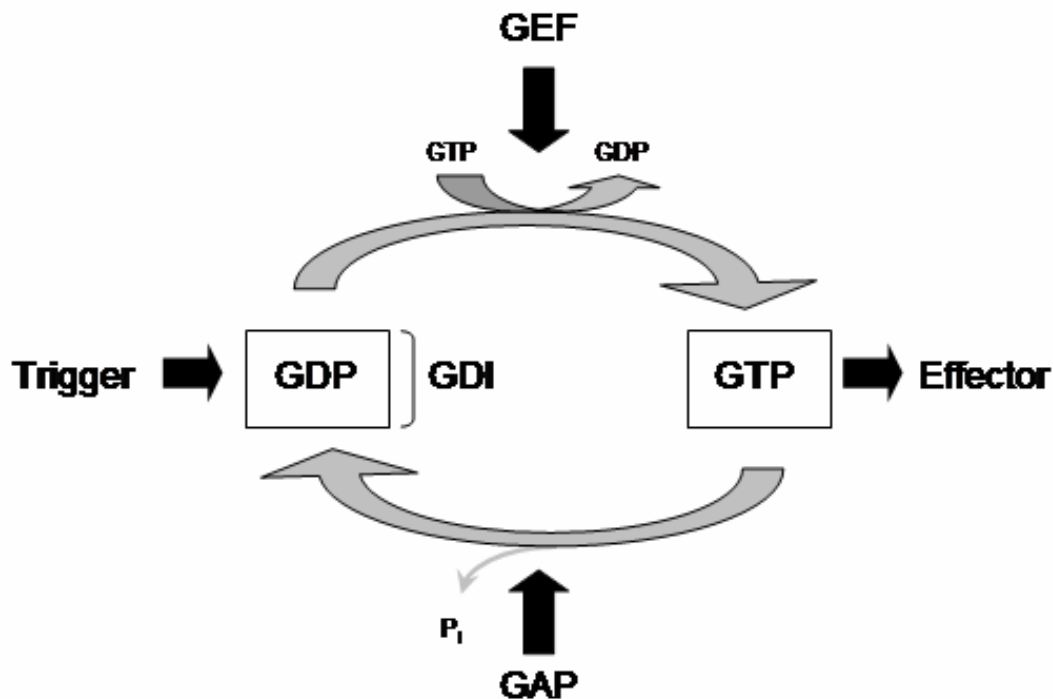


Figure I2: Simplified scheme of the GTPase cycle.

Activation of the GDP bound GTPase by a trigger is achieved by exchange of GDP for GTP. This exchange is often mediated by the activation of exchange factors (GEF). The GTP bound GTPase interacts with molecules termed effectors mediating its downstream effects. GTP hydrolysis and dissociation of the γ -phosphate leads to the inactivation of the GTPase. The often low intrinsic hydrolytic activity can be accelerated by activating proteins (GAP). Some GDP bound GTPases are kept inactive by the action of guanine nucleotide dissociation inhibitors (GDI) (99-101).

Due to their ability to be regulated in multiple ways and to give complex reactions a direction, GTPases are central regulators and mediators of membrane traffic and membrane association is essential for their function.

Arf GTPases for example regulate COP mediated vesicular budding (105). The inactive GDP bound form is cytosolic but upon nucleotide exchange from GDP to GTP Arf exposes an N-terminal myristoyl-group and an amphipathic helix hidden within the molecule anchoring the protein in the lipid bilayer (106, 107). At the membrane Arf interacts with other molecules to initiate vesicular budding (105).

Rab GTPases in contrast are isoprenylated at their C-terminus and are kept soluble in the cytosol by the interaction with RabGDI burying the large C-terminal isoprenyl-group in a hydrophobic pocket (44, 105). Activation of Rab by nucleotide exchange from GDP to GTP leads to dissociation of Rab from RabGDI and subsequent membrane association.

At the membrane Rab GTPases interact with various effectors thereby determining specificity of vesicular transport and organelle identity (44).

Rho GTPases are yet another family of GTP binding proteins belonging, like Arf and Rab, to the p21 Ras superfamily of GTPases. Rho GTPases such as RhoA, CDC42 and Rac1 regulate actin dynamics (108-110) and function in phagosome formation (111-113) and maturation by recruiting the phagosome oxidase complex to the phagosomal membrane (114). In addition they have various other cellular functions (108). Activation of Rho GTPases results in membrane association which is, as in the case of Rab, mediated by a C-terminal isoprenyl-group (115). The GDP bound form of Rho GTPases is found in the cytosol in a complex with RhoGDI (116). Upon exchange of GDP for GTP Rho GTPases bind to intracellular membranes collectively called endomembranes and the plasma membrane (117, 118). In all cases nucleotide exchange and membrane association are strictly coupled.

1.6 Dynamin

Dynamins are GTPases which mediate scission of vesicles budding from the donor membrane. Overexpression of dominant negative mutants of dynamin interferes with the formation of clathrin-coated vesicles, budding from caveolae and phagosome formation. Dynamins differ in several key aspects from the p21 Ras superfamily of GTPases (98, 102, 119).

Dynamins are with a molecular weight of about 100 kDa much larger than Arf, Rab and Rho GTPases which are 20-30 kDa in size. Since their discovery it is under debate whether dynamins function by generating force or are molecular switches analogous to the members of the Ras superfamily of GTPases, or both (98, 102, 120-122).

The N-terminal nucleotide binding domain of dynamin is followed by the middle domain implicated in self-assembly, a pleckstrin homology domain (PH domain) involved in membrane targeting, a GTPase effector domain accelerating GTP hydrolysis and a C-terminal proline-rich domain interacting with other proteins (98). Although many proteins have been shown to interact with dynamin no proteins, apart from dynamin itself, could be identified so far interacting with dynamin in a nucleotide dependent manner (98, 102). Compared to Ras-like GTPases dynamins bind guanine nucleotides with a rather low affinity in the μM range and have high turn over rates of hydrolysis. Dynamin self associates in a GTP dependent manner which increases the specific activity of the dynamin subunits (123). Thus nucleotide hydrolysis of dynamin

is cooperative. Dynamin associates with negatively charged liposomes *in vitro* and this association accelerates hydrolysis about 100 fold (123, 102).

In the presence of GTP-analogues dynamin tubulates lipids *in vitro* by forming ring-like structures around liposomes (124). Upon hydrolysis the diameter of the tubulated liposomes decreases (122). *In vivo* dynamin was observed to form spiral-like structures around the neck of budding vesicles (124). The presence of lipids massively accelerates GTP hydrolysis and enhances nucleotide dependent oligomerization and self-assembly (102, 123).

Membrane binding is essential for the function of dynamin itself and probably also for the other members of the dynamin superfamily of which the mammalian dynamin 1, 2 and 3 are the prototypes (98). The PH domain of dynamin is involved in targeting of dynamin to membranes mediated by its low affinity for the lipid head group inositol 1,4,5-triphosphate. Mutations in the PH domain of dynamin have a dominant negative effect on endocytosis (125-127). However other members of the dynamin superfamily lack a PH domain but are still capable of lipid binding as for example the Mx proteins (128, 45).

1.7 The antiviral Mx proteins

Mouse Mx was the first member of the dynamin superfamily discovered and was initially identified as a dominant locus in A2G mice conferring resistance to infections by orthomyxoviridae (129). Mapping and subsequent cloning of the gene led to the identification of mouse Mx1 (48, 130) and the human homologue MxA (131). Surprisingly, in contrast to most out bred mice, most laboratory mouse strains do not carry a functional allele of Mx (132, 133).

Mx proteins exhibit nucleotide dependent oligomerization and cooperative hydrolysis (47, 134, 135). A direct interaction of Mx with viral particles has been shown and is proposed to be important for its antiviral activity (47). However a mutant Mx protein, defective in GTP hydrolysis and oligomerization still shows antiviral activity questioning the role of self assembly for its antiviral function (136).

Recently human MxA has been reported to localize to the smooth ER and to tubulate lipids in a nucleotide dependent manner (45). The meaning of membrane deformation by MxA for its biological function however is unclear recalling that dynamin has been first isolated as a protein assembling around microtubules (137) but there is still no *in vivo* function described giving this finding significance. A hallmark of the Mx proteins

is their exclusive inducibility by type I IFN (138) and low or absent level in resting cells.

1.8 Other Interferon inducible GTPases

The induction of high molecular weight GTPases by IFNs turns out to be an important component of their biological function. There are at least three more families of GTP binding proteins which are massively induced by IFN and whose functions are dedicated to host resistance.

The p65 family of GTPases has 5 members (GBP1-5) in mouse and human (139). Homologues are found in all vertebrates analyzed so far (60). The p65 GTPases are abundantly induced by type I and type II IFN from low resting levels (60). When expressed in Hela cells human GBP1 (hGBP1) shows a cell-autonomous antiviral effect against VSV and EMCV (58). Besides its antiviral activity members of the p65 family have been implicated in the regulation of cell proliferation (140-142). The crystal structure of hGBP1 reveals a three domain protein having an N-terminal GTP binding domain, followed by a helical middle domain and a C-terminal GTPase effector domain (143). Some family members are isoprenylated mediated by a C-terminal CAAX motif (C, cysteine; A, large hydrophobic residues; X, any residue) and this isoprenylation appears to be responsible for the localization in enigmatic cytoplasmic dots (59) (H. Kashkar, unpublished results). The structure of hGBP1 has attracted much attention because it is generally believed that its overall structural organization is shared with dynamin (143).

Recently a family of gigantic GTP binding proteins with a molecular weight of 280 kDa has been published (144). This very large inducible GTPases (VLIGs) are massively induced by type I and type II IFNs, at least in the mouse. No anti-microbial effect for the VLIGs has been shown so far but VLIG-1, the prototype of the VLIG family, shows highest homology to GTPases mediating cell-autonomous resistance within the GTPase superfamily (144). This suggests, in addition to their IFN inducibility, a role in intracellular defence.

The third family of IFN inducible GTP binding proteins are the p47 GTPases.

1.9 The p47 GTPases

There is now compelling evidence that the p47 GTPases are an essential component of the immune response against intracellular pathogens in the mouse (40). So far 6 p47 GTPases have been published, namely TGTP (145), IRG-47 (146), IIGP1 (60), IGTP (147), GTPI (60) and LRG-47 (148) but the total number of p47 genes in the *Mus musculus domesticus* genome is 23 of which 4 are pseudogenes by one or another criterion (Julia Hunn, Cemali Bekpen and Jonathan C. Howard, personal communication). Figure I3 shows a phylogeny of the p47 GTPases of *Mus musculus domesticus*.

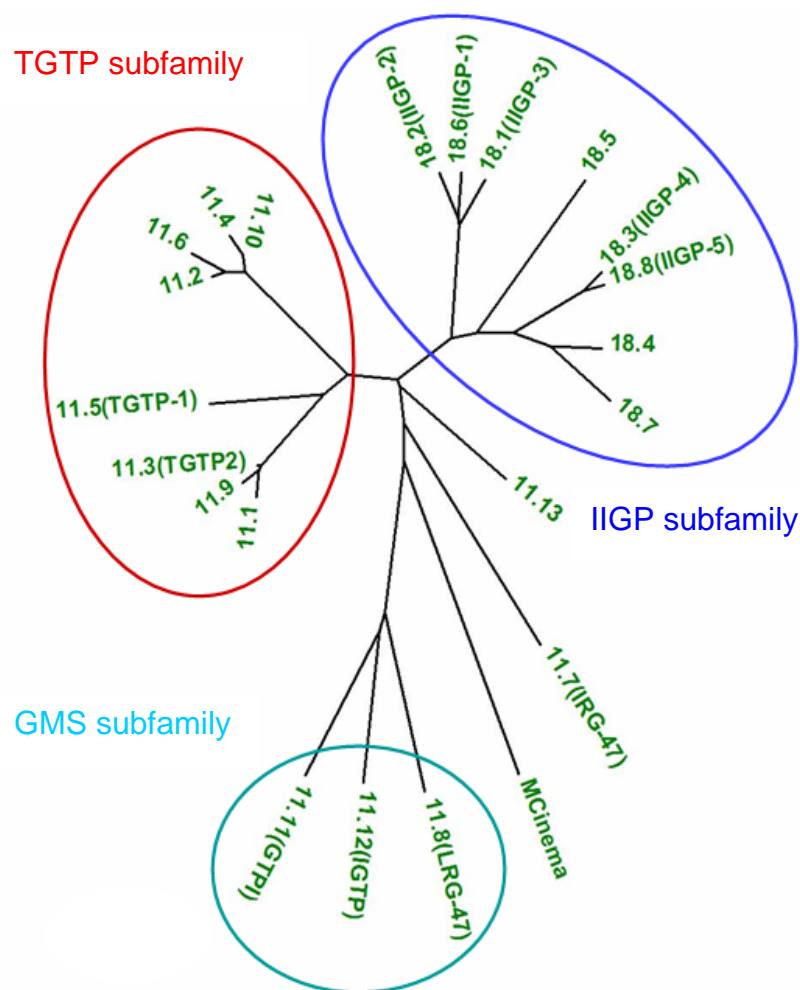


Figure I3: Phylogenetic Tree based on the protein sequence of the GTPase domain of the mouse p47 GTPases (courtesy of Cemali Bekpen) showing 22 out of the 23 members. The neighbour joining tree is based on the distance method using the MEGA2 program.

The phylogeny reveals a complex protein family which can be subdivided into several subgroups namely the TGTP, IIGP and GMS subfamily. In addition, the phylogeny

includes p47 GTPases which do not belong to any of this subgroup like IRG-47 and mCinema. The GMS GTPases carry an unusual methionine instead of the universally conserved lysine in the G1 motif changing its sequence from GX₄GKS to GX₄GMS (60). In human the p47 GTPase family is far less complex including only a very close homologue of mCINEMA called hCINEMA and a small fragment showing homology to the mouse GMS GTPases carrying the same unusual lysine to methionine substitution in the G1 motif (Cemali Bekpen and Jonathan C. Howard, personal communication).

IRG-47	MDQFISAFLK	GASENSFOOL	AKEFLPQYSA	LISKAGGMLS	PETLTGHIKA	LOEGNLSDVM	IQIQKAISAA	ENAILLEVAVI	GOSGTGKSSF
Mg21/TGTPMA	WASSFDAPFK	NFKRESKIIIS	EYDITLIMTY	IBENKLOKAV	SVIEKVLKDI	ESAPLHIAVT	GETGAGKSTF
IIGPMGQLF	SSPKSDENNND	LPSSFTGYFK	KPNTGRKIIIS	QEIILNLELR	MRKGNLQLTN	SAISDALKEI	DSSVLNVAVT	GETGSGKSSF
LRG-47MK	PSHSSCEAAP	LLPNMAETHY	APLSSAFPFF	TSYQGTSSRL	PEVSRSTERA	LREGKLELV	YGKQETVATL	GDSGNGMSSF
IGTP	MDLVTKLPQN	IWKFTFLFIN	MANYLKRLIS	PWSKSMTAGE	SLYSSQSSS	PEVIEDIGKA	VTEGNLQKVI	GIVKDEIQSK	SRYRVKIAVT	GDSGNGMSSF
GTPI	MEEAVESPEV	KEFEYFSDAV	FIPKDGNTLS	VGVIKRIETA	VKEGEVVKV	SIVKEIIQNV	SRNKIKIAVT	GDSGNGMSSF
GBP motifs										GXXXGKS
IRG-47	INALRGLGHE	ADESADVGVV	ETTMCKTPYQ	H.PKYEKVIF	WDLPGTGTGN	PHADAVLDQV	GFANYDFPII	ISSSRFSLND	ALLAQKTKDA	GKKFYFVVRTK
Mg21/TGTP	INTLRGVGHE	EKGAAPTGAI	ETTMKRTYPV	H.PKLENVVI	WDLPGIGSTN	PTPQNYLTEM	KFGEYDFPII	ISATRFKEND	AQLAKATAQM	GMNFYFVVRTK
IIGP	INTLRVIGNE	EEGAKTGVV	EVTMERHPYK	H.PNIENNVF	WDLPGIGSTN	PPNTVLEKRM	KFGEYDFPII	ISATRFKEND	IDIKAESMM	KKPFYFVVRTK
LRG-47	INALRVIGHD	EDASAPTVV	RTTKTRTEYS	S.SHFENVVL	WDLPLGLGATA	QTVEDVVEEM	KFTCDLPII	EASQFSSNH	VKLSKIQSM	QKRFYFVVRTK
IGTP	INALRPIGHE	EESAPTVGV	RTTKKPAQYS	SDSHFVVEL	WDLPLGLGATA	QSVESYLEEM	QISTFDLIII	VASEQFSSNH	VKLAITMORM	RKRFYFVVRTK
GTPI	INALRLIGHD	EKDSAPTVGV	RTTKQKTCYF	S.SHFFVVEL	WDLPLGLGATA	QSVESYLEEM	QISYDLDLII	VASEQFSSNH	VKLAITMORM	RKRFYFVVRTK
GBP motifs					DXKG					NK TQ
IRG-47	VDSLDYNEQK	AKPIAFKKEK	VLQQRIDYCV	TNLIKTVTE	ECIFLISNLD	LGAFDFPEKLE	ET.LLKEEFG	HRRHMFALLI	PNISDASIEL	KKHFIREKIV
Mg21/TGTP	VDSLDYNEQK	FKPKSFNKEE	VKNIKIDYCS	NHLQESLDSE	PFVFLVSNVD	ISKYDFPEKLE	.TKLLQDLPA	HKRHFVLSLI	QSLTEATINY	KRSLDKQKVF
IIGP	VDSIDTNEAD	GKQTFDKER	VLDQIRLNCV	NTPRENGIAB	PEIFLISNKN	VCHYDFPVEM	D.KLISDLEI	VKRHFVMSI	PNITDSVIEK	KRPFKQKVF
LRG-47	LDRLD.....	.STSVLSEVR	LLQNIQENIR	ENLQKKEKVV	PFVFLVSSLD	PLLYDFPEKLR	DT.LHKDESN	TRCCPEKTLI	YGTVEKIVGD	KVAWVKQRIA
IGTP	LDRLD.....	.STSTFPEPQ	LLQSIQENIR	ENLQCAQVRD	PEFLISCFSS	PSFHDPEELR	NT.LOKDIFS	IRYDPLEIIT	QVCCKIEN	KAFSLKEDQM
GTPI	LDRLD.....	.STSTFPEPQ	LLQSIQENIR	DSLQKKEKVV	HEMFLVSVFK	PESHDFPEKLR	ET.LOKDLEP	IKYHGLVETI	YQVCEKTVNE	RVESIKKSID
GBP motifs					XD					
IRG-47	LEALKSAAVS	FIFMFTFFKG	FDLPEQEQL	KDYRSYFGLD	DSQIKEIIEK	LGAPLADIKG	ELKCLDFWSL	VKDNSIIAQA	TSAAEAFCV	KGGPESSAFQ
Mg21/TGTP	LEAMKAGALA	TIFLGGMI.S	DILENLDETF	NLYRSYFGLD	DASLENIQD	LNMSVDDFKV	HLRFPHLFAE	HNDESLEDKL	FRYIKHISV	TGGPVAAVTV
IIGP	LEGFAADLVN	IIFSLTFLLD	SDLETLKKS	KFYRTVFGVD	ETSLEQLARD	WEIEVDQVEA	MKSPAVFKP	TDEETIQERL	RREYQECFLA	NGYLLPKNSF
LRG-47	NESLKNLSGV	RDDDNMGE..CL	KVYRLIFGVD	DESVOQVAQS	MGTVVMEYKD	NMKSQNFYTL	RREDWKLRML	TCIAVNAFFR	LLRFLPCVCC
IGTP	EMKLEAAVS	SEDDTANL..ERGL	QTYQKLFQVD	DGSLQCVARS	TGRLEMGRA	LQF.QDLIKM	...DRRLELM	MCFAVNKFLR	LLSSSWYGL
GTPI	EDNLHTEPGI	SDEGNAIE..IR	KAFQKTEGLD	DISLHLVLE	MKNKHPNTSM	ES..QETQRY	QDDDWLRLR	YRTGTRVGS	GFDMKCCFT
IRG-47	ALKV..YYR	TQF...ENIV	VDDAKHLERK	IETVNVVA*						
Mg21/TGTP	YRMA..YYLQ	NLF...LDTA	ANDAIALENS	KALFEKKVGP	YISEPPEYWE A*					
IIGP	LKEI..FYLK	YYP...LDMV	TEDAKTLLEK	ICLRN*						
LRG-47	CL.....RR	LRHKRMFLV	ADTKNILEK	ILRDSIFPPQ	I*					
IGTP	WNVVTRYFRH	QRHKLVIETV	SENTKTSLRK	ALKDSVLPPE	IH*					
GTPI	S...HHSRC	KQQKDIIDET	AKAKREVLLK	ILRLSIFHP*						

Figure I4: Amino acid alignment of the 6 published p47 GTPases (60).

The N- and C-terminal domains show low homology between the family members containing unique sequence patches. The core of the proteins is conserved showing stretches of identical sequence. The conserved GTP binding motifs are shown below the sequence.

The 6 published p47 GTPases show an identity between 25% and 55% which is clustered in the core of the proteins (Figure I4). The N-terminal and the C-terminal domains in contrast are rather divergent containing unique sequence patches with no similarity to other family members (60).

Nearly all family members are inducible by type II and to a minor extent by type I IFN in all cell-types tested so far including immune and non-immune cells (60, 92) (Cemali Bekpen, personal communication). Cinema appears to be an exception in this respect since it was not found to be IFN inducible in any cell-type tested so far (Christoph Rohde, personal communication) In general the basal expression of the p47 GTPases is low although exceptions to this rule are emerging. IIGP1 for example shows a high type I and type II IFN receptor independent basal expression level in liver which is rising

even further after infection with *Listeria monocytogenes* (Jia Zheng, personal communication).

Recently the crystal structure of IIGP1 has been determined (149) (Figure I5).

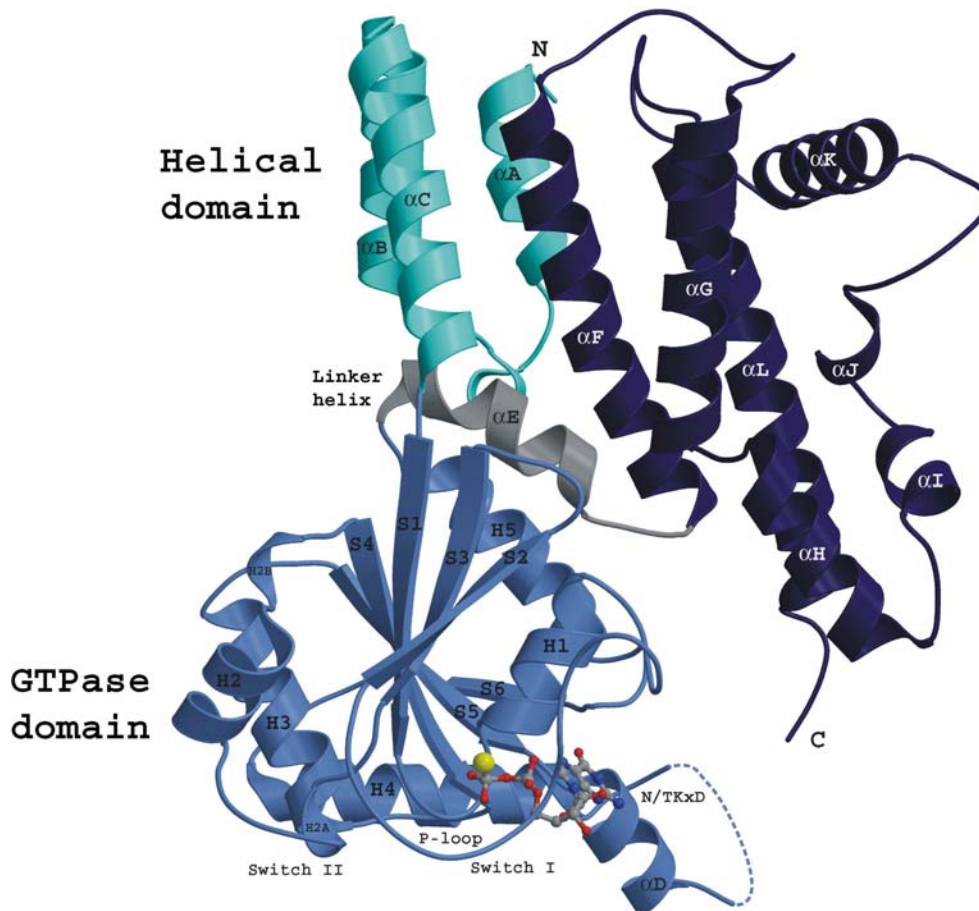


Figure I5: Crystal structure of IIGP1 in the GDP bound form (149).

The first 13 amino acids of IIGP1 are not resolved in the structure and therefore not shown. The N-terminal domain (cyan) is composed of three α helices and is followed by the GTP binding domain (light blue) which is similar to the G-domain of Ras. The helical C-terminal domain (dark blue) is connected to the G-domain by the linker helix α E (grey)

The GTP binding domain which is structurally similar to the canonical GTPase domain of Ras is preceded by an N-terminal domain composed of 3 α helices. The first 13 amino acids are not resolved and therefore missing in the structure. The GTPase domain is connected with the C-terminal helical domain by the linker helix α E. The C-terminal domain folds back to come into close proximity to the GTP binding domain. The N- and C-terminal helical domains correspond to the regions of low sequence similarity shown in the alignment. In particular the region around α K shows virtually no sequence similarity between the published p47 GTPases. However patches of sequence identity throughout the whole sequence and secondary structure predictions suggest that the overall structure of IIGP1 is representative for the whole family (149). IIGP1

crystallized as dimer with the two molecules making contact at the N-terminal and GTPase domain involving α B and H3. The dimer appears to be relevant for the properties of IIGP1 as mutations designed to disrupt dimer formation alter the enzymatic properties of IIGP1 (149).

IIGP1 behaves strikingly similar to dynamins regarding several key features of its enzymatic behaviour (150). IIGP1 binds nucleotides with a rather low affinity in the μ M range, shows cooperative activity and nucleotide dependent oligomerization. Upon hydrolysis the oligomers dissolve showing that multimerization is a reversible process (150).

Experiments with mice carrying targeted deletions of single genes of the p47 GTPase family have shown that the p47s are essential, non-redundant resistance factors against intracellular pathogens in the mouse (40, 94-95). Table 2 summarizes the results obtained with IGTP, IRG-47 and LRG-47 knock out mice (40).

Mouse	Intracellular protozoa			Intracellular bacteria			
	<i>T. gondii</i>	<i>L. major</i>	<i>T. cruzi</i>	<i>L. monocytogenes</i>	<i>S. typhimurium</i>	<i>M. tuberculosis</i>	<i>M. avium</i>
Wild-type	R	R	R	R	R	R	R
IFN- γ knockout	S (acute)	S	S	S	S	S	S
Igtp knockout	S (acute)	S	R	R	R	R	R
Lrg47 knockout	S (acute)	S	N.T.	S	S	S	S
Irg47 knockout	S (chronic)	N.T.	N.T.	R	R	R	N.T.

Table 2: The table, taken from a review by Taylor et al. (40), summarizes the phenotypes obtained with the shown knock out mice (S, sensitive; R; resistant).

LRG-47 and IGTP are required in the acute phase of infection. Mice carrying a targeted deletion of the LRG-47 gene die within 5 days after infection with *Listeria monocytogenes* (96) which is too fast for the adaptive immune system to mount an effective immune response. In view of the fact that IFN- γ induces at least several hundreds if not thousands of genes the profound loss of host resistance after deletion of single p47 GTPases is remarkable.

The resistance conferred by the p47 GTPases appears to be at least in some cases cell-autonomous. Astrocytes isolated from IGTP^{-/-} mice show no IFN- γ mediated growth inhibition of *Toxoplasma gondii* (151). The finding of Carlow et al. reporting that TGTP expressing HeLa cells are less susceptible to the cytopathic effects caused by VSV supports (152) the hypothesis of the p47 GTPases functioning in a cell-autonomous manner. In addition a small antiviral effect of IGTP against Coxsackievirus B3 when overexpressed in HeLa cells has been observed (69). However both antiviral effects were rather small and no *in vivo* experiments underline their significance.

The cell-biology and thus the mode of function of the p47 GTPases is totally unknown although recent experiments begin to shed light on their mechanism of resistance. IIGP1 has been reported to localize to the ER and Golgi complex in bone marrow derived macrophages (92) and recently a physical interaction of IIGP1 with Hook3, a Golgi localized microtubule binding protein, has been published but the biological significance of this interaction remains to be established (225). IGTP was shown to localize to the ER in mammary gland derived C127 cells in a GTP independent manner (93). The nature of their membrane attachment is unexplored but none of the p47 GTPases contains a signal peptide for co-translational translocation into the ER or any other predictable transmembrane segment. LRG-47 was co-purified with phagosomes from *Mycobacterium tuberculosis* infected macrophages (95). This co-purification was sensitive to BrefeldinA treatment and targeted deletion of the LRG-47 gene resulted in a reduced acidification and thus maturation of the *Mycobacterium* containing phagosome (95). Where LRG-47 localizes, how it interacts with membrane and how it is recruited to the phagosome is totally unknown. The initial observation that LRG-47 functions in phagosome maturation however might provide the key for the understanding how the p47 GTPases and in particular LRG-47 mediate resistance against such a variety of pathogens with completely different intracellular life styles (40).

1.10 Phagocytosis of microbes

Phagocytosis describes the process of uptake of large particles by cells (10, 153). Phagocytosis is of central importance for the function of innate immune cells such as neutrophils and macrophages but also non-immune cells are able to take up large particles as for example in the case of collagen-phagocytosis in fibroblasts (154). Phagocytosis is an extraordinarily complex process whereby upon particle recognition, cytoskeletal dynamics and membrane traffic are co-ordinately orchestrated involving several hundreds of proteins (10, 114, 155). The recognition and engulfment of the phagocytosed particle is accompanied by the activation of several signal transduction pathways (10).

The initial recognition of a microbe or particle is followed by the formation of a so called phagocytic cup marked with actin filaments and subsequent closure of the phagocytic cup to form the phagosome (112). Recently the ER has been reported to supply membranes for the formation of the vacuole at least in macrophages (156). The initial steps of phagosome formation involve the generation, modification and cleavage

of phosphoinositides by the action of enzymes such as PI3K and PLC (10, 114). After closure of the phagocytic cup the resulting phagosome matures by sequential interactions with the endosomal compartment of the cell to form the phagolysosome (157). Maturation includes the recruitment of the phagosome oxidase complex to the phagosomal membrane by Rac2 (113), acidification and activation of hydrolytic enzymes, recruitment of iNOS and other antimicrobial proteins such as NRAMP1 to the phagosomal membrane (10, 158-159). Nearly all steps of phagosome formation and maturation involve the action of GTP binding proteins of the Rho, Arf, Rab and dynamin family of GTPases (43, 157, 160-165).

During maturation the phagosomal lumen becomes very soon uninhabitable for the internalized pathogen. It is therefore not surprising that pathogens attempt to control phagosomal maturation and vesicular traffic by secretion of virulence factors interfering with host cell processes promoting maturation of the phagosome (97). The host in contrast tries to accelerate phagosomal maturation before the pathogen takes over control. IFN- γ strongly increases the speed with which phagosomes mature (166) for example by the induction of Rab5a (43, 167).

Not all intracellular pathogens are passively taken up by phagocytosis like *Mycobacterium tuberculosis* (168, 169) but actively induce their uptake (97, 170). Common to all mechanisms of entry into the host cell however is that the pathogen has to cross the plasma membrane and to control the fate of the resulting membrane bound compartment regardless of whether they reside in an intracellular vacuole (169, 171) or escape into the cytosol soon after uptake (172, 173).

1.11 The aim of this study

The introductory remarks outline above intended to emphasize the intimate relationship of intracellular pathogens and host cell membranes. The p47 are a battery of diverse cell-autonomous resistance factors and association with cellular membranes has been described for some members. The mechanism and dynamics of membrane association however is totally unexplored and is the subject of investigation in this work. The assumption is that information about the membrane association properties of the p47 GTPases reveals an essential part of their cell-biology in order to get further insights how the p47 GTPases contribute to host resistance.

Therefore the p47 GTPases LRG-47 and IIGP1 were analyzed in detail regarding their membrane association properties. LRG-47 is until now by far the most potent resistance

factor among the p47 GTPases whereas the biochemical characteristics of IIGP1 have been thoroughly investigated. This information is used to design and interpret the experiments shown in this work. The results obtained for LRG-47 and IIGP1 are extrapolated to other family members and similarities and differences are discussed in the context of intracellular defence.

2. Material and Methods

2.1 Reagents and Cells

2.1.1 Chemicals, Reagents and Accessories

All chemicals were purchased from Aldrich (Steinheim), Amersham-Pharmacia (Freiburg), Applichem (Darmstadt), Baker (Deventer, Netherlands), Boehringer Mannheim (Mannheim), Fluka (Neu-Ulm), GERBU (Gaiberg), Merck (Darmstadt), Pharma-Waldhof (Düsseldorf), Qiagen (Hilden), Riedel de Haen (Seelze), Roth (Karlsruhe), Serva (Heidelberg), Sigma-Aldrich (Deisenhofen) or ICN biochemicals, Oxoid, (Hampshire UK). DNA size standards from Gibco-BRL (Eggenstein), electrophoresis chambers from FMC Bioproducts (Rockland Maine US), developing and fixing solutions for Western Blot detection from Amersham Pharmacia (Freiburg), Luminol from Sigma Aldrich (Deisenhofen), Coumaric acid from Fluka (Neu-Ulm) and “Complete Mini” protease inhibitor cocktail from Boehringer (Ingelheim). Deionised and sterile water (Seral™) was used for all the buffers and solutions, Ultra pure water derived from Beta 75/delta UV/UF from USF Seral Reinstwassersysteme GmbH, (Baumbach) equipped with UV (185/254nm) and ultrafiltration (5000 kd cut off), or from Milli-Q-Synthesis (Millipore).

2.1.2 Equipment

Centrifuges used were: Biofuge 13, Heraeus; Sigma 204; Sigma 3K10; Labofuge 400R, Heraeus; Sorvall RC-5B, Du Pont instruments; Optima TLX Ultracentrifuge, Beckmann. BioRAD Gel dryer, Model-583; BioRad Power pack 300 or 3000; Gel Electrophoresis Chamber, Cambridge electrophoresis; Biorad Mini Protean II; PTC-100, MJ Research Inc.; Centrifuge tubes 15ml, TPP Switzerland; 50ml Falcon, Becton Dickenson; Zeiss Axioplan II fluorescence microscope equipped with a Quantix cooled CCD camera and a Z-stepping device; Odyssey confocal laser scanning device.

2.1.3 Materials

Sterile filters FP 030/3 0,2 μm and ME 24 0,2 μm (Schleicher und Schüll, Dassel); Nitrocellulose transfer membrane PROTRAN (Schleicher und Schüll, Dassel); 3MM

Whatmann Paper (purchased via LaboMedic); 100 Sterican 0,50 x 16mm hypodermic needles (Braun AG, Melsungen); 0.2µm and 0.45µm sterile filters (Schleicher und Schuell, Dassel); X-OMAT LS and AR X-ray films, Kodak.

All plastic ware for cell culture was from Sarstedt (Nümbrecht) or Greiner (Solingen)

2.1.4 Enzymes/Proteins

Restriction Enzymes were purchased from New England Biolabs (Bad Schwalbach); “Complete Mini” protease inhibitor cocktail from Boehringer (Ingelheim); *Pyrococcus furiosus* (Pfu) DNA Polymerase (Promega, Mannheim); T4 DNA ligase (New England Biolabs); RNase A (Sigma); shrimp alkaline phosphatase (SAP) (USB, Amersham); 1Kb ladder for agarose gels (Gibco); rainbow molecular weight marker precision protein standardsTM (Biorad); wide range protein standard marker (Sigma, Deisenhofen)

2.1.5 Kits

Plasmid Maxi and Midi kit (Qiagen, Hilden),
Terminator-cycle Sequencing kit version 3 (ABI),
QuikChangeTM Site directed mutagenesis kit (Stratagen),
Rapid PCR product purification Kit (Boehringer, Ingelheim),

2.1.6 Vectors

pGW1H (British Biotech, Oxford, England),
pGEX-4T-2 (Amersham Pharmacia, Freiburg),
pEGFP-C3 (Clontech),
pEGFP-N3 (Clontech),

2.1.7 Cell lines

RAW 264.7 (ATCC TIB-71), L929 mouse fibroblasts (CCL-1), mouse hepatocytes derived TIB-75 cells (ATCC TIB-75) (174)) and B6m29 cells (175) derived from a p53^{-/-} C57BL/6J mouse were cultured in IMDM supplemented with 10% FCS (Sigma, Deisenhofen), 2 mM L-Glutamine (Gibco BRL, Eggenstein), 1 mM sodium pyruvate (ICN, Eschwege), 100 U/ml penicillin (Gibco BRL) and 100 µg/ml streptomycin (Gibco

BRL). Peritoneal macrophages were isolated from the peritoneal cavity of CB20 mice and cultured in 6-well plates with coverslips. Cells were grown in IMDM and washed several times to remove non-adherent cells over a period of 36-48h before experiments.

2.1.8 Media

Luria Bertani (LB) medium

10g bacto tryptone, 5g yeast extract, 10g NaCl, distilled water 1l

LB plate medium

10g bacto tryptone, 5g yeast extract, 10g NaCl, 15g agar, distilled water 1l

IMDM (Iscove's Modified Dulbecco's Medium) Gibco BRL, Eggenstein supplemented with: 10% FCS, 2 mM 1-glutamine, 1 mM sodium pyruvate, 100 U/ml penicillin, 100 µg/ml streptomycin, 1x non-essential amino acids (Gibco BRL).

DMEM (Dulbecoo's Modified Eagle Medium), Gibco BRL, Eggenstein supplemented with: 10% FCS, 2 mM 1-glutamine, 1 mM sodium pyruvate, 100 U/ml penicillin, 100 µg/ml streptomycin, 1x non-essential amino acids (Gibco BRL).

2.1.9 Bacterial strains

Escherichia coli XL1-Blue: recA1, end A1, gyrA96, thi-1, hsdR17, supE44, relA1, lac, [F', pro AB, lacI^qZΔM15, Tn10 (Tet^r)]

Escherichia coli DH5α: 80dlacZΔM15, recA1, endA1, gyrA96, thi-1, hsdR17 (r_B⁻, m_B⁺), supE44, relA1, deoR, Δ(lacZYA-argF)U169

Escherichia coli BL-21: *E. coli* B, F⁻, omp T, hsd S (r_B⁻ m_B⁻), gal, dcm

Salmonella typhimurium strain SL1344 (Hoiseh and Stocker 1981)

2.1.10 Serological reagents

Primary antibodies and antisera:

NAME	IMMUNOGEN	SPECIES	CONCENTRATION	DILUTION	ORIGIN
1D4B	mouse LAMP-1	rat monoclonal		IB: 1:100 IF: 1:1000	DSHB, University of Iowa
α giantin	human giantin	mouse monoclonal		IF: 1:1000	Hans Peter Hauri, Basel (176)
α IGTP clone 7	mouse IGTP aa 283-423	mouse monoclonal	0.25 μ g/ μ l	IB: 1:5000 IF: 1:250	BD Transduction Laboratories
α MII	mouse α mannosidase II	rabbit polyclonal		IF: 1:100	Paul Slusarewicz via Albert Haas, Bonn
α CI-M6PR	CI-M6PR	rabbit polyclonal		IF: 1:100	Gus Lienhard via Albert Haas, Bonn (177)
M2	Flag-epitope DTKDDDDK	mouse monoclonal	4.9mg/ml	IB 1:1000 IF 1:4000	Sigma Aldrich
2078	mouse IRG-47 peptides CKTPYQHPKY PKVIF and CDAKHLRKI ETVNVA	rabbit polyclonal		IB: 1:1000	Eurogentec double X programme
N20 (sc-894)	N-terminal peptide of human Caveolin- 1	rabbit-polyclonal	0.2 μ g/ μ l	IB: 1:1000 IF: 1:100	Santa Cruz
L115	mouse LRG-47 peptides QTGSSRLPEVS RSTE and NESLKNSLGV RDDD	rabbit-polyclonal		IB: 1:1000	Eurogentec double X programme
A19 (sc-11075)	N-terminal peptide of mouse LRG-47	goat-polyclonal	0.2 μ g/ μ l	IB: 1:200 IF: 1:100	Santa Cruz
A20 (sc-11079)	N-terminal peptide of mouse TGTP	goat-polyclonal	0.2 μ g/ μ l	IB: 1:500 IF: 1:100	Santa Cruz
M14 (sc-11088)	C-terminal peptide of mouse GTPI	goat-polyclonal	0.2 μ g/ μ l	IB: 1:100	Santa Cruz
V9	pig eye lens vimentin	mouse monoclonal		IF: 1:40	Sigma
SPA-865	N-terminal peptide of canine calnexin	rabbit-polyclonal		IB: 1:10000 IF: 1:200	StessGen

α ERP60	ERP60	rabbit-polyclonal		IF: 1:1000	Tom Wileman, Pirbright
α Rab6	human Rab6	rabbit-polyclonal		IF: 1:100	Bruno Goud, Paris
G65120	C-terminus of Rat-GM130	mouse monoclonal		IB: 1:100 IF 1:1000	BD Transduction Laboratories
165	recombinant mouse IIGP1	rabbit polyclonal		IB: 1:25000 IF: 1:8000	
10E7	recombinant mouse IIGP1	mouse- monoclonal	1-3 μ g/ μ l	IB: 1:1000 IF: 1:200	Jens Zerrahn, Berlin
10D7	recombinant mouse IIGP1	mouse- monoclonal	1-3 μ g/ μ l	IB: 1:1000	Jens Zerrahn, Berlin
C15 (sc-6414)	peptide mapping to the C- terminus of human EEA1	goat-polyclonal	0.2 μ g/ μ l	IB: 1:100	Santa Cruz

Secondary antibodies and antisera

goat anti-mouse Alexa 546/488, goat anti-rabbit Alexa 546/488, donkey anti-goat Alexa 546/488, donkey anti-mouse Alexa 488, donkey anti-rabbit Alexa 488, donkey anti-rat Alexa 488, goat anti-mouse Alexa 680, goat anti-rabbit Alexa 680, goat anti-rat Alexa 680, donkey anti-goat Alexa 680 (all Molecular Probes), donkey anti-rabbit HRP (Amersham), donkey anti-goat HRP (Santa Cruz), goat anti-mouse HRP (Amersham), goat anti-mouse IRDye 800, goat anti-rabbit IRDye 800, goat anti-rat IRDye 800 (all Rockland Immunochemicals Inc.).

2.2 Molecular Biology

All plasmids and constructs were amplified, cloned or propagated using protocols adapted from Sambrook, J., Fritsch, E.F., and Maniatis, T., Vol. 1, 2, 3 (1989), or from the cited references.

2.2.1 Agarose gel electrophoresis

DNA was analyzed by agarose gel electrophoresis (1x TAE; 0.04 M Tris, 0.5 mM EDTA, pH adjusted to 7.5 with acetic acid) The DNA was stained with ethidium bromide (0.3 μ g/ml), a fluorescent dye which intercalates between nucleotide bases, and the migration of the DNA molecules was visualized by using bromophenol blue.

2.2.2 Generation of p47 GTPase expression constructs

The coding regions of p47 GTPases were amplified either by PCR from full length cDNAs described in (60) from IFN- γ (1000U/ml) stimulated mouse embryonic fibroblasts (MEFs) according to standard procedures using Pfu-polymerase (Promega) and primers ordered from Invitrogen. Restriction enzymes were ordered from “New England Biolabs”.

Primers used were

IIGP1 forward 5'-CCCCCCCCGTCGACCACCATGGGTCAGCTGTTCTCTTC-3',

IIGP1 reverse 5'-CCCCCCCCGTCGACCTAGTTTCTTAAACATATCTCTTTAAG-3',

IIGP1 aa 1-287 reverse 5'-CCCCCCCCGTCGACCTAAAAATCCTTCCAGCCAAATCCTC-3',

LRG-47 forward 5'-CCCCCCCCGTCGACCACCATGAAACCATCACACAGTTCC-3',

LRG-47 reverse 5'-CCCCCCCCGTCGACCACCTAGATCTGCGGAGGGAAG-3',

LRG-47 aa 1-285 reverse 5'-CCCCCCCCGTCGACCTACAGGATTTTCTCTAGGATG-3'

introducing a Sall site (underlined) at both ends. The PCR products were cloned into the Sall site of pGW1H (British Biotech).

IGTP forward: 5'-CCCCCCCCGTCGACCACCATGGATTAGTCACAAAGTTGCC-3',

IGTP reverse: 3'-CCCCCCCCGTCGACTCAGTGAATTCGGGAGGGAG-3',

The PCR fragments were cut with Sall and cloned into pEGFP-C3 (Clontech) expression vector.

Primers to generate a C-terminal Flag tagged version of TGTP were

TGTP-Flag 5 5'-CCCCCCCCGTCGACCTAACTACTTAGTGAGC-3',

TGTP-Flag 3' 5'-

CCCCCCCCGAATTCCTACTGTGCATCGTCGTCCTTGTAAATCACCGGATCCAGCTTCCCAGTACTCGGGGGG-3',

The PCR products were Sall and EcoRI cut and cloned into the appropriately cut pGW1H expression vector.

Primers used to clone N-terminal fragments of IIGP1 and LRG-47 into pEGFP-N3 (Clontech) were

pGW1H 5' 5'-CTTTCCATGGGTCTTTTCTG-3',

IIGP1 aa 1-69 reverse 5'-CCCCCCCCGTCGACCACACTACTATCGATTCTTTAATG-3',

LRG-47 aa 1-76 reverse 5'-CCCCCCCCGTCGACTGGAATCTGGGACAATGTTGC-3'.

Fragments were amplified from the respective pGW1H constructs, cut with Sall, gel purified and cloned into pEGFP-N3.

Primers used to clone the G-domain, the C-terminal domain and C-terminal fragments of LRG-47 and IIGP1 into pGW1H were

IIGP1 G-domain 5': 5'-CCCCCCCCGTCGACCACCATGAGTGTGCTCAATGTTGCTGTC-3',

IIGP1 G-Domain 3' Flag:

5'-CCCCCCCCGTCGACCTAACCTTATCGTCATCGTCCTTGTAAATCAGGGAGGTCACCTATCAGCTTG-3',

IIGP C-domain 5': 5'-CCCCCCCCGTCGACCACCATGGCTGACCTAGTGAATATCATC-3',

LRG-47 G-domain 5': 5'-CCCCCCCCGTCGACCACCATGATTCCAGTGAGCATCTTTGTG-3',

LRG-47 G-domain 3': 5'-

CCCCCCCCGTCGACTAGACCCTTATCGTCATCGTCCTTGTAAATCGGAGAGATCTTTATGAAGTGTG-3',

LRG-47 C-domain 5': 5'-CCCCCCCCGTCGACCACCATGAAGAATTCTCTCGGTGTCAG-3',

LRG-47 alphaH 5': 5'-CCCCCCCCGTCGACCACCATGTTTGGTGTAGATGACGAATCAG-3',

LRG-47 alphaI 5': 5'-CCCCCCCCGTCGACCACCATGGGGACAGTAGTCATGGAG-3',

LRG-47 alphaJ 5': 5'-CCCCCCCCGTCGACCACCATGAAGTCCAAAACCTTTATAC-3',

LRG-47 alphaK 5': 5'-CCCCCCCCGTCGACCACCATGAAACTGAGGCTATGACATGTG-3',

LRG-47 alphaL 5': 5'-CCCCCCCCGTCGACCACCATGTGTTAAAGACGCTTGAGACATAAAC-3',

PCR products were cut with Sall and ligated to Sall cut pGW1H in case of the G-domain constructs and into pEGFP-C3 in case of the C-terminal domain constructs.

Primers used to clone α K fragments of LRG-47, GTPI and IGTP into pEGFP-N3 (Clontech) were

LRG-47 α K 5': 5'-CCCCCCCCGTCGACCACCATGAACTGAAGGCTGATGACATG-3',

LRG-47 α K 3': 5'-CCCCCCCCGTCGACCTAGCAGCATAACGCATGGGAGAAATC-3',

IGTP α K 5': 5'-CCCCCCCCGTCGACCACCATGGATGTGTTTGCCGTGAAC-3',

IGTP α K 3': 5'-CCCCCCCCGTCGACCTAGCGGGTGACGACGTTCCACAAG-3',

GTPI α K 5': 5'-CCCCCCCCGTCGACCACCATGGTGTGCTCGGTTGATACG-3',

GTPI α K 3': 5'-CCCCCCCCGTCGACCTAATGAGAGGTAAAGCAGCACTTC-3',

Fragments were amplified from the respective pGW1H constructs, cut with Sall, gel purified and cloned into pEGFP-C3.

Mutation into the ORFs of LRG-47 and IIGP1 were introduced according to the "QuikChange" site directed mutagenesis kit (Stratagene) protocol using the respective pGW1H and pEGFP-C3 constructs as template. Primers used were

LRG-47 S90N forward: 5'-GGGACTCTGGCAATGGCATGAATTCTTTCATCAATGCACTTCG-3',

LRG-47 S90N reverse: 5'-CGAAGTGCATTGATGAAAGAATTCATGCCATTGCCAGAGTCCC-3',

LRG-47 ins 359E forward: 5'-ATGACATGTGCAATTGAAGTGAATGCATTCTTC-3',

LRG-47 ins 359E reverse: 5'-GAAGAATCGATTCACTTCAATTGCACATGTCAT-3',

LRG-47 ins 362E forward: 5'-GCAATTGTGAATGCAGAATTCTCCGTTTGTG-3',

LRG-47 ins 362E reverse: 5'-CAACAAACGGAAGAATTCTGCATTCACAATTGC-3',

LRG-47 ins 362, 367E forward: 5'-

GCAATTGTGAATGCAGAATTCTCCGTTTGGAAATTGAGATTCTCCCA-3',

LRG-47 ins 362, 367E reverse: 5'-

TGGGAGAAATCTCAATTCCAAACGGAAGAAATTCTGCATTACAATTGC-3',

IIGP1 G76, 81V forward: 5'-GTTGCTGTACCCGTGGAGACGGGATCAGTGAAGTCCAGCTTC-3',

IIGP1 G76, 81V reverse: 5'-GAAGCTGGACTTCACTGATCCCGTCTCCACGGTGACAGCAAC-3',

IIGP1 G2A forward: 5'-GAGTCGACCACCATGGCTCAGCTGTTCTCTTCA-3',

IIGP1 G2A reverse: 5'-TGTAGAGAACAGCTGAGCCAGGGTGGTCGACTC-3',

TGTP G63, 68V forward: 5'-CATAGCTGTGACAGTGGAAACAGGCGCAGTGAAGTCCACTTTC-3',

TGTP G63, 68V reverse: 5'-GAAAGTGGACTTCACTGCGCCTGTTTCCACTGTCACAGCTATG-3',

All constructs were verified by sequencing.

2.2.3 Cloning of PCR amplification products

Amplified PCR products were purified using the rapid PCR purification Kit (Boehringer) and eluted with 100 µl 10mM Tris, pH 8.5. DNA yield was monitored by agarose gel electrophoresis and DNA fragments were digested with the appropriate restriction endonuclease (New England Biolabs) according to the suppliers' protocol. Restriction enzymes were used at a 5-10 fold over digestion. Following restriction, DNA fragments were again column purified using the rapid PCR purification Kit (Boehringer) and DNA yield was monitored by agarose gel electrophoresis.

2.2.4 Purification of DNA fragments from agarose gels

DNA Fragments were loaded on agarose gels of the suitable percentage after incubation with appropriate restriction endonucleases. After proper separation of the fragments DNA was visualized under a low energy UV source and cut out of the gel using a clean blade. DNA fragments were eluted from the gel with the rapid PCR purification Kit (Boehringer) according to the manufactures protocol. Purity and yield of the DNA was determined by agarose gel electrophoresis and UV spectroscopy.

2.2.5 Ligation

The appropriate cloning vector was cut with the respective restriction enzyme(s) (10U/1µg DNA) for 1h under according to the restriction enzyme suppliers' protocol. After the first hour the same amount of restriction enzyme and 0.1U of shrimp alkaline

phosphatase were added to the reaction followed by 1.5h incubation. Following restriction DNA fragments were column purified using the rapid PCR purification Kit (Boehringer) and DNA yield was monitored by agarose gel electrophoresis. Vector and the appropriate cut insert were mixed at a ratio of 1:3 and ligated with T4-DNA ligase in a total volume of 10 μ l at 16⁰C over night according to the manufactures protocol. As control the same reaction without insert was carried out which should not yield any colonies after transformation into competent DH5 α .

2.2.6 Preparation of competent cells

A single colony from a particular *E. coli* strain was grown overnight in 2 ml LB medium with 0.02 M MgSO₄, 0.01 M KCl with vigorous shaking (~300 rpm). It was diluted 1:10 into fresh medium with the same constituents and grown for 90', at 37°C to an OD₆₀₀ of 0.45. Cultures were incubated on ice for 10 min after which the cells were pelleted by centrifugation at 6000 rpm, 4°C for 5'. Cells were resuspended in TFB I (30 ml/100 ml culture), incubated 5' on ice, pelleted again by centrifugation at 6000 rpm, 4°C for 5' and finally resuspended in TFB II (4 ml per 100 ml culture). 100 μ l aliquots of the competent bacteria were frozen at -80°C.

Composition of the buffers:

TFB I (30 mM KOAc, 50 mM MnCl₂, 100 mM RbCl₂, 10 mM CaCl₂, 15% w/v glycerin, pH 5.8)

TFBII (10 mM MOPS, pH 7.5, 75 mM CaCl₂, 100 mM RbCl₂, 15% w/v glycerin)

Both the solutions were sterilized and stored at 4°C.

2.2.7 Transformation of competent bacteria

100 μ l of competent bacteria were thawed on ice and gently mixed 3-4 times. 5 μ l of the ligation reaction was added to the cells followed by incubation for 20' on ice. Cells were then heat-shocked for 45'' at 42⁰C followed by a further incubation on ice for 2'. Antibiotic free LB medium was added to a total volume of 1ml and cells were rolled at 37⁰C for 1h. The culture was spun at 9000 rpm in a table top centrifuge for 2' and 800 μ l of the supernatant was removed. The cell pellet was resuspended in the 200 μ l medium left over in the 1.5 ml reaction tube and plated on a LB agar plate supplemented with the appropriate antibiotics.

2.2.8 Plasmid isolation

For screening a large number cultures for clones containing the desired insert 4ml LB cultures with the appropriate antibiotics were inoculated with single colonies picked from a ligation plate and grown over night at 37⁰C, 250 rpm. All following steps were performed at room temperature. 1.5ml of the cultures was transferred into a 1.5ml reaction tube and pelleted by centrifugation at 23000g for 5'. The supernatant was discarded and pellet resuspended in 100µl P1 (50 mM Tris, pH 8.0, 10 mM EDTA, 100µg/ml RNase A). After addition of 100µl P2 (200mM NaOH, 1% SDS) the reaction was gently mixed and incubated for 5'. 140µl of P3 (3M potassium acetate, pH 5.5) was added and the reaction was spun for 15' at 23000g. The supernatant (~340 µl) was transferred into a new tube and 700µl of 100% EtOH was added. After mixing the reaction was spun for 15' at 23000g and the supernatant was removed. The pellet was washed by addition of 700µl of 70% EtOH and spun at 23.000g. After removal of the supernatant the pellet was air dried and resuspended in 50 µl 10mM Tris pH 8.0. 5µl of the plasmid preparation was cut with the appropriate restriction enzyme(s) in a total volume of 50 µl for 1h and 10µl of the reactions were subjected to agarose gel electrophoresis to identify insert containing clones.

For preparation of large amounts of plasmid the Qiagen Midi and Maxi Plasmid Preparation Kits were used according to the manufactures instructions.

2.2.9 Determination of the concentration of DNA

The concentration of DNA was measured using a spectrophotometer at 260 nm. The purity of the DNA solution was determined using the ratio of OD readings at 260 nm and 280 nm. Pure preparations of DNA have an OD₂₆₀/OD₂₈₀ ratio of 1.8. The concentration was calculated according to the following equation. $c = A_{260} \times 50 \mu\text{g/ml} \times \text{dilution factor}$.

2.2.10 Site directed mutagenesis

Site directed mutagenesis was carried out using the using a modified protocol supplied with "QuikChangeTM XL Site-Directed Mutagenesis" Kit from Stratagene. The amplification was carried out using 20ng plasmid as template, 125ng of the sense and antisense oligonucleotide as primers and 2.5U of Pfu-polymerase (Promega) in a total volume of 50 µl. The following program was used: 1. 30'', 95⁰C; 2. 30'', 95⁰C; 1',

55°C; 13'', 72°C (back to step 2 15 times); 15', 72°C. The annealing temperature was adjusted depending on the nature of the mutation introduced into the plasmid (QuikChange™ XL Site-Directed Mutagenesis protocol). After amplification 1 µl DpnI (20U, New England Biolabs) was added to the reaction and incubated for 1.5h at 37°C. 20 µl of the reaction was used to transform 200µl competent DH5α. As control the whole procedure was carried out without addition of Pfu-polymerase. Ideally no colonies are found on the final LB agar plate for the control reaction.

2.2.11 DNA Sequencing

All constructs generated were verified by sequencing. DNA was sequenced using the *ABI Prism^R BigDyeTM* Terminator Cycle Sequencing Ready Reaction Kit (PE Applied Biosystems), using fluorescently labeled dideoxynucleotides based on the dideoxy-chain termination method by Sanger et al. 1977. Template DNA (0.5 µg), the respective primer (10 pmole) and 2 µl *Big DyeTM* terminator ready reaction mix (ABI) were combined in a total volume of 10 µl and the sequencing reaction was carried out as follows :

5', 96°C; 25x (30'', 96°C; 15'' 50°C; 4', 60°C).

The DNA was precipitated with 3M sodium acetate and 2 volumes of 100% ethanol (Maniatis *et al.* 1989), spun at 23000g , 4°C for 15 min. The pellet was washed with 70% ethanol and finally air dried. Sequencing was done on an automated sequencer (ABI 373A) by Rita Lange.

2.3 Cell Biology

2.3.1 Transfections

Cells were transiently transfected with Fugene 6 (Boehringer, Ingelheim) according to the manufacturer's protocol using a ratio of 1µg DNA/3µl FuGene6 reagent and 1µg DNA per well of a 6 well plate, 2µg DNA for 4cm plates and 8µg for 10cm plates.

2.3.2 Bead uptake experiments

500 μ l 2 μ m carboxylated latex beads (Polysciences) were coated with collagen as follows. Beads were washed 2x with 1ml 0.1 M NaHCO₃ pH 9.6 followed by 3 washes with 1ml 0.02 M phosphate buffer pH 4.5. The beads were resuspended in 675 μ l phosphate buffer pH 4.5 and 675 μ l 2% carbodiimide (Sigma) in phosphate buffer pH 4.5 was added. After an incubation of 4h on a rotator at room temperature the beads were washed 3 times with 1ml phosphate buffer pH 4.5, resuspended in 1.2 ml borate buffer pH 8.5 containing 500 μ g collagen (type I from rat tail (Sigma)) and incubated over-night at room temperature on a rotator. 50 μ l 0.25 M ethanolamine was added and the beads were incubated for another 30 minutes. The beads were pelleted and resuspended in borate buffer pH 8.5, 10 mg/ml BSA (fraction V, Roth), and incubated for 30 minutes. The beads were washed with 1ml borate buffer pH 8.5, 10 mg/ml BSA and stored in 500 μ l 0.02 M phosphate buffer pH 7.4, 0.15 M NaCl, 1 % BSA, 5% glycerol, 0.1% NaN₃.

L929 cells were grown on coverslips and induced with 200U/ml IFN- γ . Twenty hours after induction the collagen coated beads were added and the cells were incubated for an additional 4h. Finally the cells were fixed with 3% paraformaldehyde (PFA) for 20 minutes at room temperature.

3x 10⁷ RAW 264.7 cells were induced with 200U/ml IFN- γ for 48h and incubated with 2 μ m latex beads not coated with collagen (Polyscience) diluted 1:1000 in IMDM for 30'-4h.

2.3.3 Transferrin uptake experiments

Cells were grown on coverslips and serum starved for 1h. Alexa-546 labeled human Transferrin (Molecular Probes) was diluted 1:1000 (to a final concentration of 5 μ g/ml) into culture medium not supplemented with FCS and cells were incubated at 37⁰C, 7.5 CO₂ for 5' to 1h. Finally cells were fixed with 3% PFA in PBS for 20' at room temperature followed by four washes with PBS.

2.3.4 Indirect immunofluorescence

All steps were performed at room temperature unless otherwise stated. Cells were grown on coverslips, fixed with 3% paraformaldehyde (PFA) in PBS for 20' and subsequently washed 4 times with PBS. Cells were permeabilized with 0.1% saponin in PBS

(washing buffer) followed by a blocking step with 0.1% saponin, 3% BSA (fraction V) in PBS (blocking buffer) for 1h. Incubation with primary antibodies (diluted in blocking buffer) was done in a humid chamber either at room temperature or at 4⁰C for periods ranging from 1h to over night. The incubation was followed by three washing steps with 3-5 ml washing buffer for 5'. Incubation with secondary antibodies was done as described for primary antibodies with an incubation time of 30' followed by three washes as described above. Coverslips were mounted on slides with Mowiol, sealed with nail polish and cleaned with deionized water. DAPI used to stain DNA (300nM) and Alexa-labeled phalloidin (used according to the protocol supplied by Molecular Probes) used to stain F-actin was added to the secondary antibody solutions. Nocodazole (Sigma, Deisenhofen) was used at a concentration of 100µg/ml.

2.3.5 Image acquisition and processing

Images were taken with a Zeiss Axioplan II fluorescence microscope equipped with a cooled CCD camera (Quantix) using the Metamorph software. The Metamorph software (version 4.5r3, Universal Imaging Corp.) was also used for acquisition of Z-series, 3D reconstruction, 2D deconvolution and general processing of raw images. 3D deconvolution was performed using the Auto Deblur software (version 6.001, AutoQuant Imaging Inc.). Overlays of fluorescence images with phasecontrast images were created using Adobe Photoshop version 5.5.

2.3.6 Triton X-114 partitioning assay

L929 cells were lysed in PBS, 1% Triton X-114 (Sigma) including “complete mini” protease inhibitors (Roche) 24h after IFN- γ induction (200U/ml) and 48h after transfection for 1h on ice. Lysates were centrifuged for 15' at 3000g at 4°C to remove nuclei. Supernatants were incubated for 5' at room temperature and subsequently centrifuged for 1' at 23.000g at room temperature. The aqueous phase was transferred into a new tube and washed by an additional centrifugation step. The detergent phase was washed by addition of PBS followed by an additional centrifugation step and finally brought to the same volume as the aqueous phase by addition of PBS. Equal amounts were loaded on a 12% polyacrylamide gel.

The sequential Triton X-114 partitioning assay was conducted as follows:

L929 cells growing on a 10 cm plate were induced with 200U/ml IFN- γ and harvested 24h later with a cell scraper (cells were 80% confluent corresponding to $\sim 6 \times 10^6$ cells). Cells were washed with PBS, resuspended in 1ml ice cold 1% Triton X-114 and incubated for 1h on ice. Cells were spun at 3000g at 4⁰C for 15'. The supernatant was transferred into a new tube and incubated at room temperature for 5' to induce phase separation. After the solution turned cloudy the tube was spun for 1' with 23.000g at room temperature. The aqueous phase ($\sim 800 \mu\text{l}$) was transferred into new tube and the detergent phase was adjusted to the same volume as the aqueous phase and stored on ice. 100 μl of the aqueous phase was taken and stored on ice. The remaining 700 μl of the aqueous phase were adjusted to 1% Triton X-114 by addition of an appropriate volume of ice cold 10% Triton X-114 ($\sim 77 \mu\text{l}$). The tube was incubated on ice until the solution turned clear and was again shifted to room temperature to induce phase separation. The following steps are described above. The procedure was repeated 4 times. The volume of the aqueous and detergent phases progressively decreased with increasing number of repetitions. Equal volumes (15 μl) were subjected Western Blotting using the anti-IIGP1 165 antiserum.

2.3.7 Membrane extraction experiments

IFN- γ induced or transfected L929 cells were lysed for 1h in hypotonic buffer (10mM HEPES, 5.1mM MgCl₂, pH7.5) on ice. Cells were disrupted by passing the lysates 10 times through a 25G needle. Nuclei were removed by centrifugation at 1000g, 4⁰C for 5'. The supernatant was centrifuged at 100000g for 30' at 4⁰C and resulting supernatant was stored on ice as hypotonic supernatant. The membrane pellet was washed with hypotonic buffer and centrifuged for another 15'. The washed pellet was resuspended in hypotonic buffer, PBS, 1M NaCl, 100mM Na₂CO₃ pH 11.75, 2M Urea, 4M Urea, 6M Urea or 1% Triton X-100 in PBS respectively followed by incubation on a rotator at 4⁰C for 30'. Samples were again centrifuged at 100.000g for 30' at 4⁰C. Supernatants were stored on ice and the pellet was washed by addition of the respective buffer and centrifugation for 15' at 100000g at 4⁰C. Finally the pellets were resuspended in PBS, 0.5% SDS to the same volumes as the supernatants and equal volumes were loaded on 10%, 12% or 15% polyacrylamide gels and subjected to Western Blotting.

2.3.8 Preparation of artificial lipid vesicles

Recombinant IIGP1 was produced as previously described in (150). Liposomes were prepared from synthetic phosphatidylserine (1,2-Dioleoyl-sn-glycero-3-[phospho-L-serine] (Avanti)). Lipids dissolved in chloroform were dried under nitrogen and additionally in a rotatory evaporator to remove residual chloroform. The resulting lipid cake, hydrated by addition of HBS (HEPES buffered saline), was left undisturbed for 1h at room temperature and finally vortexed to resuspend the lipids. The lipid suspension was extruded 21 times through polycarbonate membranes with a pore size of 100 nm (Avestin). For co-sedimentation assays 0.25 mM phosphatidylserine lipids and 0.25 μ M IIGP1 in HBS were incubated for 30' at 37°C followed by centrifugation for 30' with 125.000g at 4°C. The samples were further processed as described for the cellular membranes.

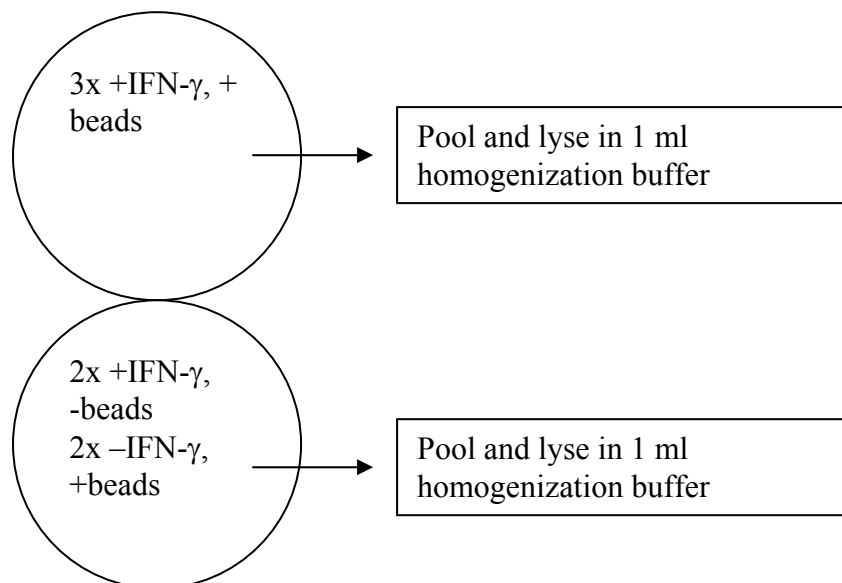
2.3.9 Western Blotting

After SDS-PAGE proteins were transferred to nitrocellulose membranes by electroblotting. The gel was placed in contact to a nitrocellulose transfer membrane, and was sandwiched between four sheets of 3 MM Whatmann paper, two porous pads, and two plastic supports on either side, soaked in a transfer buffer containing 25 mM Tris, 190 mM Glycine. The sandwich was then placed between platinum plate electrodes, with the nitrocellulose membrane facing the anode, and the transfer was carried out at RT for 1h with a current of 0.5V. Ponceau S staining was used to locate proteins (0.1% (w/v) Ponceau S (Sigma) in 5% (v/v) acetic acid) after Western Blotting. Membranes were blocked with PBS, 5% milk powder, 0.1% Tween 20 or Roche Western Blotting blocking reagent at room temperature for 1h or over night at 4°C. Antisera/antibodies were diluted in PBS, 5% FCS, 0.1% Tween 20 or PBS, 5% Roche blocking reagent. Bands were visualized with enhanced chemiluminescence (ECL) substrate or using the Odyssey system.

2.3.10 Isolation of phagosomes

Phagosomes were isolated according to the protocol described by Dejardins et al. (157). 2.5×10^6 RAW 264.7 cells were split on 7 15 cm culture plates. 48h later the cells on 5 plates were induced with 200U/ml IFN- γ . After 48h 2 μ m latex beads (Polysciences) were added to the cells at a concentration of 1 μ l beads per 2 ml medium with a total

amount of 15 ml per plate. No beads were added to two plates with IFN- γ induced cells. The cells were incubated for 4h under standard cell culture conditions, washed 3x with ice cold PBS, scraped into ice cold PBS, pelleted and washed for 5' with homogenization buffer (250mM sucrose, 3mM imidazole, pH 7,4 including "Complete Mini" protease inhibitors (Roche)). Cells from three IFN- γ induced culture plates plus beads (+/+) and two IFN- γ induced culture plates without beads and two uninduced culture plates plus beads (+/-, -/+) were pooled and resuspended in 1 ml homogenization buffer after 5' centrifugation at 500g, 4⁰C (summarized in the scheme below). Homogenization was done with a 2ml tight fitting Dounce Homogenizer until 90% of the cells were disrupted (100 strokes). Homogenization was monitored by light microscopy. Unbroken cells were pelleted by centrifugation for 5', 140g, 4⁰C. The cell homogenate was brought to 40% sucrose by addition of an equal amount of 62% sucrose. (All sucrose solutions were in 3mM imidazole, pH 7.4) Lysates were placed on top of 1ml 62% sucrose and overlaid with 2ml 35% sucrose, 2ml 25% sucrose and finally 2ml 10% sucrose. The gradient was spun for 1h, 4⁰C, 100000g in a SW41 rotor (Beckman) without deceleration. The 10%-25% interface was collected with a Pasteur pipette, diluted in 12 ml PBS and spun for 15', 40C, 40000g in a SW41 rotor to collect the phagosomes. The final pellet was resuspended in 200 μ l PBS, 0.5% SDS, complete mini protease inhibitors. 5 μ l of the lysates and 20 μ l of the isolated phagosomes were loaded on 7.5%-12% polyacrylamide gels.



2.3.11 Nucleotide agarose binding assay

L929 cells were induced with 200U/ml IFN- γ and 6×10^6 cells were lysed in 600 μ l 1% digitonin/ TBS, 3mM MgCl₂ for LRG-47 and 0.1% Triton X-100 in PBS for IIGP1 24h after induction. After incubation for 30' on ice cells were spun for 30' with 25000g at 4⁰C. In the meantime GMP, GDP and GTP agaroses were washed 3 times with TBS. 100 μ l of the GTP agarose was used for each sample. The volume of the GMP and GDP agarose was adjusted in order to include the same number of cross-linked guanine nucleotide molecules per experiment. After centrifugation the cell lysate was equally divided into 3 aliquots and incubated with GMP, GDP and GTP agarose, respectively, for 30' at 4⁰C on a rotator. Samples were spun for 30' with 25000g at 4⁰C and pellets were washed 4x with 1ml TBS, 3mM MgCl₂. Pellets were resuspended in 100 μ l Laemmli buffer, shaken for 15' at room temperature and spun for 5' at 23000g at room temperature. The supernatant was transferred into a new tube, boiled and 25 μ l were loaded on a 12% (LRG-47) polyacrylamide gel. LRG-47 was detected by Western Blotting using the anti-LRG-47 A19 antiserum, IIGP1 was detected using the anti-IIGP1 165 antiserum.

2.3.12 Preparation of infectious *Salmonella typhimurium*

A 2ml LB culture supplemented with 30 μ g/ml streptomycin was inoculated with a single colony of *Salmonella typhimurium* growing on a LB plate. The culture was incubated for 16h at 37⁰C with 225 rpm. The LB culture was diluted 1:100 into 30ml IMDM cell culture medium containing 30 μ g/ml streptomycin and incubated 16h at 37⁰C, 7.5% CO₂ without shaking. The culture was transferred into a 50 ml Falcon tube and spun at 8800g for 10' at room temperature. The bacterial pellet was resuspended in 10 ml IMDM. 250 μ l were used for infection of B6m29 cells per well of a 6 well plate. The experiments with *Salmonella typhimurium* were conducted under the supervision of Dr. Christine Kocks.

2.3.13 Infection of B6m26 cells with *Salmonella typhimurium*

10⁴ B6m29 cells were split on heat sterilized cover slips placed in 6 well plates and induced with 100U/ml IFN- γ after 24h. 48h later the medium was exchanged for 2ml per IMDM plus 250 μ l of the infectious *Salmonella typhimurium*. Cells were incubated with the bacteria for 30' under the standard cell culture conditions described above,

thoroughly washed to remove extracellular bacteria and incubated for additional 2h in IMDM supplemented with 100 µg/ml gentamycin (Gibco BRL). After 2h cells were fixed with 3% PFA and stained with anti-IIGP1 165 antiserum and DAPI, anti-IGTP antibody and DAPI or anti-LAMP1 1D4B antibody and DAPI. The experiments with *Salmonella typhimurium* were conducted under the supervision of Dr. Christine Kocks.

2.3.14 *In vitro* passage of *Toxoplasma gondii*

Toxoplasma gondii, strain ME49, was passaged *in vitro* in HS27 human foreskin fibroblasts. Under these conditions the parasite mainly replicates in the tachyzoite stage. Confluent fibroblast monolayers in 25 cm² flasks were inoculated with 1x10⁶ parasites in IMDM, 5% FCS, 2mM L-Glutamin, 50µM 2-mercaptoethanol. Parasites actively invade the host cells, replicate intracellularly and egress from their host cells approximately 3 days later. At this time point extracellular parasites were harvested with the supernatant and purified from host cell debris by differential centrifugation. To this end, the supernatant was first centrifuged for 5' at 50g (room temperature) and a second time at 1500g for 15'. Parasites were resuspended in culture medium, counted in a Neubauer chamber and immediately used for inoculation of host cells. The *In vitro* passage of *Toxoplasma gondii* was conducted by Dr. Gaby Reichmann, Düsseldorf.

2.3.15 Preparation and culture of murine primary astrocytes

Newborn C57BL/6 mice (1 day old) were killed in CO₂, desinfected in 70 % ethanol and decapitated. After removal of the skin and the skull, cortex were prepared and freed from the meninges using a binocular. Tissue was then placed in DMEM and disrupted mechanically by repeated passage through a pasteur pipette until a homogenous cell suspension was obtained. The suspension was filtered through a 70µm cell strainer and centrifuged for 10' at 220g at 6°C. The pellet was resuspended in DMEM, 10 % FCS, 2mM L-glutamine, 50µM 2-mercaptoethanol and seeded in 6-well plates at 1x10⁶ cells per well. Starting from day 3 (with the growth of adherent cells) medium was changed every 3-4 days. At day 10, when a confluent glial cell monolayer had developed, cells were harvested by trypsinization and replated in 6-well plates. After reaching confluence again, the cells were trypsinized a second time and seeded in 48-well plates onto glass coverslips (1x10⁵ cells/1ml DMEM complete). When monolayers were confluent again they were used for experiments (usually cultures were 3-6 weeks old). In general, these

mixed glial cell cultures contained approximately 90 % glial fibrillary acidic protein (GFAP)-positive astrocytes and less than 10% microglia (as controlled by immunofluorescence staining). The Preparation and culture of murine primary astrocytes was conducted by Dr. Gaby Reichmann, Düsseldorf.

2.3.16 *In vitro* infection experiments and inoculation of primary astrocytes with *Toxoplasma gondii*

Murine primary astrocytes were left untreated or stimulated with 100 U/ml IFN- γ for 18-24h. Then cultures were inoculated at a multiplicity of infection (MOI) of 20 with *T. gondii* ME49 tachyzoites. Non-invaded parasites were removed 2h later by extensive washing with PBS (3-5x1ml/well). Then, some cultures were fixed with PFA (3% paraformaldehyde in PBS) for 20 min at room temperature. The remaining cultures were incubated in fresh medium in the absence or presence of IFN- γ as before. 24 h later, when intracellular parasitophorous vacuoles contained on average 8 parasites, these cultures were fixed in PFA as described above. *In vitro* infection experiments and inoculation of primary astrocytes with *Toxoplasma gondii* were conducted by Dr. Gaby Reichmann, Düsseldorf. After 1 wash in PBS, fixed cultures were stored with PBS in the cold until immunostaining was performed.

3. Results

3.1 The p47 GTPases are induced by IFN- γ in L929 and TIB-75 cells.

To test the inducibility of the p47 GTPases in the cell lines used in this study, L929 and TIB-75 cells were stimulated with 200U/ml IFN- γ for 24h and lysed in PBS, 1% Triton X-100 (Figure 1). Equal amounts of the post nuclear supernatants were subjected to SDS-PAGE and single members of the p47 family were detected by Western Blotting with specific serological reagents. All 6 proteins tested were abundantly induced from low or undetectable resting levels. The same result was found for RAW-264.7 cells, mouse primary astrocytes and mouse primary embryonic fibroblasts (not shown). Thus the p47 GTPases will be considered absent in cells not induced with IFN- γ .

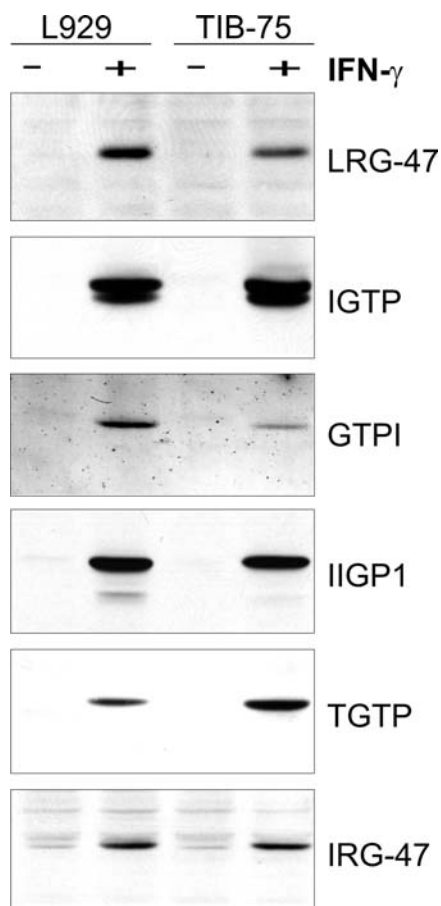


Figure 1

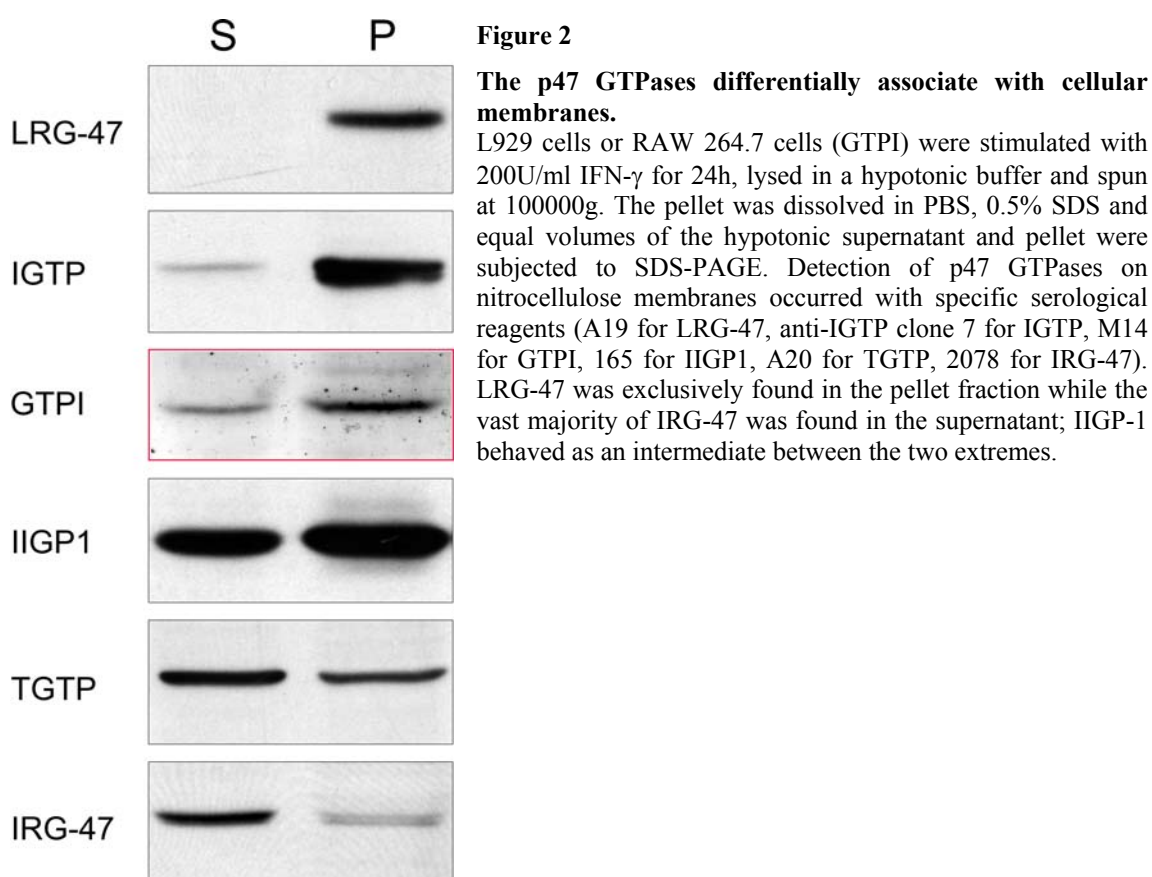
The p47 GTPases are induced by IFN- γ in L929 and TIB-75 cells.

L929 and TIB-75 cells were induced with 200U/ml IFN- γ for 24h or left untreated and lysed with 1% Triton X-100. Equal volumes of the lysates representing the equivalent of 10^5 cells were subjected to Western Blotting using specific serological reagents (A19 for LRG-47, anti-IGTP clone 7 for IGTP, M14 for GTPI, 165 for IIGP1, A20 for TGTP, 2078 for IRG-47). All p47 GTPases tested were abundantly induced from low or absent resting levels.

3.2 The p47 GTPases show different levels of membrane association.

L929 cells were induced with IFN- γ for 24h, disrupted in a hypotonic buffer and spun at 100000g. Equal amounts of the pellet and supernatant were loaded on 10%-12% polyacrylamide gels and the partitioning of the 6 p47 GTPases between cytosol

(supernatant) and membrane (pellet) was determined by Western Blotting (Figure 2). LRG-47 was exclusively found in the pellet while IRG-47 was nearly completely found in the supernatant. IIGP1 is an intermediate between these two extremes. In general the proportion of membrane bound protein appears to be higher for the GMS GTPases LRG-47, IGTP and GTPI. The GTPI experiment was, in contrast to the other proteins, conducted with RAW 264.7 cells. The ratio of membrane bound vs. cytosolic GTPI is likely to be very similar in L929 cells as all the other GTPases tested (LRG-47, IGTP and IRG-47) were found to partition in the same manner in RAW 264.7 and L929 cells. The IGTP result is in agreement with the results by Taylor et al. (93).



3.3 LRG-47 binds GDP and localizes to the Golgi apparatus and the ER.

To determine the sub-cellular localization of LRG-47 the anti-LRG-47 A19 purified goat polyclonal antiserum (Santa Cruz Biotechnology) was used. A19 showed an adnuclear signal with a diffuse granular background throughout the cytoplasm fainting at the periphery only in IFN- γ induced cells (Figure 3) which is consistent with the Western Blot result (Figure 1). LRG-47 was consistently observed to run smaller than the calculated molecular weight of 46.5 kDa with different specific serological reagents

(A19 and anti-LRG-47 L115 antiserum) by Western Blotting. Instead the molecule run as a 40 kDa band in SDS-PAGE analysis. N-terminal and C-terminal cleavage was excluded as possible explanation for the aberrant running behaviour in this assay by transfection of tagged constructs into several cell lines (not shown).

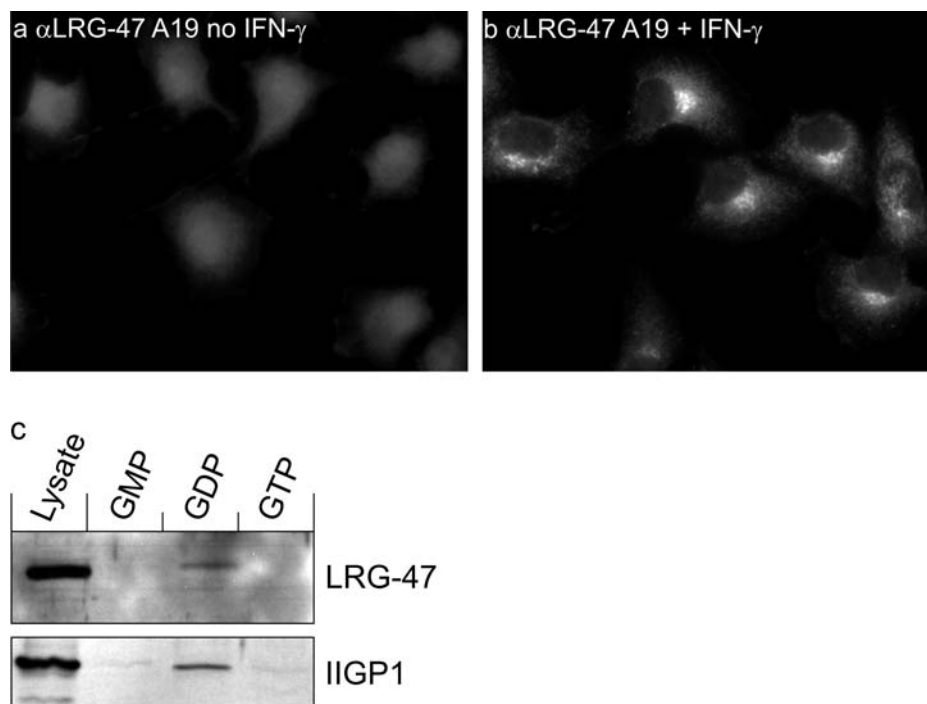


Figure 3

The anti-LRG-47 A19 antiserum detects an IFN- γ induced, adnuclear signal with diffuse granular background throughout the cell; LRG-47 binds to GDP agarose.

L929 cells were induced with 200 U/ml IFN- γ for 24h (a) or left untreated (b), fixed with 3% PFA and stained with the α LRG-47 A19 antiserum diluted 1:20. Bound A19 was detected with the donkey anti-goat-Alexa 546 antiserum. In IFN- γ induced cells an adnuclear signal and a diffuse granular background throughout the cell fainting at the periphery was detected. No signal was detected in uninduced cells. The images were taken with a Zeiss Axioplan II microscope equipped with a cooled CCD camera (Quantix) using the Metamorph software (version 4.5). The magnification is 630x. (c) Nucleotide agarose binding assay with 1% digitonin (LRG-47) or 0.1% Triton X-100 (IIGP1) lysates of IFN- γ induced L929 cells using GMP, GDP or GTP crosslinked agaroses. The final nucleotide agarose pellets were incubated in Laemmli buffer and co-pelleting of LRG-47 and IIGP1 was analyzed by immunoblotting with A19 for LRG-47 and 165 for IIGP1.

Lysates of IFN- γ induced L929 cells were subjected to nucleotide binding assay using guanine nucleotides crosslinked to agarose beads. The binding of LRG-47 was determined by Western Blotting of the proteins recovered in the final pellet which were released from the nucleotide agarose by incubation with Laemmli buffer. When cells were lysed in 1% digitonin a faint signal for LRG-47 was observed in the GDP agarose track but not in the GMP or GTP track (Figure 3c). No binding for LRG-47 was detected when cells were lysed in 0.1% Triton X-100 or CHAPS whereas weak binding was also detected for the Triton X-114 aqueous phase (not shown). As a control the

samples of a nucleotide binding experiment conducted with 0.1% Triton X-100 lysates were probed for IIGP1 by Western Blotting using the anti-IIGP1 165 antiserum. As for LRG-47 a clear signal was only observed for the GDP agarose which is consistent with the approximately 15 fold higher affinity of recombinant IIGP1 for GDP than GTP *in vitro* (150).

The A19 signal overlapped with various proteins localizing to the Golgi apparatus in L929 cells (Figure 4). The highest degree of co-localization of LRG-47 was seen for Rab6, involved in intra-Golgi trafficking (178), (Figure 4a-c) and the *cis*-Golgi protein Gm130 (179) (Figure 4d-f). The A19 signal also overlapped with α -mannosidase II, a *medial*-Golgi protein (180-182), although less precise (Figure 4g-i). No or very little co-localization was seen for LRG-47 and the cation-independent mannose 6-phosphate receptor (CI-M6PR) (Figure 4j-l) localizing to the *trans*-Golgi, *trans*-Golgi network (TGN) and the late endosomal compartment (183).

The sub-cellular localization of LRG-47 is very similar in RAW 264.7 macrophage-like cells (Figure 5). A19 showed an adnuclear concentration in IFN- γ induced RAW 264.7 cells. The cytoplasmic granular background is higher in RAW 264.7 compared to L929 cells (Figure 4). As in L929 cells, co-localization of LRG-47 was found for α -mannosidase II (Figure 5a-g) but not for CI-M6PR (Figure 5h-j).

The diffuse granular stain partly co-localizes with ER proteins like Calnexin (184) (Figure 6a-f) and IGTP (Figure 6g-l) (93). The degree of co-localization of LRG-47 appeared slightly higher for IGTP although the co-localization is in both cases restricted to single isolated dots. No co-localization between IGTP and LRG-47 was seen in the Golgi region consistent with the absence of IGTP from the Golgi apparatus (not shown). In conclusion, LRG-47 is a *cis*- and *medial*-Golgi associated protein with a small proportion of it being associated with the ER. Its sub-cellular localization is therefore different from its close relative IGTP (93).

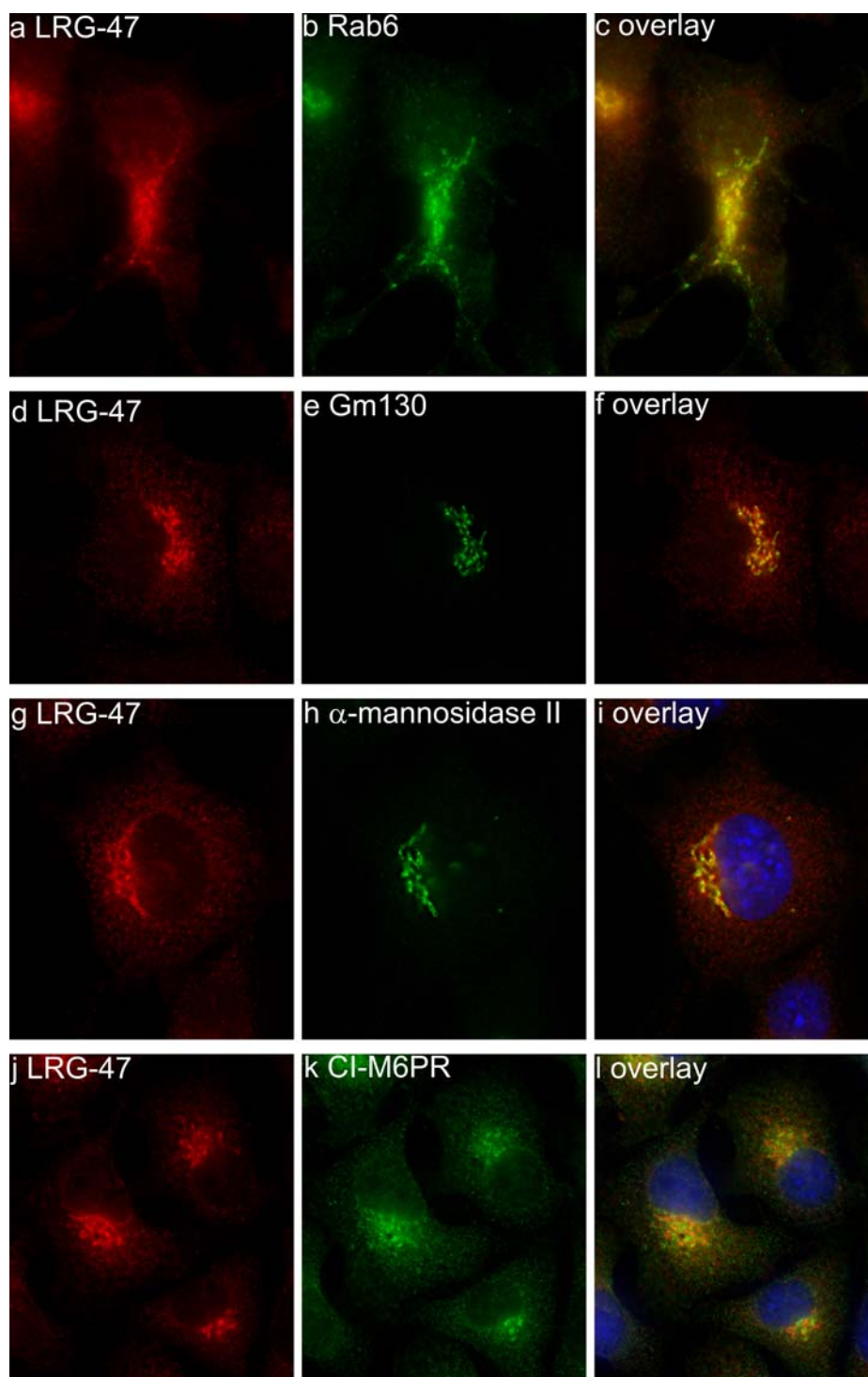
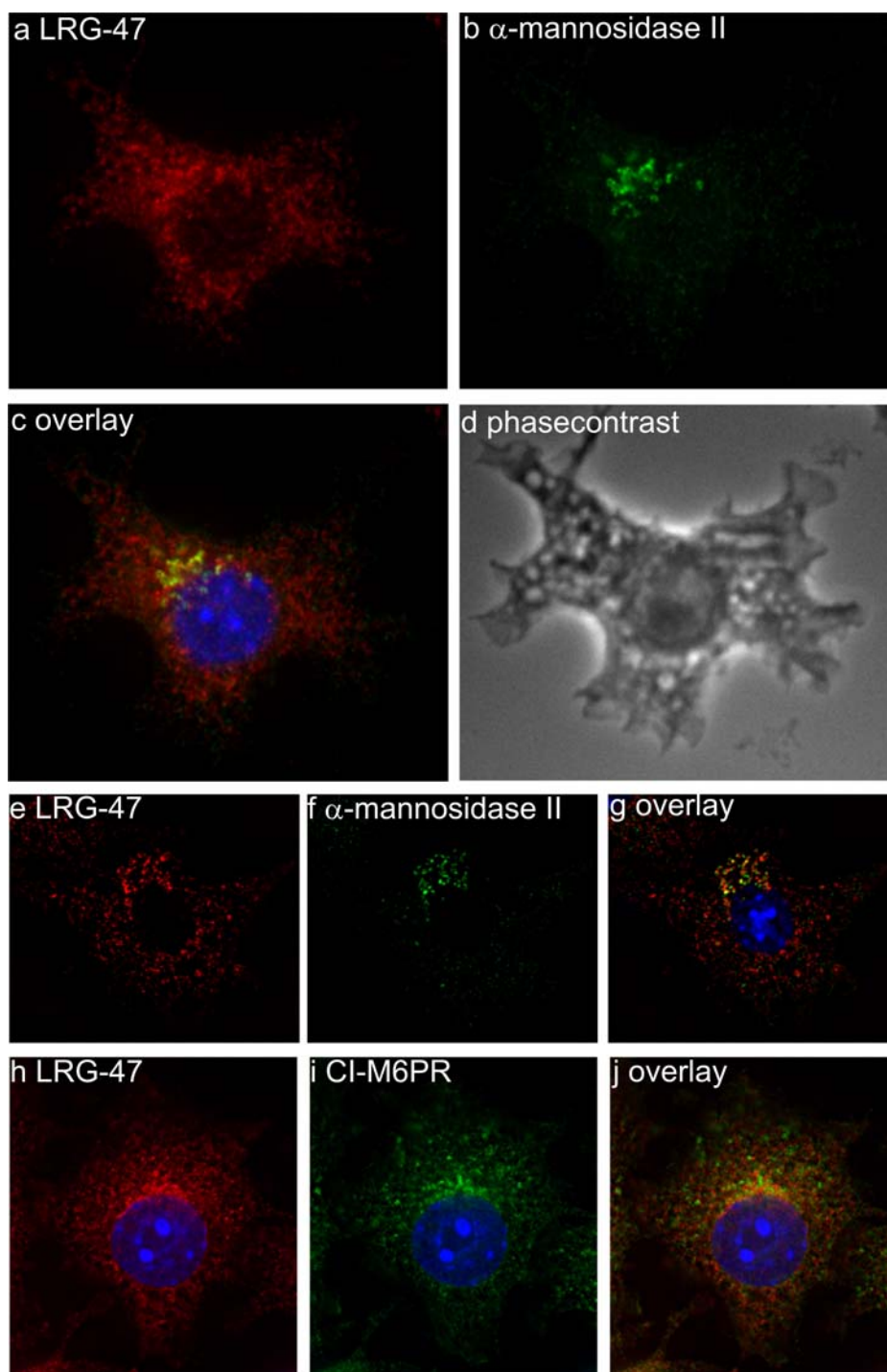


Figure 4

LRG-47 localizes to the *cis*- and *medial*-Golgi apparatus in L929 cells.

L929 cells were induced with 200 U/ml IFN- γ for 24h, fixed with 3% PFA and stained for the indicated proteins by indirect immunofluorescence. The adnuclear signal accurately overlapped with Rab6 (a-c) and Gm130 (d-f). Co-localization, although less precise, was also seen for LRG-47 and α -mannosidase II. Very little overlap was detected with CI-M6PR in the adnuclear region and the periphery (j-l). The images were taken with a Zeiss Axioplan II microscope equipped with a cooled CCD camera (Quantix) using the Metamorph software (version 4.5). The magnification is 630x for a-f and j-l and 1000x for g-i. Nuclei were labelled with DAPI.

**Figure 5****LRG-47 localizes to the Golgi apparatus also in RAW 264.7 cells.**

RAW 264.7 cells were induced with 200 U/ml IFN- γ for 24h, fixed with 3% PFA and stained for the indicated proteins by indirect immunofluorescence. The adnuclear A19 signal partially overlapped with α -mannosidase II (a-d) as revealed by 3D deconvolution (e-g). No co-localization was detected for LRG-47 and CI-M6PR (h-j). The images were taken with a Zeiss Axioplan II microscope equipped with a cooled CCD camera (Quantix) using the Metamorph software (version 4.5). The magnification is 630x for a-g and 1000x for h-j. e-f show a plane of a 3D deconvoluted Z-series. Nuclei were labelled with DAPI.

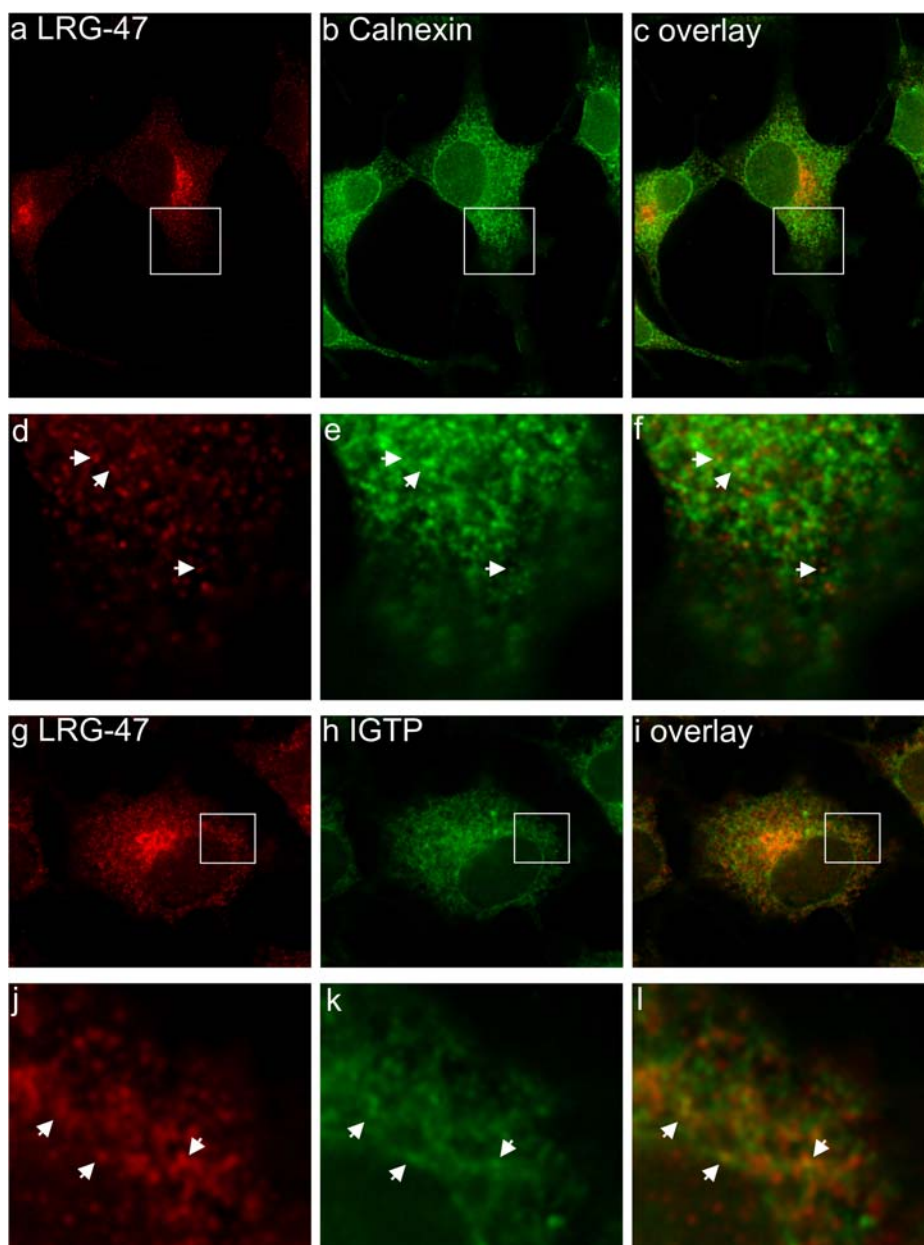


Figure 6

LRG-47 partially localizes to the ER in the periphery of L929 cells.

L929 cells were induced with 200 U/ml IFN- γ for 24h, fixed with 3% PFA and stained for the indicated proteins by indirect immunofluorescence. Partial overlap of LRG-47 with Calnexin (a-f) and IGTP (g-l) was detected in the periphery of the cells. Arrows point to representative isolated points of co-localization. The images were taken with a Zeiss Axioplan II microscope equipped with a cooled CCD camera (Quantix) using the Metamorph software (version 4.5). The magnification is 1000x.

3.4 LRG-47 does not associate with the endosomal or lysosomal compartment.

To analyze a potential association of LRG-47 with the endocytic compartment IFN- γ stimulated L929 cells were co-stained for LRG-47 and Transferrin, Rab11 or LAMP-1 (Figure 7).

Transferrin is taken up by receptor mediated endocytosis into early lysosomes, sorted into recycling endosomes and subsequently recycled back to the plasma membrane

(185). The cell shown in Figure 7a-c was incubated for 20' with Alexa-546 labelled Transferrin marking all intracellular sorting stages of Transferrin. No co-localization of LRG-47 and Transferrin was observed (Figure 7a-c). Likewise, no overlap with Rab11, marking the recycling endosomal compartment (186) and LRG-47 was seen (Figure 7d-f). Essentially the same result was obtained for LRG-47 and LAMP-1, used to stain the late endosomal and lysosomal compartment (187) (Figure g-i).

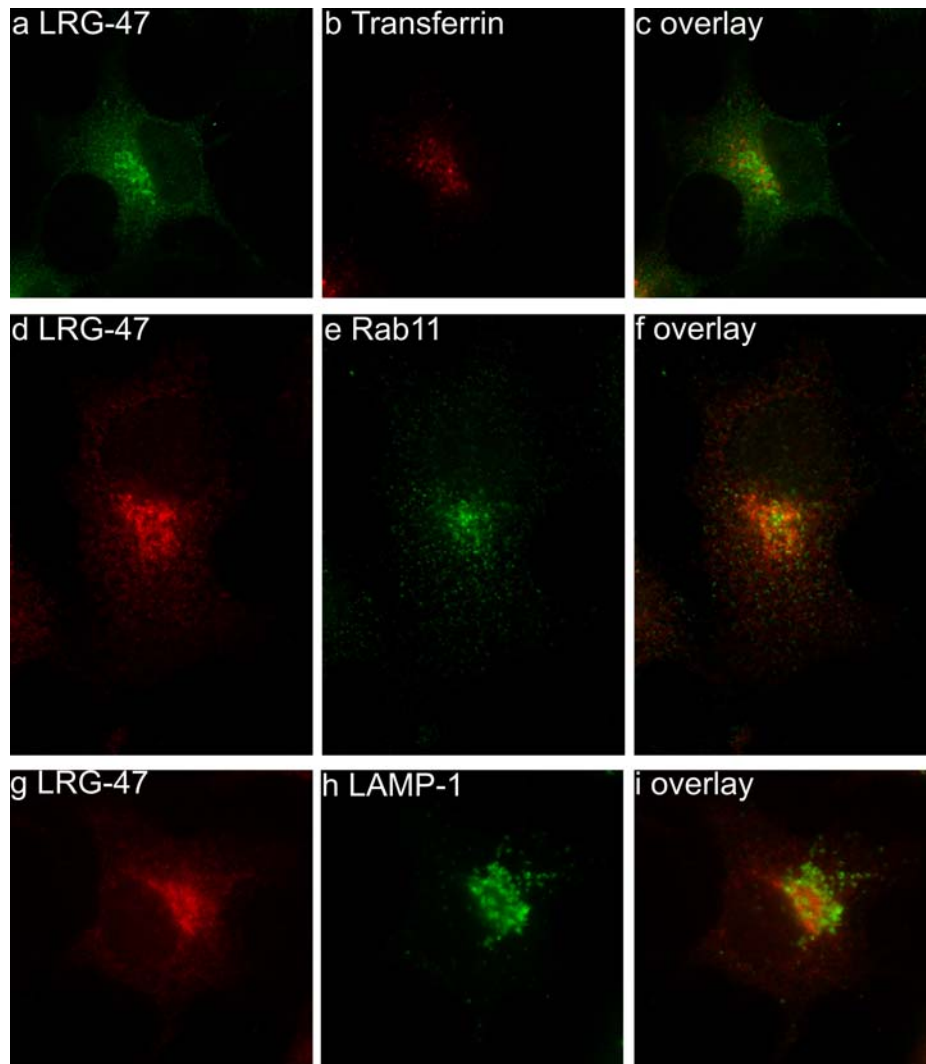


Figure 7

LRG-47 does not localize to the endocytic and lysosomal compartment in L929 cells.

L929 cells were induced with 200 U/ml IFN- γ for 24h, fixed with 3% PFA and stained for the indicated proteins by indirect immunofluorescence. To analyze the degree of co-localization of LRG-47 with the endocytic compartment, the cells were incubated with Alexa-546 conjugated Transferrin for 20' prior to fixation. No overlap with up-taken Transferrin (a-c), Rab 11 (d-f) and LAMP-1 (g-i) was detected. The images were taken with a Zeiss Axioplan II microscope equipped with a cooled CCD camera (Quantix) using the Metamorph software (version 4.5). The magnification is 630x for a-c and g-i and 1000x for d-f.

3.5 LRG-47 is recruited to the plasma membrane upon phagocytosis and remains associated with maturing phagosomes.

As shown in Figure 4-6 LRG-47 is associated with the Golgi apparatus and the ER. This localization appeared enigmatic in view of the fact that LRG-47 is a potent resistance factor against a variety of intracellular pathogens entering the cell through the plasma membrane and which have very different intracellular life styles (40, 95, 96). A possible association of LRG-47 with the plasma membrane upon its remodelling, as it occurs during phagocytosis, was therefore examined. For this purpose L929 cells were incubated with collagen-coated latex beads which are taken up by fibroblasts in a process known as collagen-phagocytosis (154) (Figure 8).

LRG-47 markedly associated with phagocytic cups and adjacent plasma membrane ruffles as shown by co-staining of L929 cells with A19 and phalloidin which stains filamentous actin (F-actin) (Figure 8a-c). LRG-47 apparently remained associated with the phagosomes as they matured to phagolysosomes shown by co-localization of LRG-47 and LAMP-1 (Figure 8d-f). No overlap was seen for the lysosomal compartment not engaged in phagocytosis (Figure 8d-f and Figure 7g-i).

To determine if the recruitment of LRG-47 to plasma membrane upon phagocytosis and its subsequent association with phagosomes is a universal process, primary macrophages, isolated from the peritoneal cavity of CB20 mice were incubated with 2 μ m latex beads for 30', fixed and stained with A19 and phalloidin (Figure 9a-e). Similar to L929 cells, LRG-47 localized to sites where the latex beads contacted the plasma membrane (Figure 9c-e). The recruitment of LRG-47 is apparently a very early and rapid process as LRG-47 associated with phagocytic cups which were not yet fully formed (middle arrow in Figure 9c-e). The same result was obtained with RAW 264.7 cells (not shown).

As demonstrated for fibroblasts, LRG-47 remained associated with the phagosomes shown by selective co-localization of LRG-47 and LAMP-1 in RAW 264.7 cells (Figure 9f-j) and peritoneal macrophages (not shown) around the phagosomes.

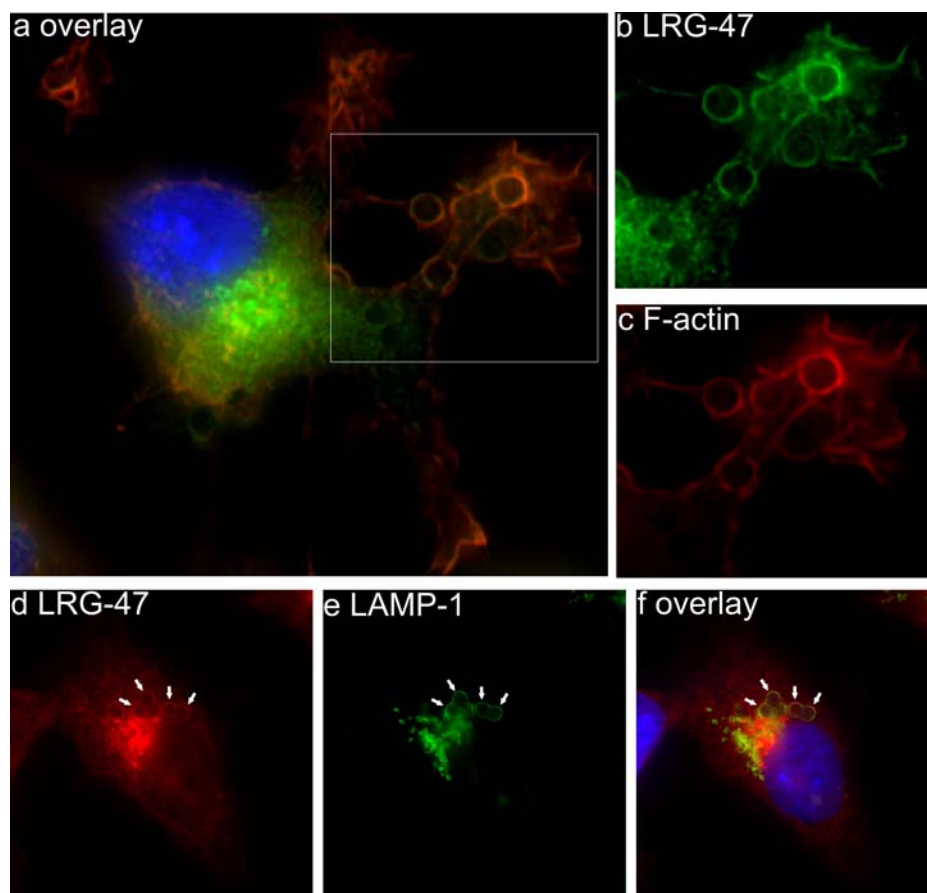


Figure 8

LRG-47 is recruited to plasma membrane upon phagocytosis and remains associated with maturing phagosomes.

L929 cells were induced with IFN- γ for 20h and incubated with collagen-coated 2 μ m latex beads for 4h in the continuous presence of IFN- γ . Cells were then fixed and stained for the indicated proteins. Filamentous actin (F-actin) was stained with TRITC conjugated phalloidin. LRG-47 co-localized with F-actin around phagocytic cups and adjacent plasma membrane ruffles (a-c). LRG-47 overlapped with LAMP-1 around the phagosomes in the centre of the cell but not with LAMP-1 containing structures not engaged in phagocytosis (d-f). The images were taken with a Zeiss Axioplan II microscope equipped with a cooled CCD camera (Quantix) using the Metamorph software (version 4.5). The magnification is 630x. Nuclei were labelled with DAPI.

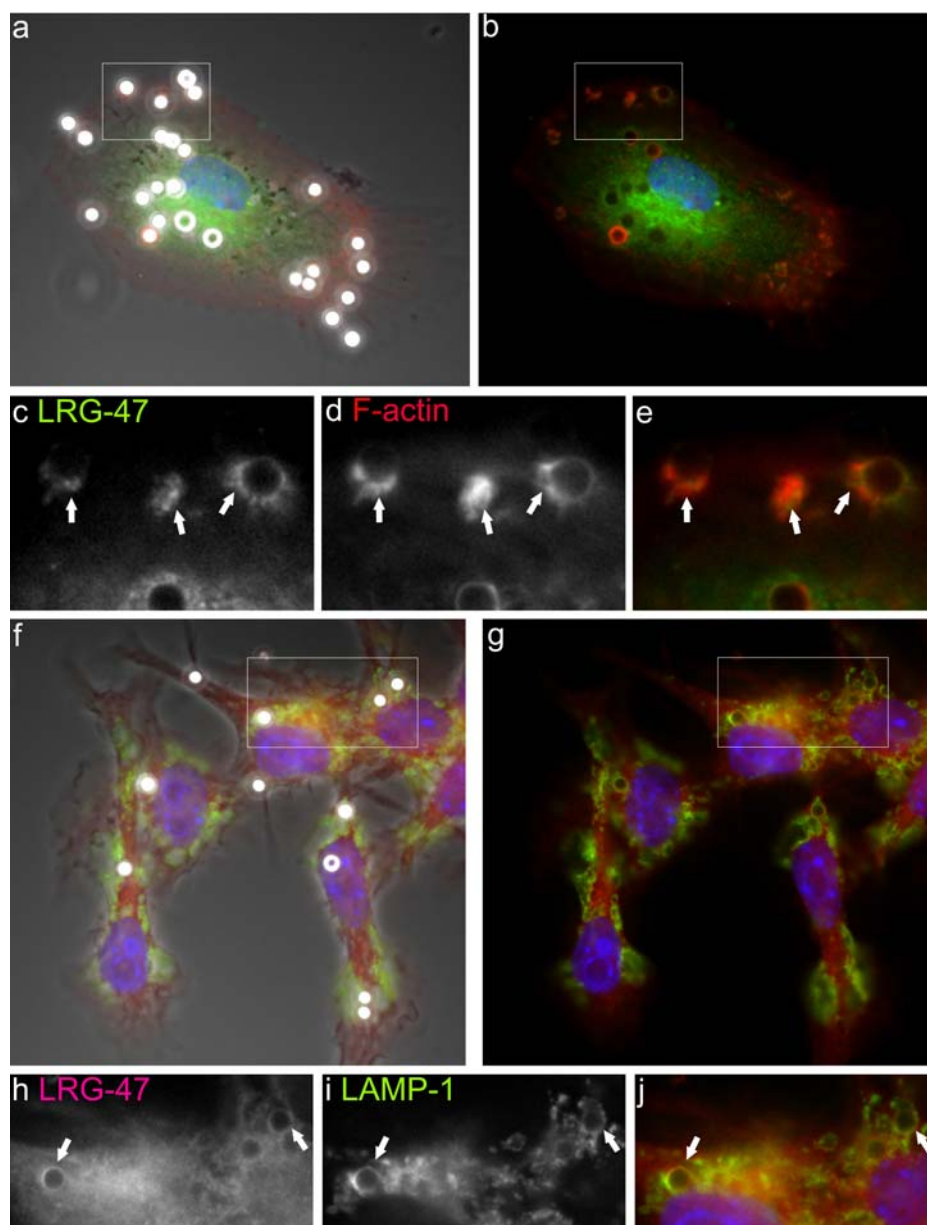


Figure 9

LRG-47 is recruited to plasma membrane and phagolysosomes also in macrophages.

Macrophages isolated from the peritoneal cavity of CB20 mice (a-e) or RAW 264.7 cells (f-j) were induced with 200 U/ml IFN- γ for 48h and incubated with 2 μ m latex beads for 30' (a-e) or 4h (f-j) in the presence of IFN- γ . Cells were fixed with 3% PFA and stained for the indicated proteins. Filamentous actin (F-actin) was visualized with Alexa-546 conjugated phalloidin. As in L929 cells LRG-47 was recruited to forming phagocytic cups (a-e) and remained associated with the maturing phagosomes (f-j). The images were taken with a Zeiss Axioplan II microscope equipped with a cooled CCD camera (Quantix) using the Metamorph software (version 4.5). The magnification is 630x. Nuclei were labelled with DAPI.

Phagosomes from RAW 264.7 cells were isolated by sub-cellular fractionation according to the protocol established by Dejardins et al. (157) (Figure 10). To control for possible contaminations, IFN- γ stimulated cells, not incubated with latex beads and uninduced cells, incubated with latex beads were mixed before lysis (+/-, -/+ track; for details see Material and Methods). The isolated phagosomal fractions (Figure 10b) and aliquots of the lysates were subjected to SDS-PAGE. Co-purification of the indicated

proteins was monitored by Western Blotting (Figure 10a). Consistent with the long incubation time of 4h the phagosomal fraction appeared to contain little or no EEA1 (early endosomal antigen 1) (157) and Calnexin (155, 156). In agreement with this, LAMP-1 was rather abundantly recovered in the phagosomal fraction. LRG-47 was also co-purified with the phagosomes although a faint signal was also detected in the track with the mixed cells representing either contamination of this fraction with other membranes or post-lyses association with phagosomes. However the signal was reproducibly higher in the *+/+* track. IGTP could not be co-purified with the phagosomes under these conditions. In a single experiment IIGP1 was found to be enriched in the *+/+* final pellet compared to the *+/-*, *-/+* final pellet (not shown). Independently MacMicking et al. reported the co-purification of LRG-47 with phagosomes isolated from macrophages infected with *Mycobacterium tuberculosis* (95).

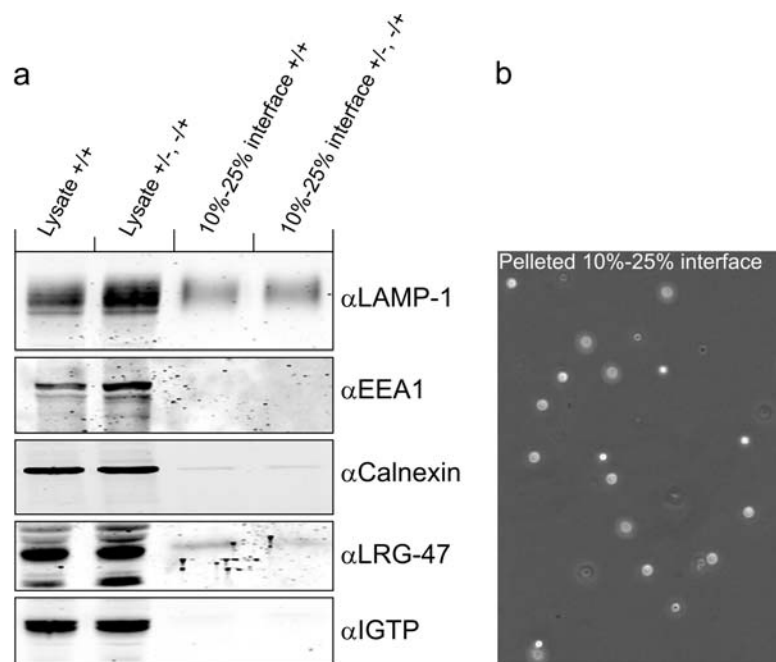


Figure 10
LRG-47 co-purifies with latex bead containing phagosomes from RAW 264.7 cells.

RAW 264.7 cells were induced with 200U/ml IFN- γ for 44h and incubated with 2 μ m latex beads for 4h in the presence of IFN- γ . Phagosomes were isolated according to (157), described in detail in the Material and Methods part. In contrast to IGTP, LRG-47 was co-purified with the phagosomal fraction (a). The recovery of the 2 μ m latex beads in the final pellet is shown in b. LRG-47 was repeatedly found to be more abundant in the *+/+* fraction compared to the *+/-*, *-/+* fraction. The absence of EEA1 and presence of LAMP-1 indicates that an abundance of late stage phagosomes.

3.6 Membrane binding of LRG-47 is IFN- γ and nucleotide independent

To examine the nucleotide dependence of membrane association of LRG-47, a mutation was introduced changing the amino acid sequence in the G1 motif from GX₄GMS to GX₄GMN. The same mutation was shown to abolish nucleotide binding of IGTP (93).

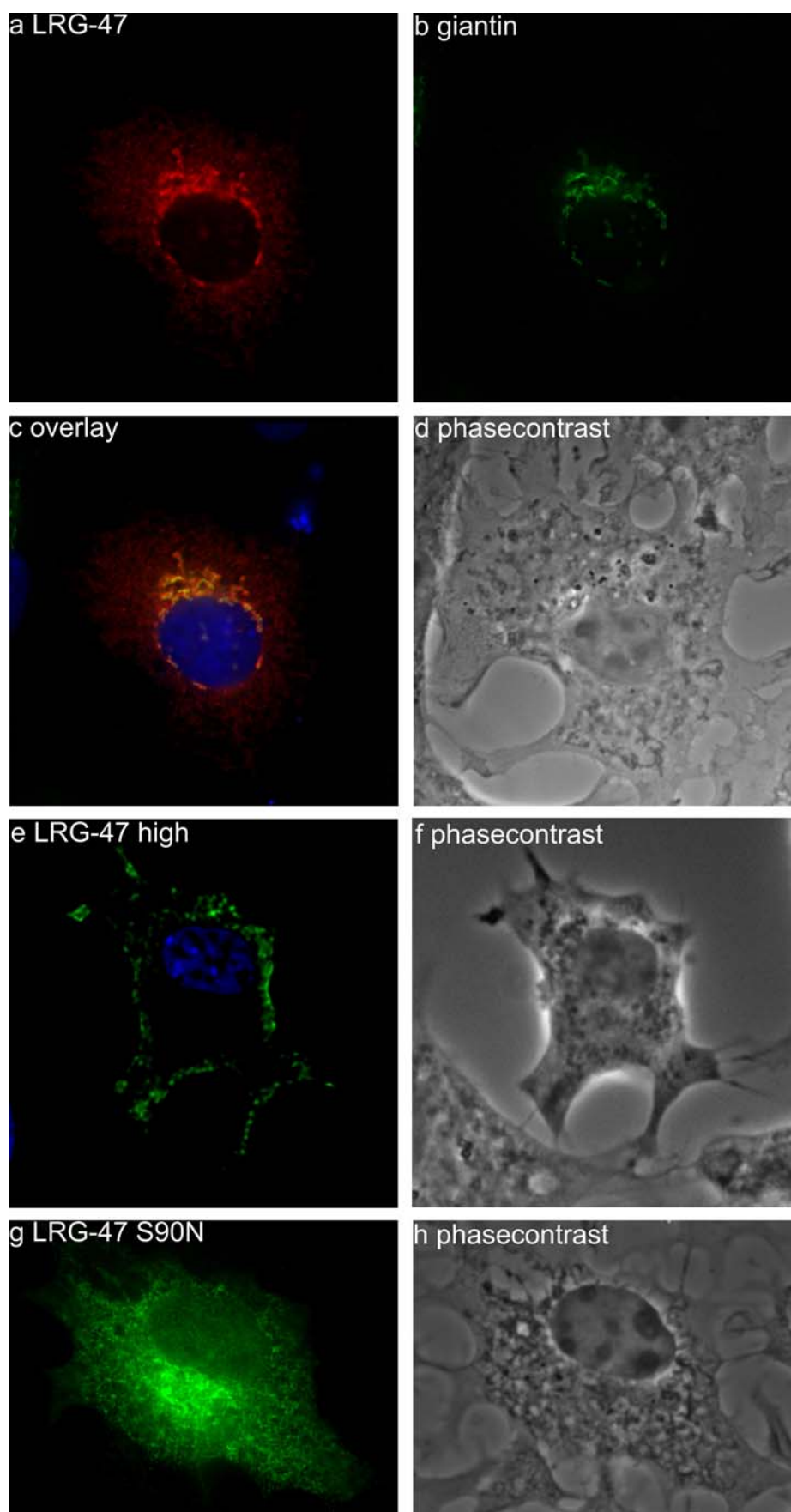


Figure 11

Membrane association of LRG-47 is independent of nucleotide binding.

Resting L929 cells were transfected with untagged, wild type or S90N mutant LRG-47 fixed with 3% PFA 24h later and stained with the A19 antiserum and anti-giantin antibody. When expressed at levels

comparable to the expression level induced by IFN- γ LRG-47 accurately co-localized to the Golgi apparatus visualized with anti-giantin staining (a-d). At higher expression levels LRG-47 exclusively associated with the plasma membrane leaving the Golgi region dark (e, f). The nucleotide binding deficient S90N mutant (g, h) still bound to membrane showing the same adnuclear concentration as the wild type protein although the peripheral signal was markedly increased. No translocation to plasma membrane was observed, regardless of the expression levels (g, h). The images were taken with a Zeiss Axioplan II microscope equipped with a cooled CCD camera (Quantix) using the Metamorph software (version 4.5). The magnification is 630x. (e) shows a plane of a 3D deconvoluted Z-series. Nuclei were labelled with DAPI.

N- and C-terminal tags caused LRG-47 to mislocalize to plasma membrane, recycling endosomes and other cellular membranes of unknown identity (Figure 23). Therefore untagged LRG-47 had to be expressed in uninduced cells.

For this purpose wild type and mutant LRG-47 was expressed in resting L929 cells by transient transfection (Figure 11). The transfection procedure itself did not induce the expression of the p47 GTPases (not shown). Transfected LRG-47 localized in a pattern indistinguishable from the endogenous protein accurately co-localizing with the Golgi protein giantin (176) (Figure 11a-d). Thus the sub-cellular localization of LRG-47 is independent of other IFN- γ induced factors.

At expression levels markedly above the levels induced by IFN- γ LRG-47 localized to the plasma membrane leaving the Golgi region dark (Figure 11e, f). This recalls the plasma membrane association of LRG-47 upon phagocytosis (Figure 8). To determine whether membrane association and plasma membrane relocalization are nucleotide dependent a mutation analogous to the G1 mutant of IGTP generated by Taylor et al. (93) abolishing nucleotide binding was introduced into the open reading frame of LRG-47. When the S90N nucleotide binding deficient mutant of LRG-47 was expressed in uninduced L929 cells the protein was found to localize very similar to the wild type protein (Figure 11g, h) although the reticular peripheral stain was noticeably increased. The adnuclear signal co-localized with the Golgi proteins Gm130 and giantin and the peripheral reticular stain with Calnexin (not shown). However no translocation of the mutant protein to plasma membrane was observed, regardless of the expression levels. To conclude, the targeting to Golgi and ER is independent of nucleotide binding and other IFN- γ stimulated factors but translocation to plasma membrane upon over expression is nucleotide dependent.

3.7 LRG-47 is targeted to the Golgi apparatus and plasma membrane by different domains.

From the results presented so far it is clear that endogenous LRG-47 has at least two localizations in the cell, the Golgi apparatus and the plasma membrane upon phagocytosis. To determine which domains are responsible for the different localizations, isolated domains were expressed in L929 cells (Figure 12). The structural domains of LRG-47 were defined by aligning the LRG-47 protein sequence to the IIGP1 crystal structure (Figure 12a) (149).

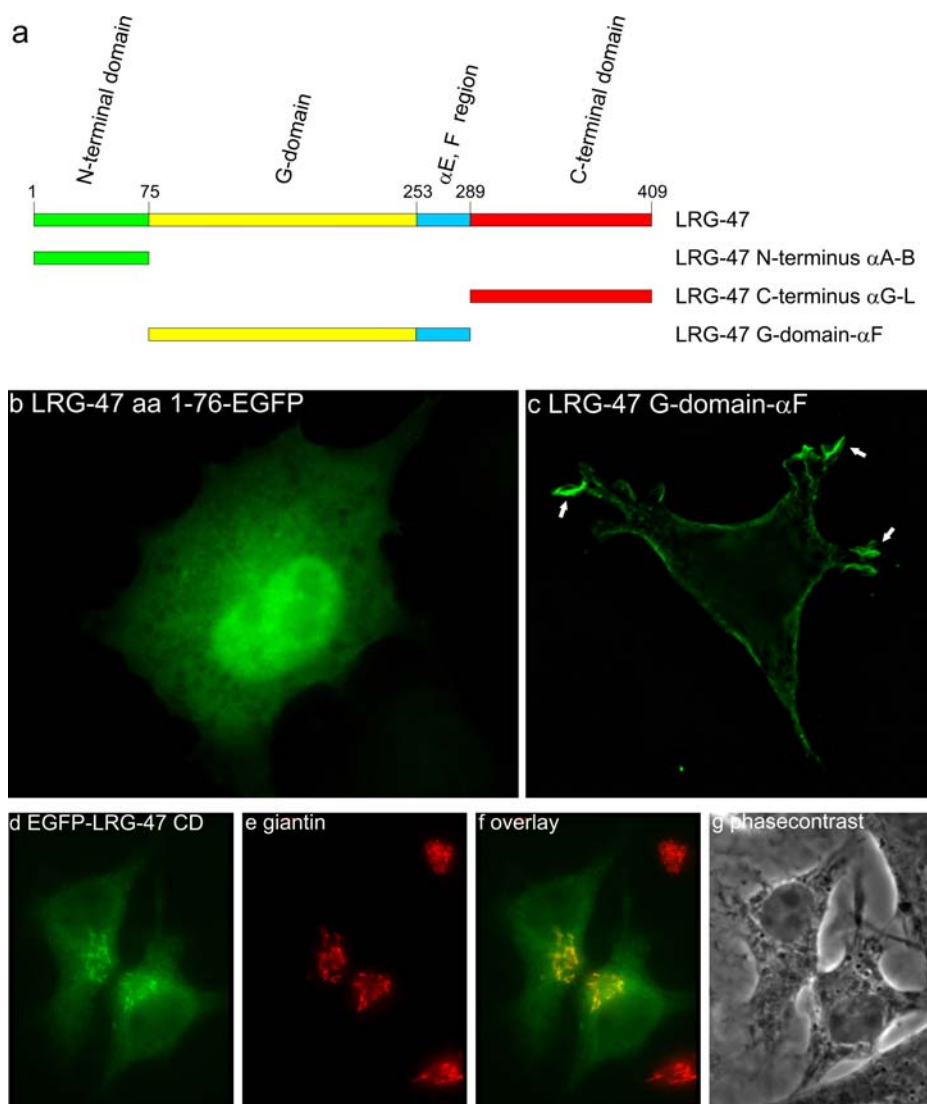


Figure 12

LRG-47 harbours a Golgi targeting signal in its C-terminal domain and a plasma membrane binding activity in the G-domain.

The linear organization of the putative domain organization of LRG-47 according to the IIGP1 crystal structure is shown in (a). Isolated domains were expressed in resting L929 cells. The N-terminal domain was C-terminally fused to EGFP (b), the G-domain- α F fragment was C-terminally Flag-tagged (c) and the C-terminal domain was fused N-terminally to the C-terminus of EGFP (d-g). No expression was detected for the isolated G-domain (not shown). Transfected cells were fixed with 3% PFA 24h after transfection and stained with the anti-Flag M2 antibody (c) or the anti-giantin antibody (d-g). No membrane targeting

activity was detected for the isolated N-terminal domain (b). The G-domain- α F fragment associated exclusively with the plasma membrane with some diffuse cytosolic stain (c). A marked accumulation of LRG-47 at plasma membrane ruffles was observed (arrows) and no signal was detected on internal membranes. The C-terminal domain associated with Golgi apparatus visualized with anti-giantin staining (d-g). A diffuse reticular signal throughout the cell was also apparent. The images were taken with a Zeiss Axioplan II microscope equipped with a cooled CCD camera (Quantix) using the Metamorph software (version 4.5). The magnification is 630x. (c) shows a plane of a 3D deconvoluted Z-series.

The isolated N-terminal domain showed no membrane targeting activity when fused to the N-terminus of EGFP (Enhanced Green Fluorescent Protein) (Figure 12b compare to Figure 20b showing EGFP alone). No expression was found for the isolated G-domain. Therefore a construct extending the G-domain C-terminally to include α F was generated and expressed in L929 cells. Strikingly the G-domain showed exclusive plasma membrane association with an additional cytosolic background (Figure 12c). The staining at membrane ruffles was particularly eminent (Figure 12c, white arrows). The C-terminal domain in contrast accurately localized EGFP to the Golgi apparatus with a diffuse reticular background (Figure 12b). This pattern is virtually identical to the transfected wild type (Figure 11a-d) and endogenous IFN- γ induced protein (Figure 4). The increased reticular background however is reminiscent of the S90N mutant (Figure 11g, h).

3.8 The α K region of LRG-47 is sufficient for Golgi targeting.

Figure 13a shows the linear organization of the putative domain organization of LRG-47 based on the crystal structure of IIGP1 (149) and several constructs designed to map the Golgi targeting activity within the C-terminal domain of LRG-47. The C-terminal domain does not contain any predictable membrane targeting motifs. Therefore a systematic approach to identify the Golgi targeting elements was chosen. All C-terminal domain constructs (Figure 13) except α L showed are more or less pronounced adnuclear signal (Figure 13b-g) co-localizing with giantin (not shown). The construct including only α L in contrast appeared fully soluble (Figure 13g), accumulating in the nucleus (Figure 13g) in the for GFP characteristic manner (Figure 20b). When the 25 amino acids (aa 350-374) that were deleted from α K-L to create α L (Figure 13a) were fused to EGFP and expressed in L929 cells the fusion protein accurately localized to the Golgi apparatus shown by co-staining with the anti-giantin antibody (Figure 13h-k). Thus the amino acids 350-374 of LRG-47 are sufficient to target EGFP to the Golgi apparatus.

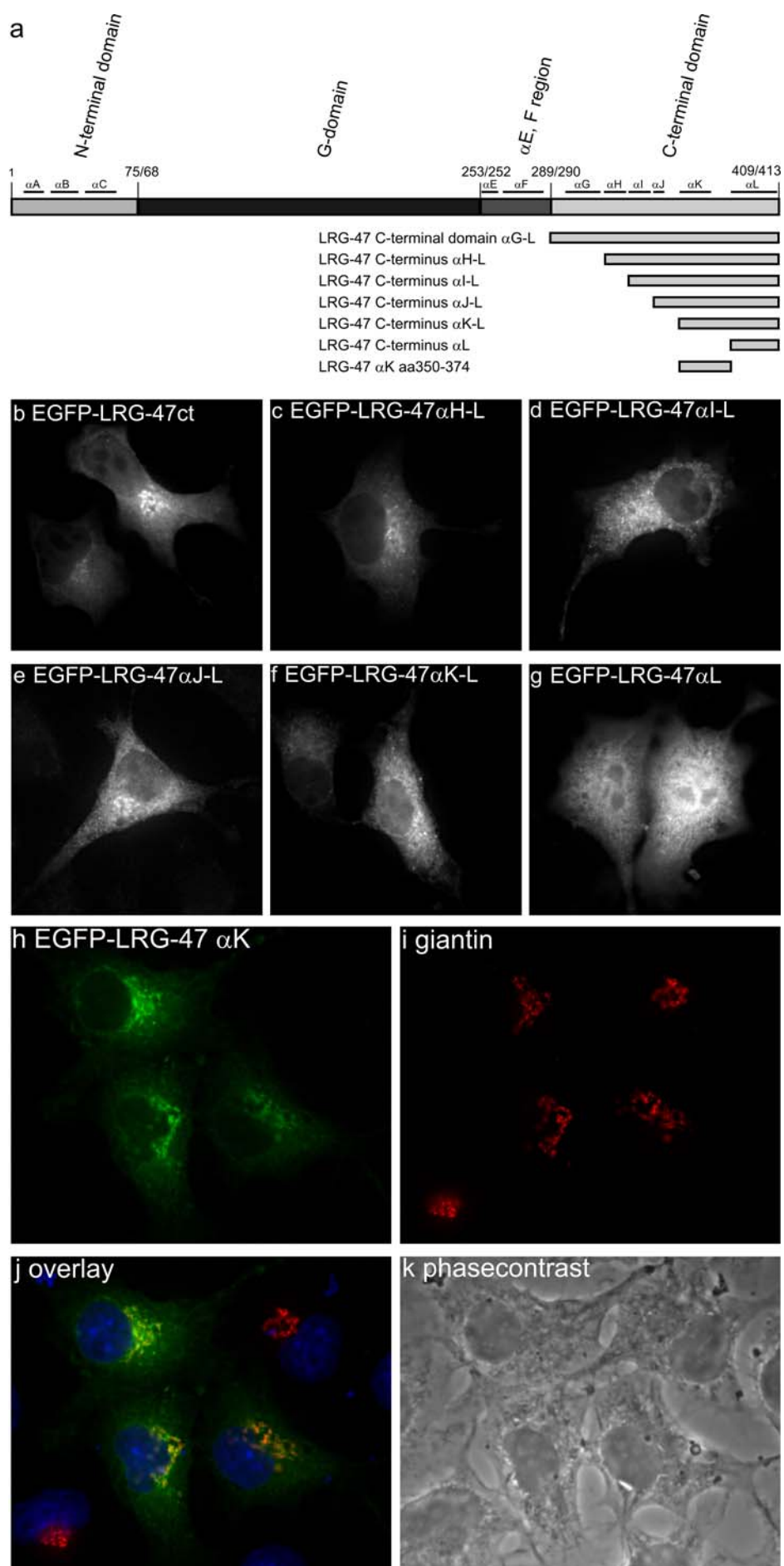


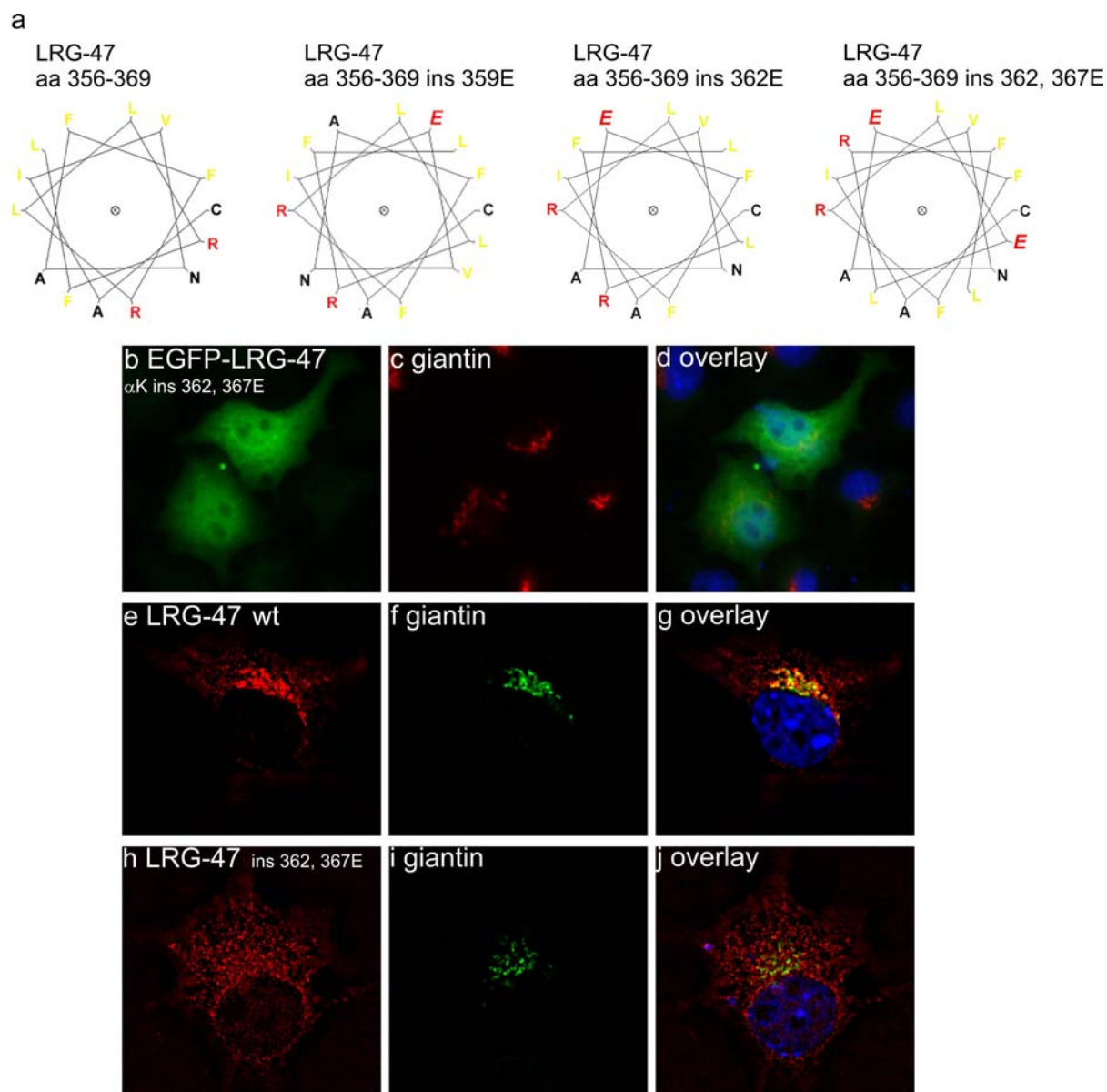
Figure 13**The Golgi targeting activity of the C-terminal domain of LRG-47 maps to a 25 amino acids long peptide corresponding to α K and the C-terminal loop in the IIGP1 structure.**

The domain organization of the p47 GTPases according to the IIGP1 crystal structure is shown in a. The numbers above the structure indicate the positions in the amino acid sequence of LRG-47 and IIGP1 respectively. Secondary structure elements outside the G-domain are drawn to scale above the structure and are indicated as small lines. Constructs designed to map the Golgi targeting activity in the C-terminal domain of LRG-47 are shown below the structure. All constructs were N-terminally fused to the C-terminus of EGFP and expressed in resting L929 cells fixed 24h after transfection. All C-terminal constructs except the one comprising only α L (g) showed a more or less pronounced adnuclear concentration (b-g). The α L construct appeared to be completely soluble with the for GFP characteristic nuclear accumulation (g). The 25 amino acids (aa 350-374) deleted from EGFP-LRG-47 α K-L to generate EGFP-LRG-47 α L accurately targeted EGFP to the Golgi apparatus (h-k) when fused to its C-terminus as shown by co-staining with anti-giantin antibody. Nuclei were labelled with DAPI.

3.9 The Golgi targeting activity of the LRG-47 α K region requires an amphipathic helix.

A core sequence of 14 amino acids (aa 356-369) within the 25 amino acids long α K Golgi targeting peptide of LRG-47 is able to form an amphipathic helix when drawn as a helical wheel (Figure 14a). In addition, by secondary structure predictions this sequence was predicted to form an α helix (149). To test whether the amphipathic character of that helix is important for membrane association, glutamate residues designed to destroy its amphipathic character were inserted into this sequence by site directed mutagenesis (Figure 14a). When introduced into the 25 amino acids long α K peptide the Golgi association of the EGFP α K fusion protein was completely abolished (compare Figure 14b-d and Figure 13h-k). Introduced into the whole open reading frame of LRG-47 all mutations interfered with Golgi targeting (Figure 14e-j and not shown). In contrast to the wild type protein the mutant proteins localized in a granular pattern throughout the cytoplasm not accumulating on Golgi membranes.

To summarize, Golgi targeting of LRG-47 is dependent on an amphipathic helix located in the C-terminal domain. This region corresponds to α K in the IIGP1 crystal structure.

**Figure 14****Golgi targeting of LRG-47 is dependent on an amphipathic helix located within the α K region.**

The amino acids 356-369 of LRG-47 are able to form an amphipathic helix when drawn as a helical wheel (a). Large hydrophobic residues are shown in yellow, charged residues in red. The helical wheels were drawn with the program found at <http://marqusee9.berkeley.edu/kael/helical.htm>. Single glutamate residues were inserted into this helix in order to destroy its amphipathic character (a). All constructs were expressed in L929 cells, fixed 24h after transfection and stained by indirect immunofluorescence with anti-giantin antibody and A19 antiserum, respectively. When introduced into the 25 amino acid long α K peptide all mutations completely abolished membrane association. A representative result is shown in b-d. When introduced into the full length ORF all mutations interfered with Golgi accumulation of the protein (h-j). The full length wild type protein in contrast accurately co-localized with giantin (e-g). The images were taken with a Zeiss Axioplan II microscope equipped with a cooled CCD camera (Quantix) using the Metamorph software (version 4.5). The magnification is 630x. e-j show planes of 3D deconvoluted Z-series. Nuclei were labelled with DAPI.

3.10 The α K regions of GTPI and IGTP also show membrane targeting activity.

Figure 15a shows an alignment of the C-terminal part of the 6 published p47 GTPases aligned to the IIGP1 structure (149).

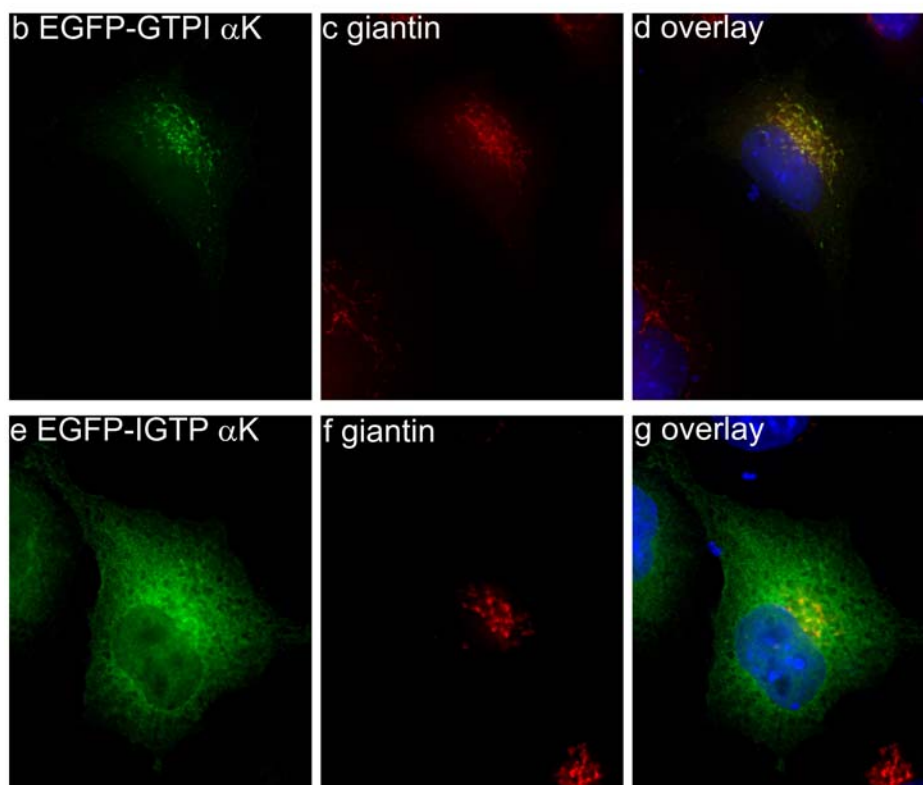
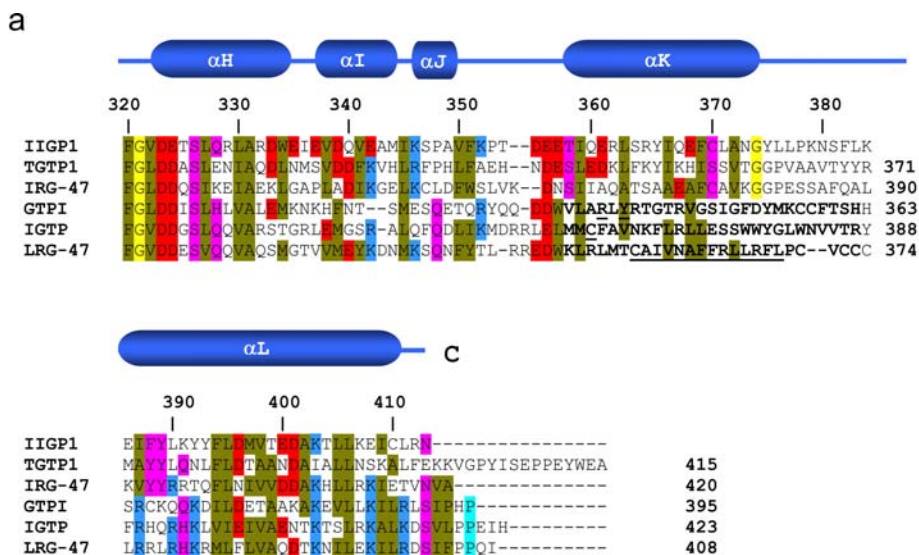


Figure 15

The α K peptides of GTPI and IGTP also show membrane targeting activity

An alignment of the C-terminal part of the p47 GTPases aligned to the crystal structure of IIGP1 is shown in (a) (The alignment was kindly provided by Dr. Eva Wolf). The 25 aa long peptide targeting LRG-47 to the Golgi apparatus is shown in bold, the amphipathic helix within this peptide is underlined. The corresponding sequences of the GTPI and IGTP comprising 27 aa were fused to the C-terminus of EGFP and expressed in resting L929 cells. The cells were fixed with 3% PFA 24h after transfection and stained with the anti-giantin antibody to visualize the Golgi apparatus. The α K peptide of GTPI accurately targeted

EGFP to the Golgi apparatus (b-d). The EGFP-IGTP α K fusion protein appeared more diffuse with an imbedded reticular pattern co-localizing only marginally with giantin (e-g). The images were taken with a Zeiss Axioplan II microscope equipped with a cooled CCD camera (Quantix) using the Metamorph software (version 4.5). The magnification is 1000x. Nuclei were labelled with DAPI.

The Golgi targeting peptide of LRG-47 is shown in bold and the amphipathic helix therein is underlined (Figure 15a). The corresponding sequences of the other two GMS p47 GTPases GTPI and IGTP (Figure 15a (bold)) were, analogous to the LRG-47 α K peptide, fused to the C-terminus of EGFP and expressed in L929 cells. The 27 amino acids long α K peptide of GTPI targeted the EGFP fusion protein accurately to the Golgi complex as shown by co-staining with the anti-giantin antibody (Figure 15b-d). The corresponding 27 amino acids long IGTP α K peptide localized in a reticular pattern throughout the cell fainting at the periphery (Figure 15e-g). The distribution of the IGTP α K fusion protein appeared noticeably more diffuse than the corresponding LRG-47 and GTPI constructs suggesting a considerable cytosolic pool of this fusion protein. The reticular pattern recalls the ER localization of IGTP reported by Taylor et al. (93) and which is shown in Figure 23e-j.

3.11 The α K peptides of GTPI and IGTP show homology to two different regions of phospholipase C.

To determine which mechanisms are used by the α K regions of GTPI and IGTP to bind to membrane both sequences were independently subjected to a BLAST search for short, nearly exact matches within the mammalian proteome using the default configuration (<http://www.ncbi.nlm.nih.gov/BLAST/>). Among other sequences two regions of phospholipase C (PLC) were found which showed significant homology to the IGTP and GTPI peptides, respectively (Figure 16a). For GTPI the highest homology among the PLC hits was for mouse PLC β (NP_062651.1) and for IGTP rabbit PLC (CAA89822.1). These peptides were aligned to the rat PLC δ sequence (P10688) for which the crystal structure in complex with inositol-1,4,5-trisphosphate (IP₃) has been determined (188) (1DJX). Surprisingly the GTPI and IGTP α K peptides do not correspond to the same region of PLC (Figure 16). They were rather found to align to two regions within the Y-region of the catalytic domain of PLC, interrupted by an 11 amino acids long sequence. After closer inspection these 11 amino acids also turned out to show low homology to rat PLC δ (Figure 16d). Strikingly, both regions make contact with the bound IP₃ (Figure 16b) in the rat PLC δ structure (188). The side chains shown

in Figure 16b make direct contact with the bound IP₃. The arginin and the tyrosine are also found in GTPI whereas the serine is a cysteine in IGTP.

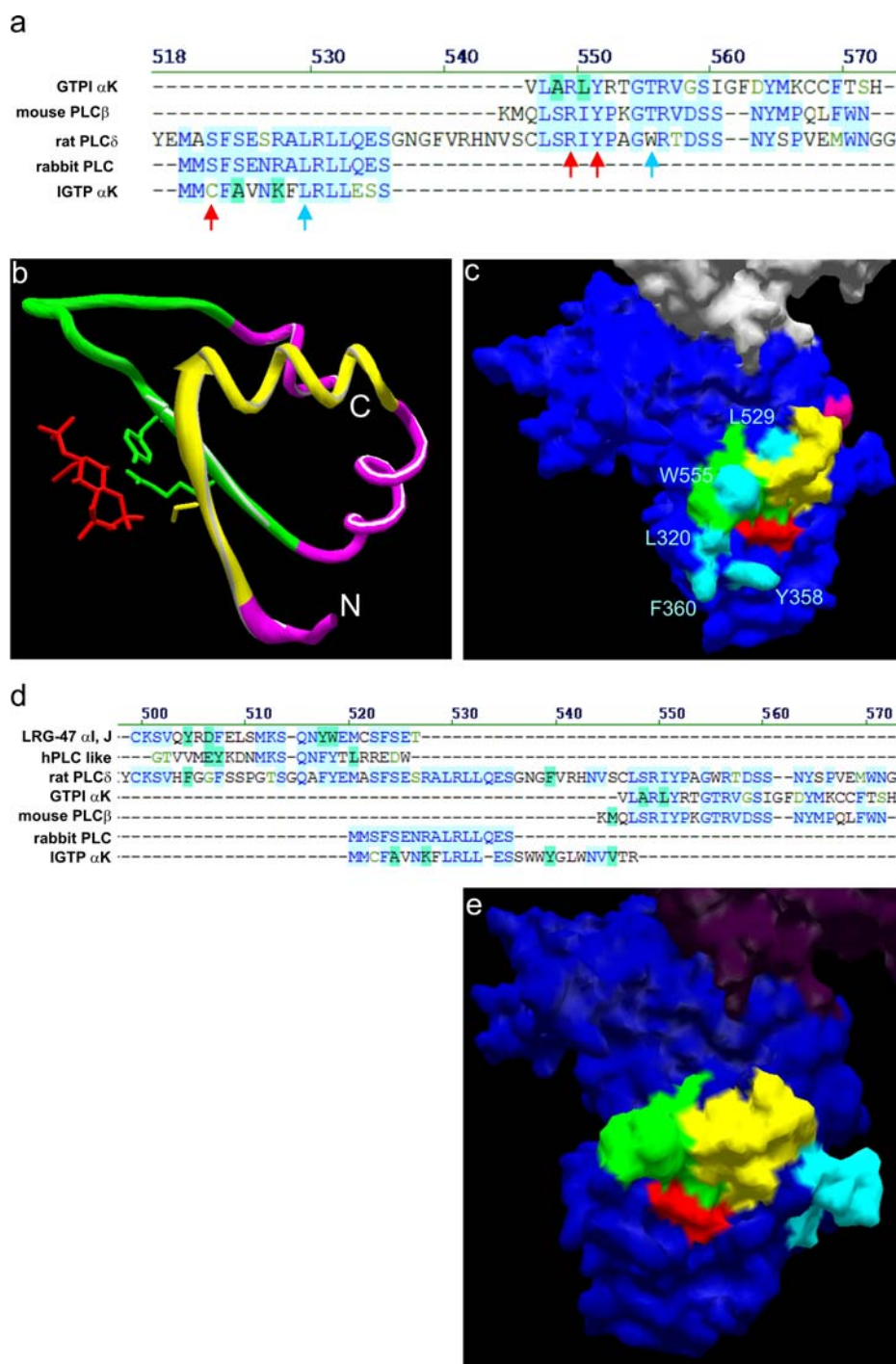


Figure 16

The α K peptides of GTPI and IGTP show homology to different regions of phospholipase C contacting the lipid bilayer; LRG-47 shows homology to human phospholipase C like protein in its α I, J region.

(a) Alignment of the GTPI and IGTP α K peptides with mouse PLC β , rabbit PLC and rat PLC δ (1DJX). The numbers above the alignment indicate the position according to the rat PLC δ sequence. Red arrows point to residues directly contacting the IP₃ molecule in the rat PLC δ structure (188). Light blue arrows point to residues in rat PLC δ implicated in direct contact to membrane (188). (b) Part of the rat PLC δ structure corresponding to the alignment shown in (a). The region homologous to IGTP and GTPI are

shown in yellow and green, respectively. The sidechains shown in (b) are highlighted with red arrows in (a). (c) View of the surface of rat PLC δ facing the membrane. Molecule one is shown in dark blue, the second molecule in the crystal dimer in white. Highlighted are the IGTP homologous region (yellow), the GTPI homologous region (green), the connecting helix (aa 536-546, magenta), the IP₃ molecule (red). Amino acids proposed to directly contact and insert into the lipid bilayer (188) are shown in light blue. (d) Amino acid alignment as in (a) including the α I, J region of LRG-47 and a short sequence of human PLC like protein. The peptide shown for the hPLC like protein was found in a BLAST search for short nearly exact matches for the LRG-47 α I, J region against the mammalian proteome. (e) shows the position of the LRG-47 α I, J homologous region on the rat PLC δ surface. The colour code is as in (c) with the exception that light blue indicates here the LRG-47 α I, J homologous region. (Gene Bank accession numbers are: hPLC-like ϵ NP_006217, ratPLC δ P10688, mouse PLC β NP_062651.1, rabbit PLC CAA89822.1). Vector NTI version 5 was used to create the alignments and the SwissPDB viewer version 3.7 was used to create the structural presentations.

In the rat PLC δ structure the serine and arginine make contact to the 4-phosphate of IP₃ while the tyrosine is proposed to form a sandwich with IP₃ (188). These amino acids were shown or proposed to be essential for PLC function (188, 189). The two regions are also implicated in making direct contact with the membrane (188) (Figure 16c). Residues suggested to form a hydrophobic ridge are shown in light blue among which leucine 529 and tryptophan 555 lie within the regions homologous to IGTP and GTPI, respectively. Tryptophan 555 is absent from IGTP but also from mouse PLC β . Both proteins have a valine instead located only 2 amino acids C-terminal of the tryptophan. The finding is therefore consistent with the α K regions of IGTP and GTPI directly contacting the lipid bilayer possibly interacting with membrane resident phosphatidyl inositol phosphates.

3.12 The α I, J region LRG-47 shows homology to human phospholipase C like protein.

No phospholipase sequences were recovered from the database when the LRG-47 α K region was used to probe the mammalian proteome for short nearly exact matches. However, when the α I, J region of LRG-47 was used to screen the database in the same unbiased manner a short peptide of human PLC like protein (NP_006217) was found to show some homology to the LRG-47 α I, J region. When the full length sequence of human PLC like protein was aligned to rat PLC δ this particular region aligned directly N-terminal of the IGTP homologous region (Figure 16d). Superimposed on the structure of rat PLC δ the LRG-47 α I, J homologous region corresponds to a loop sticking out of the rat PLC δ molecule adjacent to, but not directly involved in contacting, the lipid bilayer (Figure 16c, e). Together, the LRG-47, IGTP and GTPI homologous parts of rat

PLC δ form one side of the IP₃ binding site corresponding to the conserved Y region of phospholipases.

3.13 IIGP1 is associated with the ER.

In contrast to LRG-47, IIGP1 partitioned between cytosol and membrane (Figure 2). To study the sub-cellular localization of IIGP1 L929 cells (Figure 17a-c), peritoneal macrophages (Figure 17d-f), TIB-75 cells (Figure 17g-i) or RAW 264.7 cells (Figure 17j-m) were stimulated with IFN- γ , fixed 24 h later and stained with the anti-IIGP1 165 antiserum or anti-IIGP1 10E7 antibody to detect IIGP1. In all cell types studied IIGP1 localized in a reticular pattern fainting at the periphery. This signal overlapped with ER proteins such as TAP (transporter associated with antigen processing) (Figure 17a-c), Calnexin (Figure 17d-f) and ERP60 (190) (Figure 17g-i) in L929 cells, peritoneal macrophages and TIB-75 cells, respectively. No co-localization with Golgi proteins was detected in these cell-types. The highest degree of overlap of IIGP1 with Golgi proteins was seen in RAW 264.7 cells (Figure 17j-m, white arrows) although also in this cell type the overlap was restricted to single, isolated points. This is in contrast to the findings by Zerrahn et al. (92) reporting IIGP1 to be mainly Golgi associated.

3.14 IIGP1 forms nucleotide and C-terminal domain dependent aggregates after transfection.

When expressed at very low levels in cells not induced with IFN- γ , IIGP1 localized in a reticular pattern similar to the endogenous, IFN- γ induced protein (compare Figure 17 and Figure 18a, b). Higher expression levels resulted in the formation of aggregate-like structures, often of filamentous appearance preferentially accumulating in the centre of the cell (Figure 18c, d) also when expressed at levels comparable to the induction by IFN- γ . No aggregates were ever observed in any IFN- γ induced cell. IIGP1 forms GTP dependent oligomers *in vitro* (150). To examine the nucleotide dependence of these aggregates a nucleotide-binding deficient mutant was generated changing the sequence in the conserved G1 motif from GX₄GKS to VX₄VKS. This mutation has been shown to interfere with nucleotide binding and oligomerization (150). When expressed in L929 cells the mutant protein localized in a reticular pattern (Figure 18e, f) co-localizing with ER proteins (not shown). No aggregation was observed for the mutant protein regardless of expression levels.

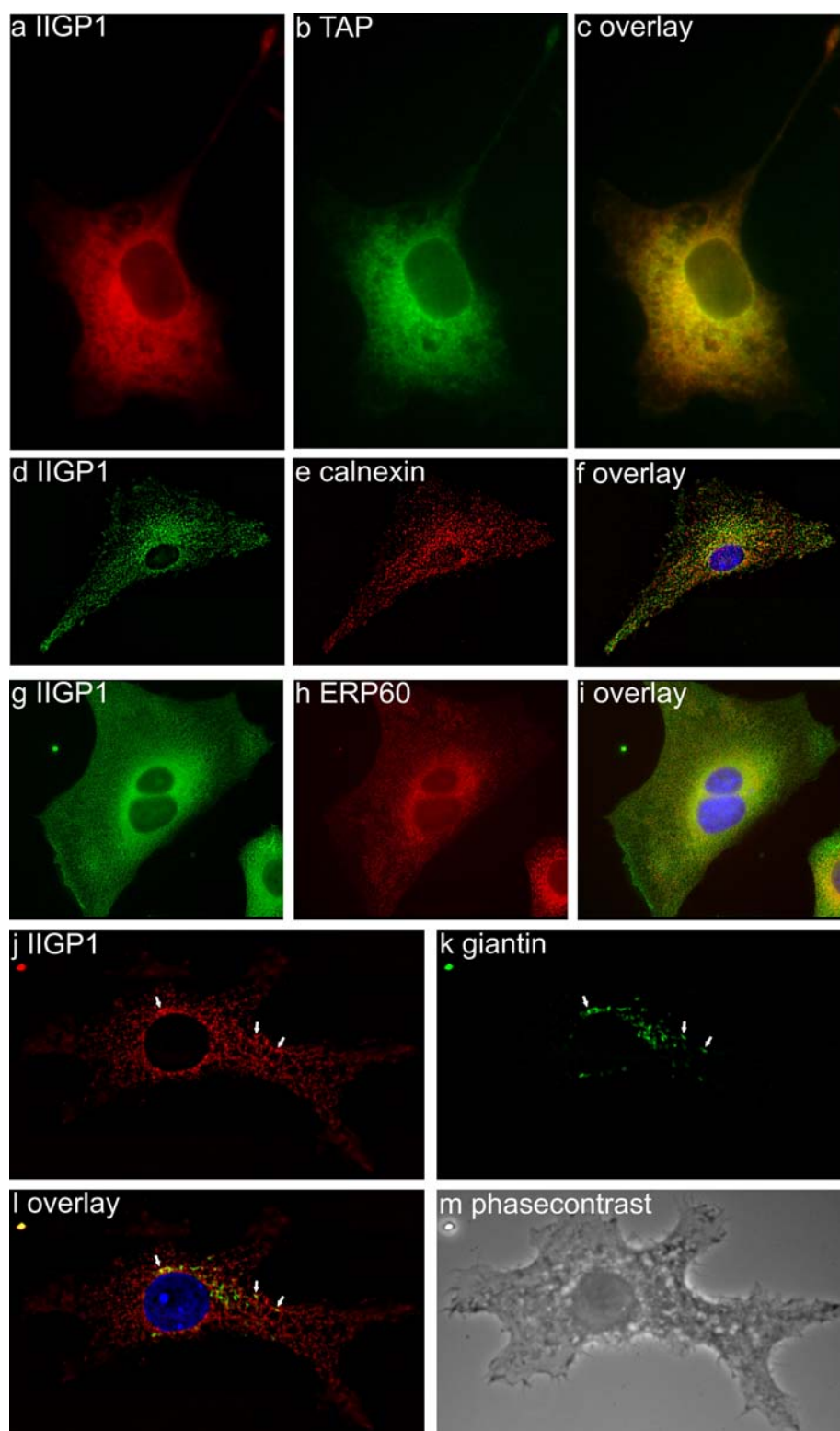


Figure 17

IIGP1 localizes to the endoplasmic reticulum in L929 cells, TIB-75 cells and primary peritoneal macrophages.

L929 cells (a-c), peritoneal macrophages (d-f), TIB-75 cells (g-i) or RAW 264.7 cells (j-m) were induced with IFN- γ for 24h, fixed and stained for the indicated proteins. IIGP1 was stained with 165 in (a) and (b). In (d) and (g) IIGP1 was stained with 10E7 to allow co-staining with the other reagents. IIGP1 co-localized with ER proteins (a-i). Only minor co-localization was observed for the Golgi protein giantin in RAW 264.7 cells (j-m). Arrows point sides of possible overlap. The images were taken with a Zeiss Axioplan II microscope equipped with a cooled CCD camera (Quantix) using the Metamorph software (version 4.5). The magnification is 1000x. (d-f and j-l) show planes of 3D deconvoluted Z-series. Nuclei were labelled with DAPI.

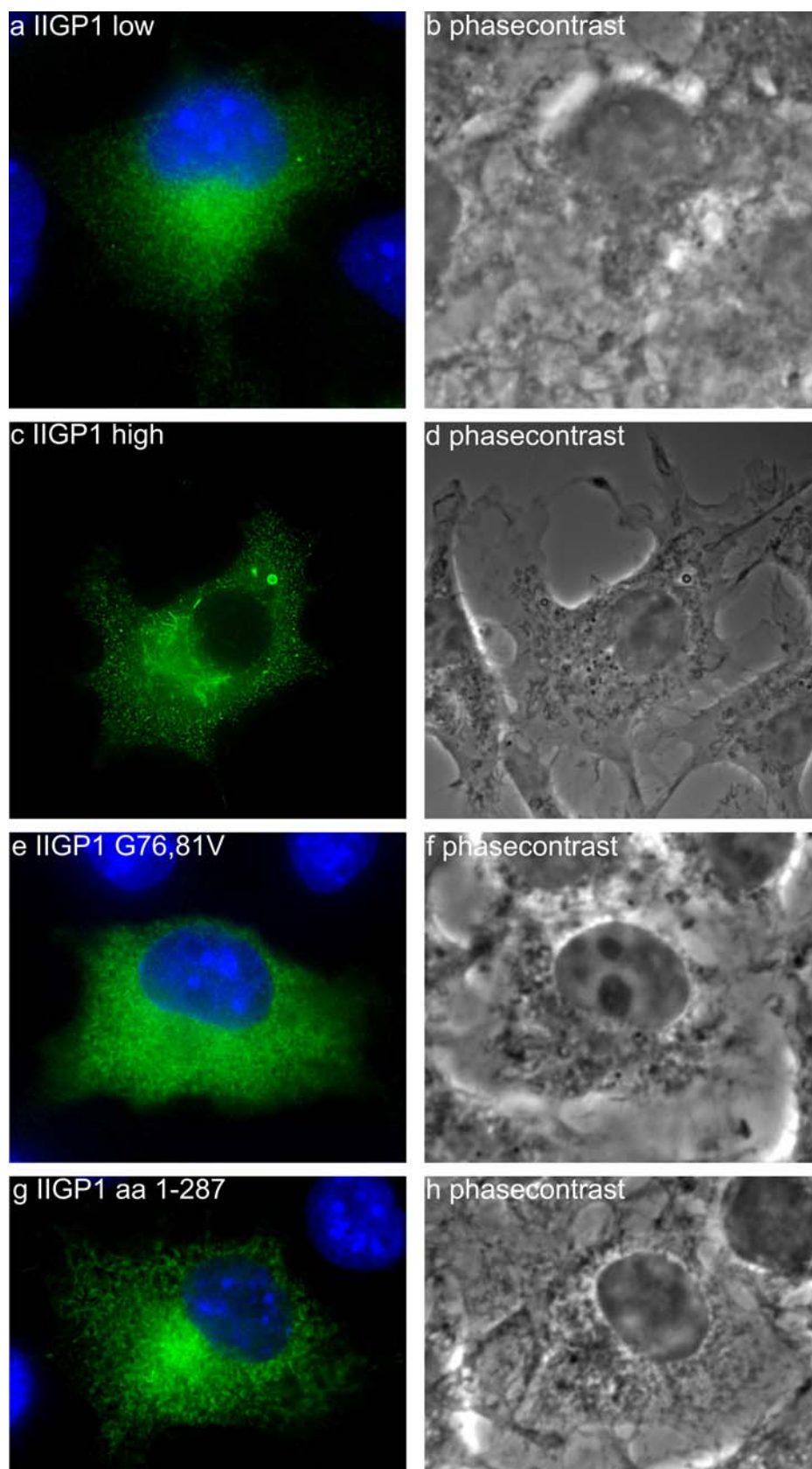


Figure 18

Expression of IIGP1 in resting cells results in a nucleotide and C-terminal domain dependent formation of IIGP1 containing aggregates; membrane association is nucleotide independent.

Resting L929 cells were grown on coverslips and transfected with wild type (a-d) or mutant IIGP1 (e-h). Cells were fixed 24h later and stained with 165 anti-IIGP1 antiserum. Low IIGP1 expression levels resulted in a pattern similar to the endogenous protein (a, b). Expression levels comparable to the

endogenous protein, or higher, resulted in formation of aggregate-like structures tending to accumulate in an adnuclear region (c, d). No aggregates were observed for a nucleotide binding deficient mutant (e, f) which still bound to membranes. Likewise, no aggregates were observed when the C-terminal domain was deleted (g-h). The images were taken with a Zeiss Axioplan II microscope equipped with a cooled CCD camera (Quantix) using the Metamorph software (version 4.5). The magnification is 630x. Nuclei were labelled with DAPI.

The C-terminus of IIGP1 has been implicated in oligomer formation *in vitro* (150). When the C-terminal domain following α F in the IIGP1 structure was deleted, the protein still localized to membranes (Figure 18g, h) although the membrane association appeared rather unspecific. However, no aggregate formation was observed independent of the expression level. Thus, aggregate formation but not membrane binding is dependent on the presence of an intact nucleotide binding site and the C-terminal domain. Nevertheless the C-terminal domain seems to contribute in some way to the exact targeting of IIGP1 to sub-cellular membranes.

3.15 IIGP1 is N-terminally myristoylated.

IIGP1 contains a predictable site for N-terminal myristoylation (191), a C14 lipid modification. In the sequence MGQLFSS glycine 2 was predicted to be myristoylated (PSORT II prediction program, <http://psort.nibb.ac.jp/form2.html>). To validate the significance of this prediction L929 cells were induced with IFN- γ and subjected to a Triton X-114 partitioning assay (Figure 19a). After a temperature shift lipid modified proteins partition in the detergent phase (192). Equal amounts of the detergent and aqueous phases were subjected to SDS-PAGE and Western Blotting. Endogenous IIGP1, induced by IFN- γ , partitioned roughly 1:1 between the two phases (Figure 19a). To determine whether the predicted N-terminal myristoylation site is responsible for the observed 1:1 partitioning glycine 2 was mutated to alanine (193). In contrast to the G2A mutant which was exclusively found in the aqueous phase, wild type IIGP1 partitioned comparable to the endogenous protein (Figure 19a). IIGP1 is the only member among the published p47 GTPases containing a predictable lipid modification sequence. Consistent with the absence of such predictable sites LRG-47 partitioned exclusively in the aqueous phase (Figure 19a). The same result was found for IGTP, TGTP and IRG-47 (not shown).

As shown in Figure 19a only ~50% of the endogenous IIGP1 protein was found in the detergent phase. Two conceivable explanations for this behaviour are: Firstly, only 50% of the cellular protein pool is myristoylated. Second, the assay is only 50% efficient for IIGP1, or both. To distinguish between the two possibilities, the first aqueous phase A_0

was consecutively subjected to a series of Triton X-114 extractions ($A_1, D_1; A_2, D_2...$) (Figure 19b). The ratio of ~50% between the two phases remained constant up to the fifth partition (A_4, D_4). This result is consistent with the assay being only 50% efficient for IIGP1 implying that practically all IIGP1 molecules are lipid modified.

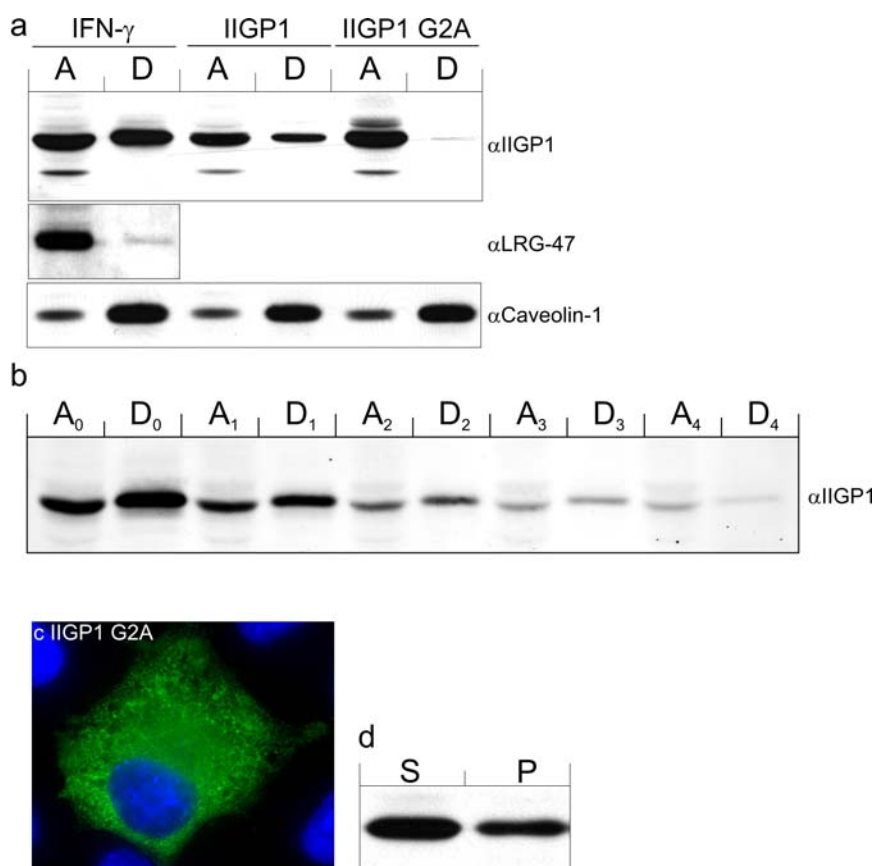


Figure 19
IIGP1 is N-terminally myristoylated.

(a) L929 cells were induced with 200U/ml IFN- γ or transfected with wild type or G2A mutant IIGP1 and subjected to Triton X-114 assays 24h later. Equal volumes of the detergent and aqueous phases were loaded and the partitioning of IIGP1, LRG-47 and Caveolin-1 was monitored by Western Blotting. IIGP1 was detected with 165, LRG-47 with A19 and Caveolin-1 with N20. Caveolin-1 served as load control for the detergent phase. (b) Triton X-114 partitioning assay with lysates of IFN- γ induced L929 cells as in (a). The aqueous phases were repeatedly subjected to Triton X-114 extractions. Note that the ratio between the aqueous and detergent phases remained constant up to the fifth partition. (c) Immunofluorescence image of a L929 cell transfected with the IIGP1 G2A mutant stained with 165. (d) Western Blot of hypotonic lysates made from IIGP1 G2A transfected L929 cells 24h after transfection. The image was taken with a Zeiss Axioplan II microscope equipped with a cooled CCD camera (Quantix) using the Metamorph software (version 4.5). The magnification is 630x. Nuclei were labelled with DAPI.

To analyze the importance of the N-terminal myristoyl-modification for the association with cellular membranes the G2A mutant IIGP1 was transiently expressed in L929 cells and visualized by immunofluorescence (Figure 19c) or subjected to a hypotonic extraction (Figure 19d). The mutant protein localized in a diffuse, granular pattern with an underlying reticulum. The hypotonic extraction showed that a considerable amount of

the protein was still found in the pellet although the ratio was shifted to the disadvantage of the pellet fraction (compare with Figure 2).

To summarize, IIGP-1 carries an N-terminal myristoyl-group which facilitates, but is not essential for membrane association.

3.16 IIGP1 is targeted to endomembranes by the N-terminal domain and to the plasma membrane by the G-domain.

Analogous to LRG-47 (Figure 12) the individual structural domains of IIGP1 were systematically analyzed for membrane association activity (Figure 20a). The N-terminal domain localized to cellular membranes when fused to the N-terminus of EGFP (Figure 20c) although in different from the endogenous protein (Figure 17). This membrane association is myristoyl-dependent as the G2A mutant N-terminal domain appeared completely soluble, indistinguishable from EGFP alone accumulating in the nucleus (Figure 20b, c). This result was confirmed by hypotonic extraction and Western Blotting of transfected L929 cells (Figure 20g). The G2A mutation led to complete shift into the supernatant. Calnexin served as load control for the pellet fraction.

The G-domain associated exclusively with the plasma membrane showing an additional cytosolic stain (Figure 20e). This localization is essentially the same as for the G-domain of LRG-47 (Figure 12c) including the accumulation on membrane ruffles (Figure 20e, white arrows). When fused to EGFP the C-terminal domain following αF appeared completely soluble (Figure 20f).

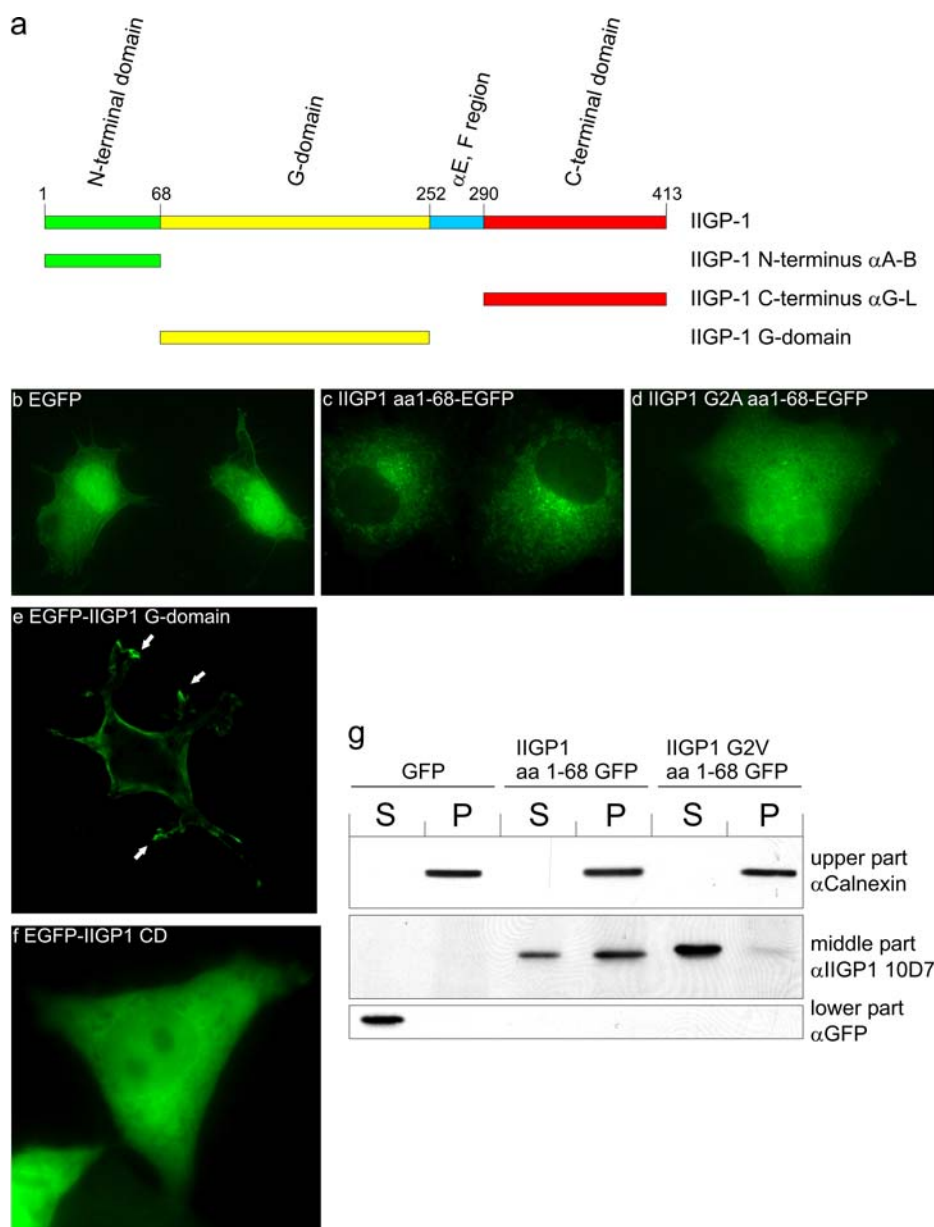


Figure 20

IIGP1 is targeted to endomembranes by the N-terminal domain in a myristoyl-dependent manner and to plasma membrane by the G-domain.

The linear domain organization IIGP1 according to the IIGP1 crystal structure is shown in (a). Isolated domains were expressed in resting L929 cells (b-g). The N-terminal domain was C-terminally fused to EGFP, the G-domain was C-terminally Flag-tagged and the C-terminal domain was fused N-terminally to the C-terminus of EGFP. Transfected cells were fixed with 3% PFA 24h after transfection and stained with anti-Flag M2 antibody (e). The N-terminal domain targeted IIGP1 to endomembranes in a glycine 2 dependent manner (b-d). The G-domain associated with the plasma membrane accumulating on membrane ruffles (e) (arrows). A diffuse cytosolic stain was also apparent. No internal membranes were stained. (f) The C-terminal domain appeared completely soluble. (g) Western Blot with hypotonic lysates of L929 cells 24h after transfection with the indicated expression constructs. The membrane was cut after blotting and the upper, middle and lower parts were incubated with the respective serological reagents. The presence of IIGP1 in the pellet is dependent on glycine 2. The images were taken with a Zeiss Axioplan II microscope equipped with a cooled CCD camera (Quantix) using the Metamorph software (version 4.5). The magnification is 630x. (e) shows a plane of a 3D deconvoluted Z-series.

3.17 The p47 GTPases bind to membrane with different strength.

The p47 GTPases use different mechanisms to associate with membrane. To analyze whether this is reflected in the strength the p47 GTPases bind to it, membranes isolated from IFN- γ induced L929 cells were incubated in a variety of different buffers and spun at 100000g. The pellet was resuspended in the same volume as the supernatant (PBS, 0.5% SDS) and equal volumes of the pellets and the supernatants were subjected to Western Blotting (Figure 21). The p47 GTPases behaved very diverse in this assay. LRG-47 and IGTP showed a low or absent cytosolic pool and behaved essentially like transmembrane proteins such as Calnexin in this assay only transferred into the supernatant by detergents such as Triton X-100 and digitonin (not shown). In contrast, IIGP1 and TGTP which had a considerable cytosolic pool (see also Figure 2) behaved like peripheral membrane proteins being released from membrane by sodium carbonate (192). The Triton X-100 resistant fraction of IIGP1 and TGTP could be aggregated protein or lipid raft associated protein (194, 195). Consistent with the latter also Caveolin-1 was found in the Triton X-100 resistant fraction and low, possibly significant co-localization of IIGP1 and Caveolin-1 was observed in TIB-75 cells (not shown).

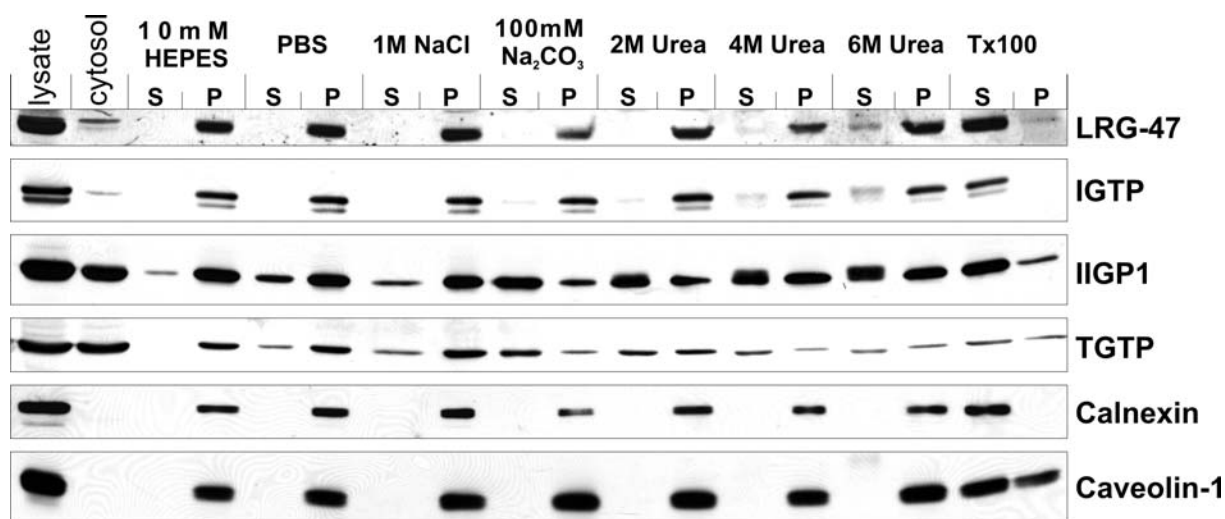


Figure 21

The p47 GTPases show different strength of membrane association.

L929 cells were induced with IFN- γ for 48h and isolated membranes were subjected to wash off experiments with the indicated buffers. The final 100000g pellets were resuspended in PBS, 0.5% SDS. Equal volumes of the supernatants and pellets were subjected to Western Blotting (A19 for LRG-47, α IGTP clone7, 165 for IIGP1, A20 for TGTP, SPA-865 for Calnexin and N20 for Caveolin-1). Note that the wash off profiles of LRG-47 and IGTP are virtually identical to the profiles Calnexin and Caveolin-1. IIGP1 and TGTP showed a different behaviour than the two GMS GTPases.

3.18 The myristoyl-group of IIGP1 does not contribute to the strength of membrane association.

To determine the influence of the N-terminal myristoyl-modification on the strength of membrane association of IIGP1, the IIGP1 G2A mutant protein was expressed in L929 cells and isolated membranes were subjected to membrane extraction experiments (Figure 22). As control the wash off profile of transfected wild type IIGP1 was determined and found to be essentially the same as the endogenous protein (Figure 21). The G2A mutant IIGP1 behaved very similar to the wild type protein despite a markedly higher Triton X-100 insoluble fraction. The same profile was found for the recombinant, not myristoylated IIGP1 bound to artificial, uni-lamellar lipid vesicles *in vitro* (The experiment with the recombinant IIGP1 was conducted by Katja Sabel and published in her “Diplomarbeit”). The myristoyl-independent interaction of IIGP1 with membranes therefore seems to be independent of other cellular proteins.

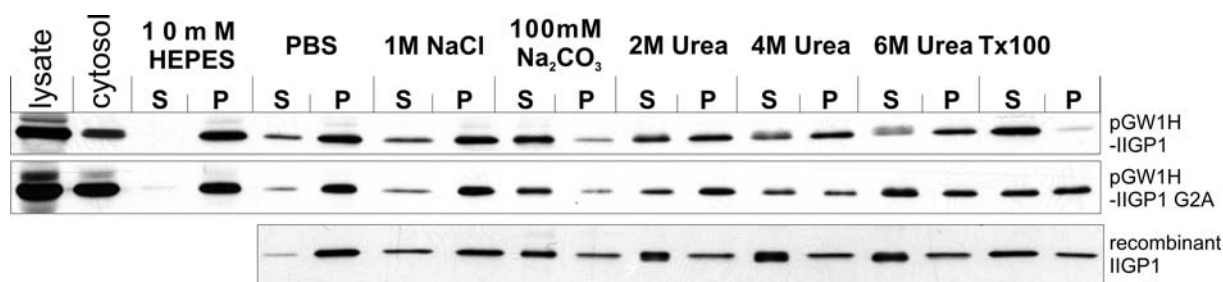


Figure 22

Myristoyl-modification of IIGP1 does not contribute to the strength of membrane association.

L929 cells were transfected with wild type or G2A mutant IIGP1 and isolated membranes were subjected to wash off experiments with the indicated buffers 24h later. The final 100000g pellets were resuspended in PBS, 0.5% SDS. Equal volumes of the supernatants and pellets were subjected to Western Blotting. Note that both wash off profiles are very similar. Purified recombinant, not myristoylated IIGP1 was incubated with artificial uni-lamellar phosphatidylserine vesicles and subjected to the same wash off procedure. The wash off profile was similar to the transfected proteins. (The experiment with the recombinant IIGP1 was conducted by Katja Sabel)

3.19 Localization of tagged GMS GTPases in L929 cells

Figure 23 shows experiments conducted to determine the sub-cellular localization of the GMS p47 GTPases with tagged constructs. Due to the lack of an appropriate serological reagent suitable for immunofluorescence studies the GTPI open reading frame was fused to the C-terminus of EGFP and expressed in L929 cells (Figure 23a-d). The EGFP-GTPI fusion protein accurately localized to the Golgi apparatus stained with anti-giantin antibody. In addition a diffuse cytosolic and vesicular stain was observed. This pattern was virtually identical to the pattern shown by the GTPI α K peptide fused to EGFP (Figure 15b-d).

To analyze a possible interference of the EGFP modification on the localization of GTPI, the IGTP open reading frame was modified in the same way and expressed in L929 cells. EGFP-IGTP localized to the ER (Figure 23h-j) in the same manner as the endogenous protein (Figure 23e-g). These results are in agreement with Taylor et al. (93). The N-terminal modification of IGTP did therefore not influence its sub-cellular localization at least at this level of resolution. However, the influence of tags and fusions of the p47 GTPases on their sub-cellular localization and behaviour has to be taken with caution since the same N-terminal modification resulted in mislocalization of LRG-47 (Figure 23k-m).

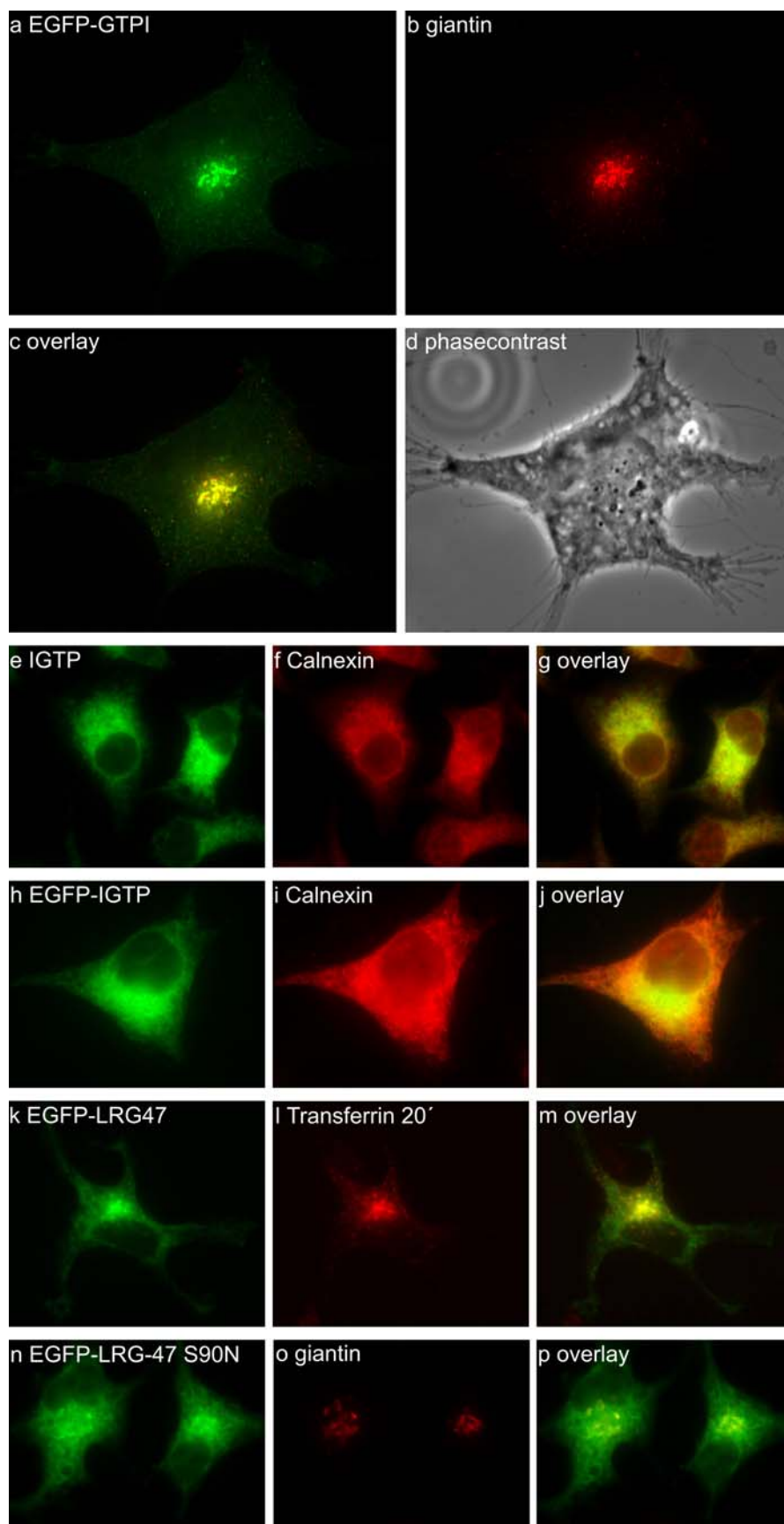


Figure 23

Localization of tagged GMS p47 GTPases in L929 cells

L929 cells were transiently transfected with the indicated constructs or induced with 200U/ml IFN- γ , fixed 24h later and stained by indirect immunofluorescence. (a-d) show a cell transfected with pEGFP-C3-GTPI. The fusion protein co-localized with giantin in an adnuclear region. Note the additional diffuse

and vesicular stain throughout the cytoplasm. (e-g) Endogenous, IFN- γ induced IGTP co-localized with Calnexin in L929 cells. (h-j) The transfected EGFP-IGTP showed a very similar pattern to the endogenous protein overlapping with Calnexin. Both proteins tended to be more intense in an adnuclear region compared to Calnexin. (k-l) L929 cell transfected with pEGFP-C3-LRG-47 and incubated with Alexa-546 conjugated Transferrin for 20'. EGFP-LRG-47 accurately co-localized with recycling endosomes in the centre of the cell and additional transferrin containing vesicles in the periphery. (n-p) EGFP-LRG-47 S90N co-localized with giantin. The images were taken with a Zeiss Axioplan II microscope equipped with a cooled CCD camera (Quantix) using the Metamorph software (version 4.5). The magnification is 630x.

EGFP-LRG-47 localized to Transferrin positive early and recycling endosomes and additional membranes of unknown origin which is in striking contrast to the endogenous protein (Figure 4-7). No co-localization with Golgi and ER proteins was detected for the EGFP-LRG-47 fusion protein (not shown). A C-terminal Flag-tag had the same effect on the intracellular localization as the C-terminal Flag tagged and the N-terminal EGFP-fused proteins accurately co-localized when expressed by co-transfection in L929 cells (not shown). Interestingly, the mislocalization was dependent on an intact nucleotide binding site because EGFP-LRG-47 S90N, the nucleotide binding deficient mutant, had the same localization as the endogenous protein (Figure 23n-p) overlapping with giantin.

3.20 Expression of TGTP in cells

In a hypotonic extraction of IFN- γ induced L929 cells the majority of TGTP was soluble (Figure 2). However a considerable fraction of the protein was found in the pellet. To study the sub-cellular localization of TGTP, L929 cells were induced with IFN- γ for 24h, fixed and stained with the anti-TGTP A20 antiserum. A20 detected an IFN- γ induced protein of the predicted size of TGTP in L929, TIB-75 and various other cell types by Western Blotting (Figure 1 and not shown). In contrast to the Western Blot results no IFN- γ induced signal was detected in L929 cells using A20 (not shown). Surprisingly, transfected TGTP was clearly recognized by A20 staining enigmatic fibrous structures surrounding the nucleus (Figure 24a-c). The same behaviour was shown by TGTP carrying a C-terminal Flag tag detected with the anti-Flag M2 antibody (Figure 24d-f). The TGTP containing filamentous structures were also observed in TGTP-Flag transfected cells stimulated with IFN- γ (not shown). Apparently expression of TGTP had a strong impact on the cellular morphology as TGTP expressing cells could be easily distinguished from untransfected cells in the phasecontrast (Figure 24f). No co-localization of these filament-like structures with F-actin was observed (Figure 24d-f). To analyze a potential role of microtubules in stabilization and formation of the TGTP containing filaments, L929 cells were transfected with TGTP-Flag and

simultaneously treated with nocodazole, a microtubule disrupting drug (196), for 42h. TGTP-Flag was detected with the anti-Flag M2 antibody by indirect immunofluorescence. The disruption of microtubules had no influence on the filament formation (Figure 24g-i). The expression of TGTP had a strong influence on the morphology of the ER in the transfected cells (Figure 24j-l). In extreme cases the complete ER marked by ERP60 or Calnexin (not shown) was crushed within cages formed by the TGTP containing filaments next to the nucleus (Figure 24l). The adnuclear, cage-like organization of these filaments was disrupted after nocodazole treatment indicating that microtubules are required for their structural organization. No deformation of the ER was ever observed in any IFN- γ induced cell. The Golgi apparatus was also buried within these cage-like structures (not shown). To analyze whether the fibre formation is dependent on the integrity of the nucleotide binding site of TGTP a mutant was generated changing the sequence in the conserved G1 motif from GX₄GKS to VX₄VKS. This mutation has been shown to abolish nucleotide binding of IIGP1 (150). Expression of the G1 mutant TGTP resulted in a diffuse cytosolic pattern having no influence on the morphology of the ER defined by ERP60 (Figure 24m-o) and Calnexin (not shown).

Another cellular structure affected by the expression of TGTP was the vimentin containing intermediate cytoskeleton. The V9 antibody used to stain vimentin does not recognize mouse vimentin. In addition the anti-Vimentin V9 antibody and anti-Flag M2 antibody are both mouse antibodies making simultaneous staining impossible. Therefore TGTP-Flag was expressed in human HeLa cells by co-transfection with pEGFP (Figure 24p). The efficiency of co-transfection was about 90%. In HeLa cells the same TGTP-Flag containing filaments as in mouse cells were observed. The filaments were often accompanied by constrictions of the nucleus (Figure 24p). Co-transfected cells were identified by EGFP expression and the intermediate cytoskeleton was visualized by staining with the V9 antibody. The vimentin containing intermediate filaments were obviously deformed adopting a structure resembling the TGTP containing filamentous cages. The distribution of Vimentin in an untreated HeLa cell is shown in Figure 25m.

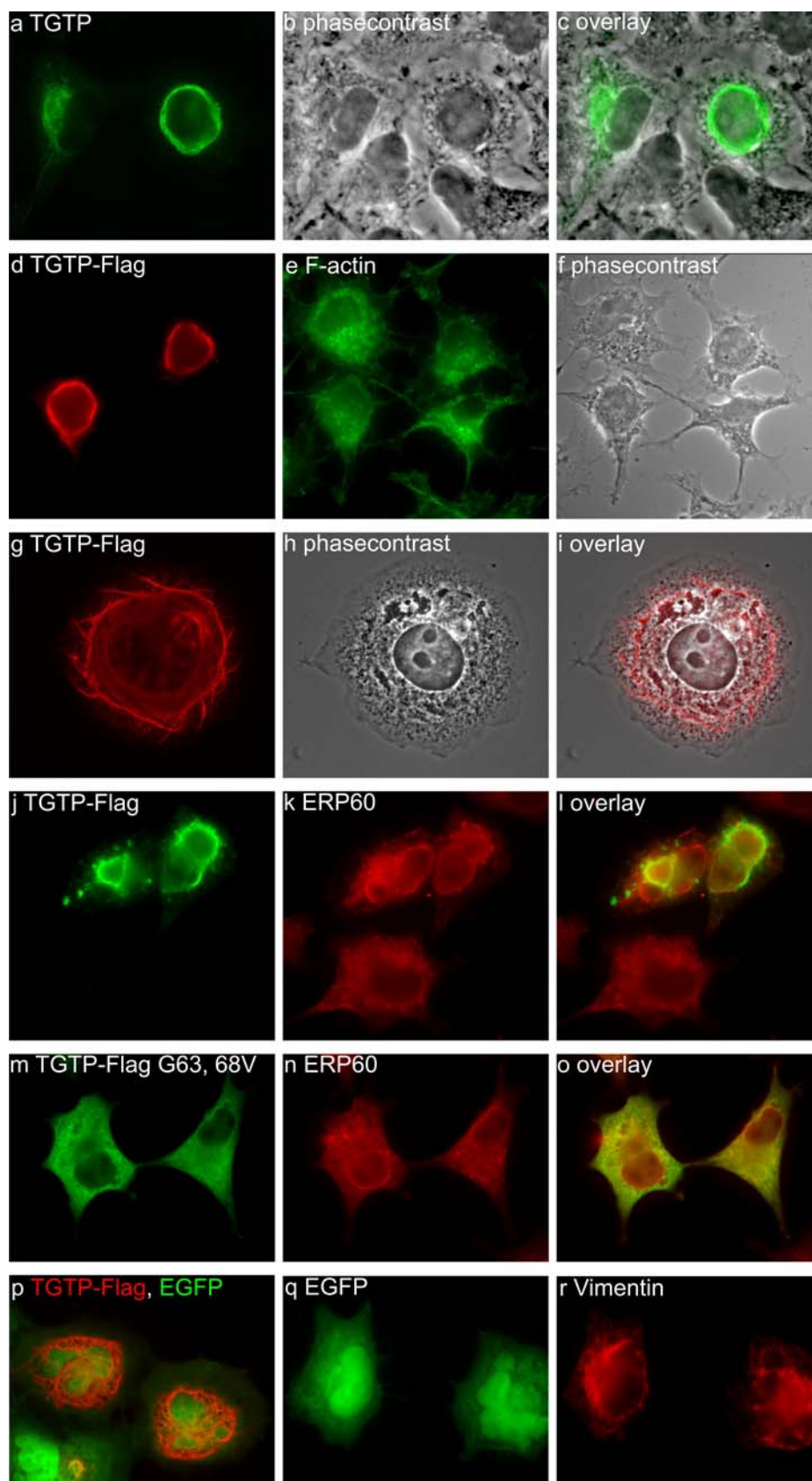


Figure 24

Expression of TGTP in cells

L929 (a-o) or HeLa cells (p-r) were transiently transfected with wild type TGTP (a-c), TGTP-Flag (d-o) or TGTP-Flag and pEGFP (p-r). Cells were fixed 24h or 42h (g-i) later and stained by indirect immunofluorescence. Wild type TGTP was detected with A20 and TGTP-Flag with M2. TGTP and TGTP-Flag were detected within filaments surrounding the centre of the cell (a-f). Note the distinct morphology of the transfected cells (f). (g-i) L929 cell transfected with TGTP-Flag and simultaneously

treated with nocodazole. (j-l) shows the deformation of the ER defined by ERP60 caused by TGTP-Flag expression. Note the distinct pattern of ERP60 in the untransfected cell. (m-o) No deformation of the ER was observed when TGTP-Flag G63, 68V was expressed. The mutant TGTP-Flag localizes in a diffuse cytosolic pattern. (p) shows HeLa cells co-transfected with pEGFP-C3 and a TGTP-Flag expression plasmid. (q, r) shows two HeLa cells co-transfected as in (p) but stained for vimentin instead of M2. The images were taken with a Zeiss Axioplan II microscope equipped with a cooled CCD camera (Quantix) using the Metamorph software (version 4.5). The magnification is 630x.

3.21 Expression of IIGP1-His in cells

Also the expression of IIGP1 and in particular of IIGP1-His, carrying a C-terminal 6xhistidine modification, had an influence on the morphology of the ER and intermediate cytoskeleton (Figure 25). The expression of IIGP1 in resting L929 cells (Figure 18c) and other cell types resulted in the formation of IIGP1 containing aggregates. These aggregate-like structures tended to accumulate in the centre of the cell. IIGP1-His, a C-terminal 6xhistidine tagged version defective in cooperative GTP hydrolysis and nucleotide dependent oligomerization (150), had the tendency to form bag-like structures in an adnuclear region constricting the ER defined by Calnexin into these bags (Figure 25a-c). Similar structures were also observed for the wild-type protein although less pronounced. The formation of the IIGP1-His aggregates was not dependent on an intact microtubule cytoskeleton as they were observed in cells treated with nocodazole (Figure 25d-f). However, the organization of the aggregated into the bag-like structures is microtubule dependent (Figure 25d-f). Similar to TGTP the expression of IIGP1-His was accompanied with morphological changes of the vimentin containing intermediate cytoskeleton (Figure 25g-i). The vimentin filaments appear to align outside of the IIGP1 bag-like structures in HeLa cells. Analogous to TGTP and wild type IIGP1 the formation of cellular aggregates of IIGP1-His was nucleotide dependent (Figure 25j-l). It is worth mentioning again that none of these morphological alterations has ever been observed in any IFN- γ stimulated cell despite the massive induction of IIGP1 and TGTP (Figure 1).

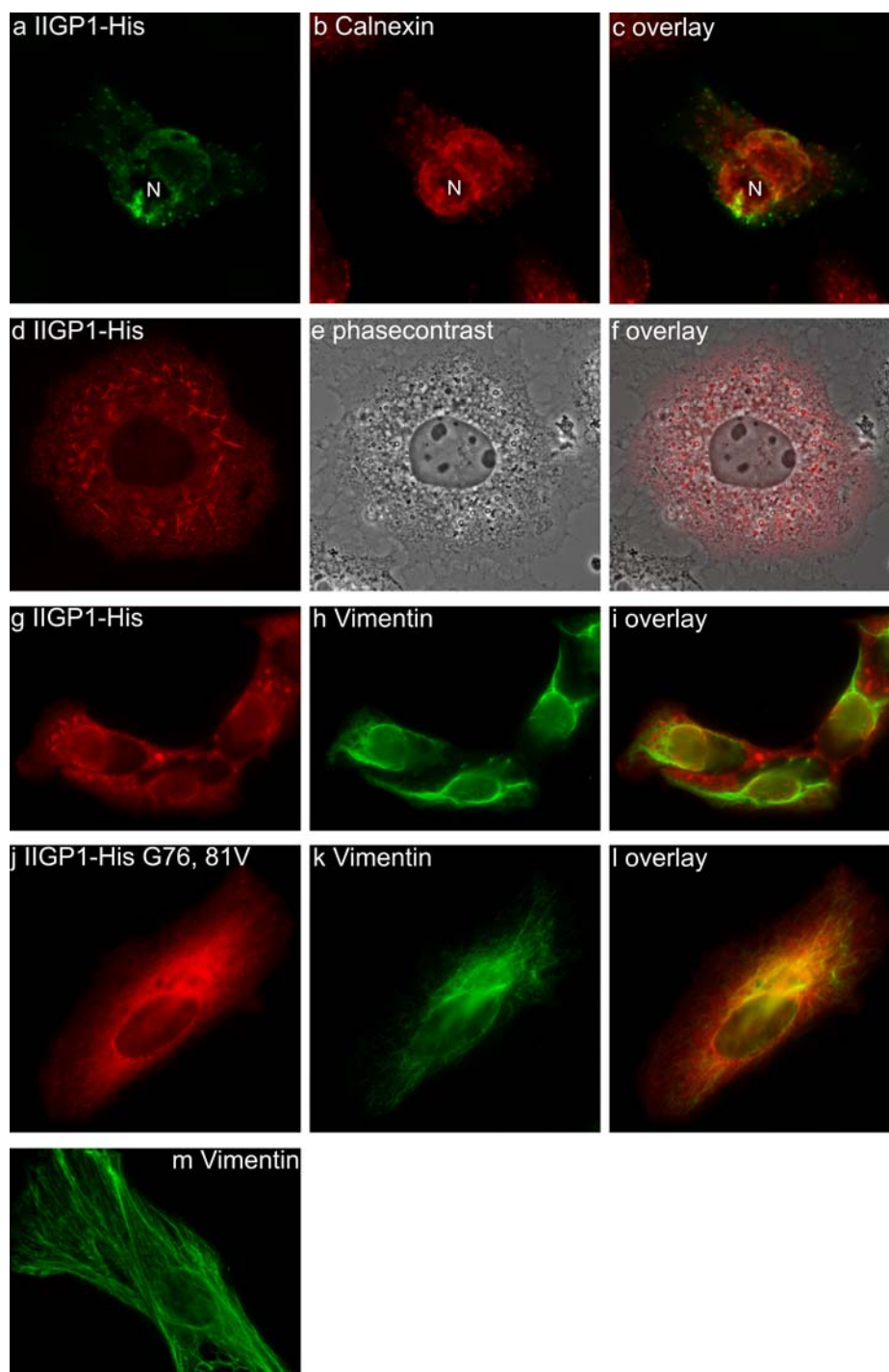


Figure 25

Expression of IIGP1-His in cells

L929 (a-f) or HeLa cells (g-l) were transfected with an IIGP1-His driving expression plasmid and stained by indirect immunofluorescence 24 or 42h (d-f) later. (a-c) IIGP1-His expression caused constriction of Calnexin into an adnuclear region. The nucleus is marked with N. Note that IIGP1-His appears to be outside of Calnexin. (d-f) L929 cell transfected with IIGP1-His and simultaneously treated with nocodazole for 42h. IIGP1-His localized in short filamentous aggregates often with round or triangle-like structures on one pole. Note that the round and triangular structures surround vesicular structures visible in the phasecontrast (f). (g-i) shows HeLa cells transfected with IIGP1-His. Vimentin surrounded the IIGP1-His containing bag-like structures. (j-l) IIGP1-His G76, 81V localized in a diffuse reticular pattern and no or little reorganization of Vimentin was observed. (m) Distribution of Vimentin in an untreated HeLa cell. The images were taken with a Zeiss Axioplan II microscope equipped with a cooled CCD camera (Quantix) using the Metamorph software (version 4.5). The magnification is 630x. (a-c) show planes of a 3D deconvoluted Z-series.

3.22 IIGP1 accumulates at *Toxoplasma gondii* containing parasitophorous vacuoles.

Primary astrocytes isolated from neonatal mouse brains were stimulated with 100U/ml IFN- γ for 24h and pulse-infected with the ME49 strain of *Toxoplasma gondii* at a multiplicity of infection (MOI) of 20. After 2h the cells were thoroughly washed to remove extracellular parasites and fixed with 3% PFA either immediately (Figure 26a-e) or 24h later (Figure 26f, g). IIGP1 was stained with the anti-IIGP1 10E7 antibody and the nuclei of the host cells and parasites were visualized by DAPI staining. The *T. gondii* parasites were identified by their 6 μ m long banana shaped particles in the phase contrast and the presence of a DAPI labelled nucleus. IIGP1 was observed to accumulate markedly around many parasites 2h after infection (solid arrowhead in Figure 26a, b) although not all parasites were found to be aligned by IIGP1 (line arrowhead). In many cases IIGP1 tended to accumulate around one pole of the parasite (Figure 26c-e shows a representative parasite). The IIGP1 stain probably corresponds to a membrane ruffle appearing darker in the phase contrast (Figure 26d).

Within 24h intracellular *Toxoplasma* parasites divide and form rosettes surrounded by the membrane of the parasitophorous vacuole (197). In some cases, IIGP1 was also found to localize around parasitophorous vacuoles after 24h (Figure 26f, g) (solid arrowhead in Figure 26f, g). The proportion of parasitophorous vacuoles showing IIGP1 nearby accumulation appeared reduced compared to the 2h time point. In particular vacuoles containing a higher number of parasites appeared to be devoid of IIGP1 accumulations (line arrowhead in Figure 26 f, g).

No accumulation of IIGP1 around vacuoles harbouring *Salmonella typhimurium* was detected in B6m29 mouse fibroblast-like cells isolated from p53^{-/-} C57BL/6J mouse embryos (175) (Figure 26h-l). The cells shown were induced with 100U/ml IFN- γ for 48h and infected with *Salmonella typhimurium* at a MOI of 9000 for 30', washed several times, incubated for 2h in the presence of 100 μ g/ml gentamycin and finally fixed with 3% PFA. IIGP1 was stained with the anti-IIGP1 165 antiserum and the DNA of host cells and bacteria was visualized by DAPI staining. As shown in Figure 26h-l IIGP1 does not accumulate near the bacteria as it does around vacuoles containing *Toxoplasma gondii*. The invasion of the B6m29 cells by *Salmonella typhimurium* was evaluated by staining for LAMP1, a membrane protein recruited to *Salmonella* containing vacuoles (not shown) (198).

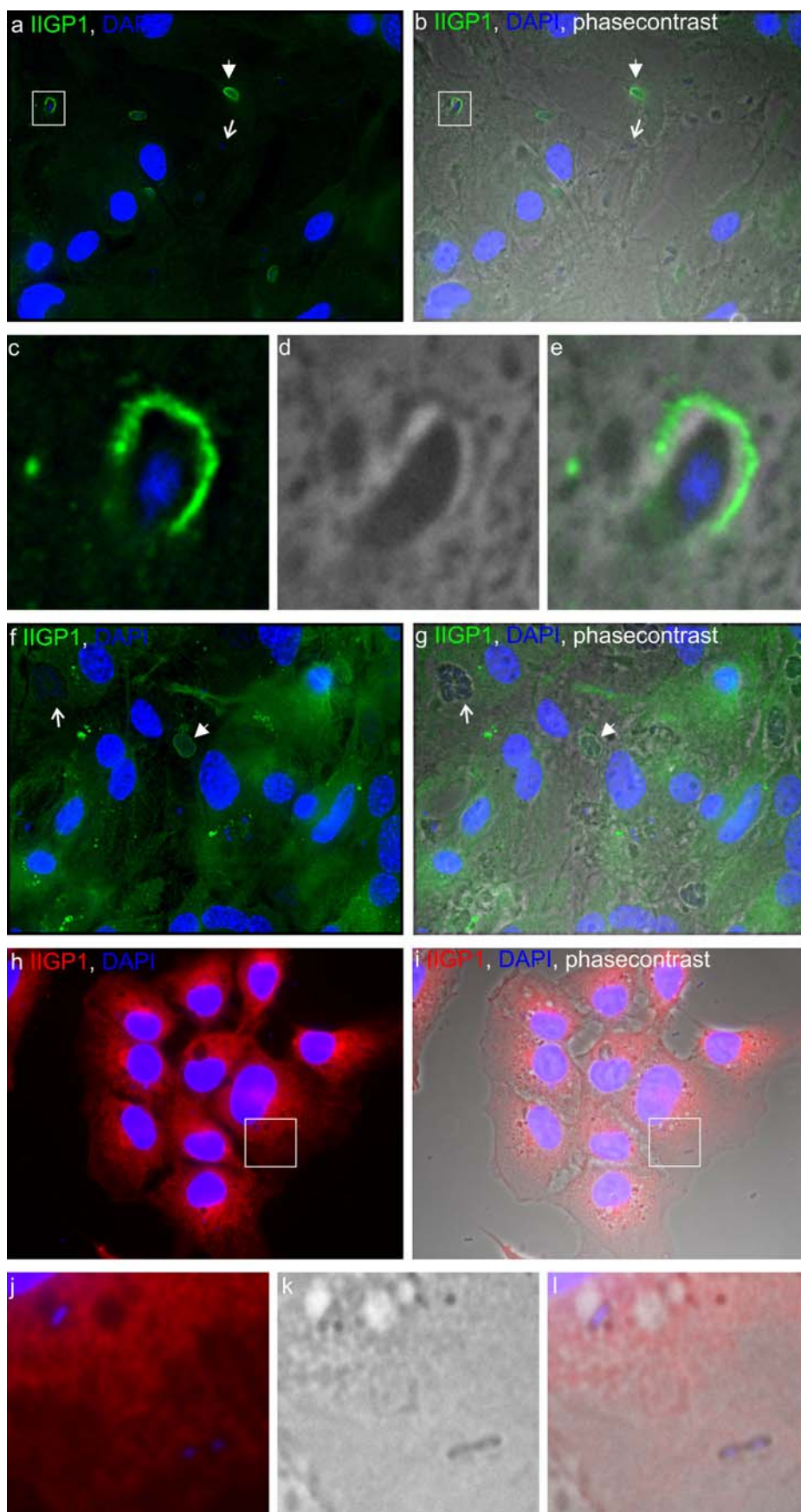


Figure 26**IIGP1 accumulates around parasitophorous vacuoles in *T. gondii* infected primary murine astrocytes.**

Primary mouse astrocytes were induced with 100U/ml IFN- γ for 24h and inoculated with the *Toxoplasma gondii* (strain ME49) at a MOI of 20. After 2h the cells were thoroughly washed several times to remove extracellular parasites and fixed immediately (a-e) or incubated 24h before fixation (f, g). The cells in (a-g) were stained by indirect immunofluorescence with the 10E7 antibody to detect IIGP1 and DAPI to mark nuclei of the host cells and parasites. Solid arrowheads point to representative parasitophorous vacuoles aligned by IIGP1; line arrowheads point to parasites without detectable IIGP1 next to them. In some cases IIGP1 appears to be concentrated around only one pole of the parasite (c-e). (h-l) shows B6m29 cells induced with 200U/ml IFN- γ for 24h and infected with *S. typhimurium* for 2h. The cells were fixed with 3% PFA and stained with anti-IIGP1 165 antiserum and DAPI to stain the DNA of the host cells and bacteria. In contrast to *T. gondii* no accumulation of IIGP1 near *Salmonella* was observed. The images were taken with a Zeiss Axioplan II microscope equipped with a cooled CCD camera (Quantix) using the Metamorph software (version 4.5). The magnification is 630x. Nuclei were labelled with DAPI.

3.23 IGTP localizes to *Toxoplasma gondii* containing parasitophorous vacuoles.

Primary astrocytes were infected with *T. gondii* as described above and stained with anti-IGTP antibody. Increased IGTP staining was found around parasites 2h after infection (Figure 27a-e) whereas hardly any increased stain near the intracellular parasites was detectable 24h after infection (Figure 27f, g). In general, the accumulation of IGTP near the intracellular parasites was not as pronounced as that of IIGP1 (Figure 26a-e).

Notably IGTP has been shown to be essential for the IFN- γ mediated inhibition of *T. gondii* in primary murine astrocytes (151). The growth inhibitory effect of IFN- γ in this particular cell type was reproduced with *T. gondii* strain ME49 in this study in collaboration with Dr. Gaby Reichmann (University of Düsseldorf) with this particular *Toxoplasma* strain (ME49) shown in Figure 26 and 27. The inhibition of *T. gondii* was reproducibly shown to be approximately 90% (not shown).

As IIGP1 (Figure 26), IGTP did not accumulate around vacuoles containing *S. typhimurium* (Figure 27h-l). The experimental procedure was as described above for IIGP1. IGTP was stained using the anti-IGTP antibody.

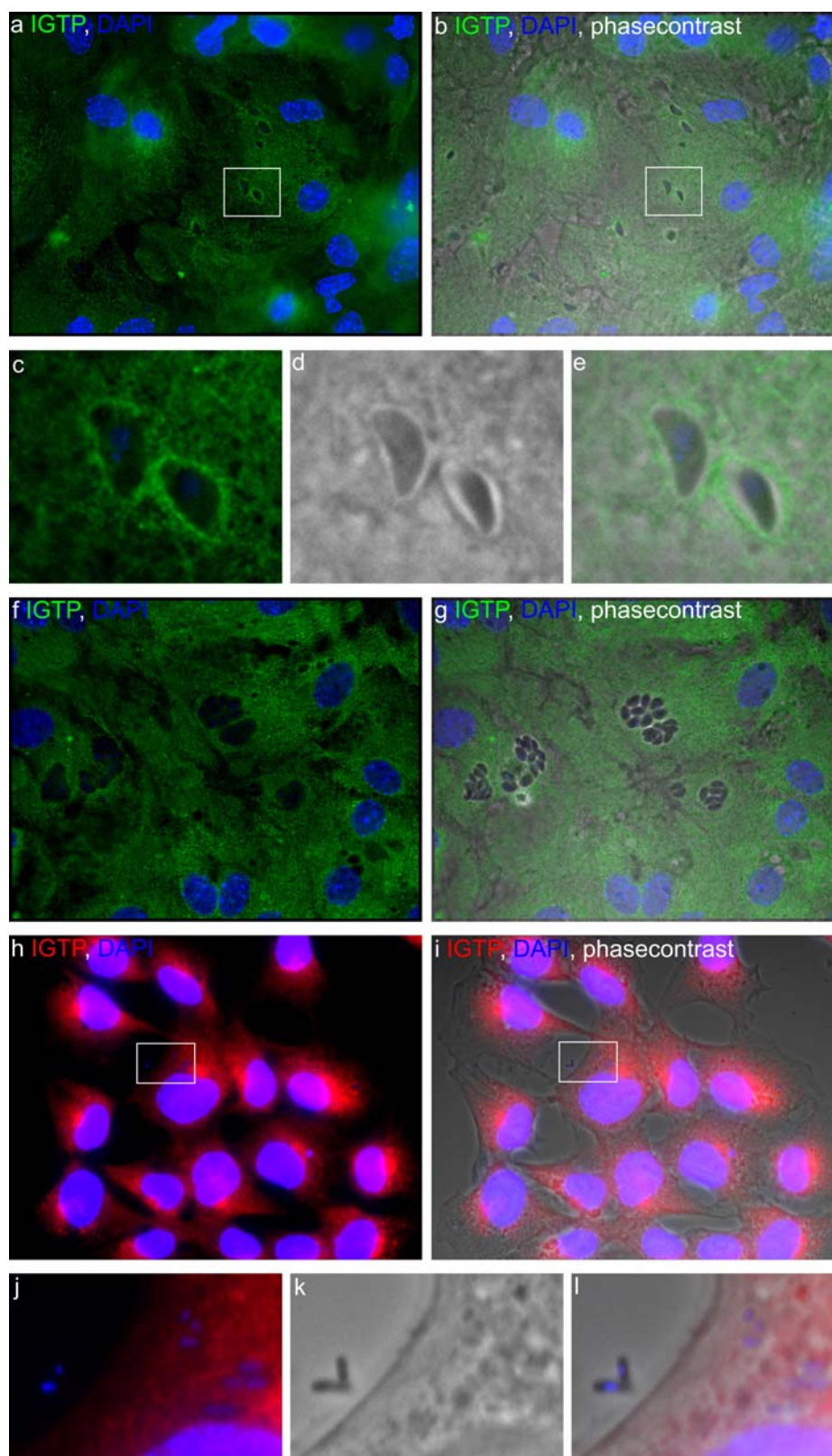


Figure 27

IGTP localizes around parasitophorous vacuoles in *T. gondii* infected mouse primary astrocytes.

Primary mouse astrocytes were induced with 100U/ml IFN- γ for 24h and inoculated with the *Toxoplasma gondii* (strain ME49) at a MOI of 20. After 2h the cells were thoroughly washed several times to remove extracellular parasites and fixed immediately (a-e) or incubated 24h before fixation (f, g). The cells in (a-g) were stained by indirect immunofluorescence with anti-IGTP antibody to detect IGTP and DAPI to mark nuclei of host cells and parasites. The staining of the anti-IGTP antibody is more intense after 2h compared to 24h (compare a-e and f, g). (h-l) shows B6m29 cells induced with 200U/ml IFN- γ for 24h and infected with *S. typhimurium* for 2h. The cells were fixed with 3% PFA and stained with anti-IGTP

antibody and DAPI to stain the DNA of the host cells and bacteria. In contrast to *T. gondii* no accumulation of IGTP near *S. typhimurium* was observed. The images were taken with a Zeiss Axioplan II microscope equipped with a cooled CCD camera (Quantix) using the Metamorph software (version 4.5). The magnification is 630x. Nuclei were labelled with DAPI.

4. Discussion

Intracellular membranes are the interface at which intracellular pathogens and host are confronted. Although the ultimate intracellular niche for survival and replication is often unique all intracellular pathogens are initially contained within a membrane bound vacuole. The host attempts to render the pathogen containing vacuole uninhabitable by its maturation to lysosomes along the endocytic pathway. Pathogens therefore express a plethora of virulence factors whose function it is to take over control of those membranes in order to determine their own subsequent intracellular fate (97). Host proteins controlling membrane traffic and cytoskeletal dynamics are therefore common targets of such virulence factors. It is becoming increasingly clear that the host responds to infection by the induction of cellular factors designed to counteract the pathogens attempt to take over control of host cell processes (table 1 and references therein). Many of these factors are only now being recognized or await their discovery.

The interferon inducible p47 GTPases are a family of at least partly membrane bound proteins which are essential for the control of intracellular bacterial and protozoan pathogens in the mouse (40). Initial observations implicate one member of the family, LRG-47, in the acidification of *Mycobacteria* containing phagosomes in mouse macrophages (95). The present study was set out to determine the sub-cellular localization of two p47 GTPases, namely IIGP1 and LRG-47, and the mechanisms used by them to associate with membrane. These findings were extended to the other family members revealing a remarkable and unexpected diverse cell-biology of the p47 family. The positioning of at least IIGP1 and LRG-47 turned out to be dynamic in response to cellular stimuli associated with pathogen invasion or phagocytosis. The implications of the experimental results presented in this study for the mechanism of action of the p47 GTPases will be discussed.

4.1 The interferon inducible p47 GTPases are remarkably diverse regarding their membrane association properties.

All 6 published p47 GTPases (and for which serological reagents are available; LRG-47, IGTP, GTPI, IIGP1, TGTP and IRG-47) are massively and synchronously induced from very low or practically absent resting levels (The number of molecules of IIGP1 proteins 24h after induction with 200U/ml IFN- γ within a single L929 cell was determined to be

2×10^6 (Jia Zheng, personal communication)). The induction of the p47 proteins by IFN- γ after 24h is shown for L929 mouse fibroblasts and TIB-75 cells, derived from mouse hepatocytes, in Figure 1 and was confirmed for RAW 264.7 macrophage like cells, primary mouse embryonic fibroblasts, mouse primary astrocytes and several other mouse cell types by Western Blotting. These findings are consistent with previous Northern Blot results (60). This result has at least two technical implications: Firstly, mouse cells are able to tolerate high levels of p47 GTPase expression, at least after IFN- γ induction. Second, resting cells, not exposed to IFN- γ or other inducing stimuli, may be considered empty in respect to p47 protein expression. This allows the expression of untagged wild type or mutant p47 proteins in resting cells and their subsequent detection with serological reagents recognizing untagged p47 proteins avoiding confusion with the respective endogenous protein.

In a hypotonic extraction of IFN- γ induced L929 cells the p47 GTPases partitioned remarkably different from each other into pellet and supernatant, interpreted as membrane bound and cytosolic, respectively. LRG-47 had no detectable cytosolic pool. IRG-47 in contrast was hardly detectable on the membrane, at least under the conditions tested. IIGP1 behaved as an intermediate between these two extremes. In contrast to the other p47 GTPases, the aqueous extraction of GTPI was conducted with IFN- γ induced RAW 264.7 cells. However the partitioning of GTPI is likely to be very similar in L929 cells, as IRG-47 and IGTP showed the same proportion of membrane bound versus cytosolic pool in RAW 264.7 and L929 cells. In general the proportion of the GMS GTPases LRG-47, IGTP and GTPI being associated with cellular membranes appears to be higher compared to the other family members.

4.2 LRG-47 binds GDP and is a Golgi associated protein

To localize LRG-47 within the cell the anti-LRG-47 A19 antiserum was used for indirect immunofluorescence. A19 detected an adnuclear signal and a diffuse granular background throughout the cell only in cells exposed to IFN- γ (Figure 3). This result is consistent with the Western Blot result shown in Figure 1. To confirm that A19 specifically detects LRG-47 resting cells were transfected with several expression constructs and a positive signal in Western Blotting and immunofluorescence was only observed when the transfected expression construct contained the LRG-47 open reading frame. Experiments with N-terminal deletion constructs of LRG-47 allowed the

localization of the epitope(s) recognized by the A19 antiserum to the N-terminal 16 amino acids (not shown).

LRG-47 binds to GDP crosslinked to agarose beads (Figure 3). A faint band recognized by the A19 and the α LRG-47 L115 antiserum (not shown) was detected only for the GDP crosslinked agarose. No signal was seen for the GMP and GTP agaroses. IIGP1 served as control for the nucleotide agarose binding assay. The nucleotide binding properties of IIGP1 have been extensively characterized (150). IIGP1 binds to GDP with a 15 fold higher affinity than GTP. Consistent with that a significant amount of IIGP1 in the final pellet was only recovered for the GDP agarose. The faint bands in the GMP and GTP tracks are most likely technical background as IIGP1 has been shown to have no significant affinity for GMP *in vitro* (150). The result for LRG-47 in this assay suggests that it might have, similar to IIGP1, a higher affinity for GDP than GTP. The nucleotide agarose experiment shows that LRG-47 binds to GDP but it does not allow any statement about hydrolysis of nucleotides by LRG-47. However, IGTP, a close relative of LRG-47, has been shown to hydrolyse GTP to GDP (93) despite the same unusual lysine to methionine substitution in the G1 motif. It is therefore likely that this property is shared by LRG-47.

Remarkably, the nucleotide agarose binding assay was extraordinarily vulnerable to the use of the detergent for cell lysis. Only the use of 1% digitonin and the aqueous phase of Triton X-114 (not shown) allowed the recovery of LRG-47 in the final GDP agarose pellet. Detergents such as Triton X-100 and CHAPS, even when used at low concentrations, did not allow recovery of LRG-47 in the final pellet for any nucleotide agarose. IIGP1 in contrast was less affected by the choice of detergent. This may suggest that membrane association is essential for nucleotide binding of LRG-47. Consistent with this, in contrast to IIGP1, LRG-47 was not recovered in the supernatant of a hypotonic extraction (Figure 2).

The adnuclear signal in IFN- γ induced cells stained with the A19 antiserum localized to the Golgi complex. The most accurate co-localization of LRG-47 and cellular markers was seen for the Golgi localized small GTP binding protein Rab6 and the Golgi matrix proteins Gm130 and giantin (Figure 4). Less accurate co-localization could be detected with α -mannosidase II and no or very little overlap was seen for CI-M6PR (Figure 4, 5). Giantin and Gm130 localize mainly to the *cis*-Golgi (176, 179), α -mannosidaseII to the *medial*-Golgi (180-182) and CI-M6PR to the *trans*-Golgi, TGN and late endosomes (183). LRG-47 is therefore associated with the *cis*- and *medial*-Golgi complex rather

than the *trans*-Golgi and TGN. Apart from L929 cells and RAW 264.7 cells shown in Figure 4 and 5, the Golgi localization of LRG-47 was also observed in several other cell types including mouse primary peritoneal macrophages, mouse primary embryonic fibroblasts, TIB-75 cells and primary murine astrocytes. The localization of LRG-47 therefore seems to be cell type independent.

The diffuse granular background throughout the cell partially co-localizes with ER proteins such as Calnexin or the p47 GTPase IGTP (93). Some overlap was also observed with ERP60, another ER resident protein (190). Therefore a small proportion of LRG-47 is associated with the ER in addition to its dominant Golgi association.

No co-localization was detected with proteins localizing to endosomal and/or lysosomal compartment (Figure 7). Under the conditions used, Transferrin stains early, sorting and recycling endosomes (185), Rab11 marks recycling endosomes (186) and LAMP-1 localizes to late endosomes and lysosomes (187). The mutual exclusive pattern of LRG-47 with all these markers strongly suggests the absence of LRG-47 from the endocytic and lysosomal compartment. In addition, as discussed above, no co-localization was seen for LRG-47 and CI-M6PR localizing, besides the *trans*-Golgi and TGN, to late endosomes (183). To conclude, in cells not engaged in phagocytosis, LRG-47 localizes to the *cis*-Golgi and ER but not the endocytic compartment.

4.3 LRG-47 is recruited to phagosomal environment and plasma membrane early upon phagocytosis.

In the recent years LRG-47 turned out to be the most powerful host resistance factor within the p47 GTPase family described so far (40, 95, 96) belonging to the most potent intracellular resistance factors known in general. Pathogens as diverse as *Toxoplasma gondii*, *Mycobacterium tuberculosis* and *Listeria monocytogenes* are targeted by LRG-47. *Toxoplasma* persists or replicates within a parasitophorous vacuole after active penetration of the cell (199). *Mycobacteria* stall the maturation of the phagosome in which they persist after their uptake through phagocytosis by macrophages (169) and *Listeria* rapidly escapes from the phagosome to replicate within the cytosol (172).

In view of the fact that LRG-47 is an essential component of intracellular immunity to these microbes having such divergent intracellular lifestyles its *cis*-Golgi and ER localization appears enigmatic. However the recruitment of LRG-47 to plasma membrane ruffles and phagocytic cups very early upon phagocytosis in macrophages taking up latex beads (Figure 9) and fibroblasts internalizing collagen-coated latex beads

(Figure 10) directly recruits LRG-47 onto the membrane which control is essential for host and pathogen. Moreover LRG-47 remains associated with the phagosomes as they mature along the endocytic pathway and acquire LAMP-1 (Figure 8, 9). The overlap of LRG-47 and LAMP-1 was restricted to the phagosomal membrane because no co-localization of the two proteins was observed in cells not engaged in phagocytosis (Figure 7).

LRG-47 was also recovered in a sub-cellular fractionation designed to purify latex bead containing phagosomes from IFN- γ induced RAW 264.7 cells (Figure 10) (157). The microscopic analysis of the final pellet of this fractionation showed that the latex beads taken up by the RAW 264.7 cells were abundantly recovered. The determination of the co-purification of LAMP-1, EEA1, Calnexin, LRG-47 and IIGP1 by Western Blotting showed that besides LAMP-1 only LRG-47 was found to be enriched in the final pellet: (In a single experiment IIGP1 was also recovered in the final pellet of the +/+ sample. This result however requires reproduction). The high experimental background in the +/-, -/+ final pellet is unsatisfactory and raises doubts on the significance of the co-purification of LRG-47 in the +/+ final pellet. However the LRG-47 was reproducibly more abundant in the +/+ final pellet which basically confirms the results obtained by immunofluorescence.

It remains to be seen whether the same early recruitment of LRG-47 to and its maintenance on the phagosomal membrane takes place in cells taking up or being invaded by intracellular microbes. During the course of this study McMicking et al. reported the co-isolation of LRG-47 with *Mycobacterium tuberculosis* containing phagosomes from primary alveolar macrophages (95). It thus appears reasonable that the experiments conducted with latex beads may be transferred to the internalization of pathogens. Unfortunately the anti-LRG-47 A19 antiserum reacts unspecifically with the membrane of *T. gondii*. Therefore the dynamics of LRG-47 in *Toxoplasma* infected cells could not be analysed.

On the other hand, the analysis of the recruitment of IIGP1 to phagosomes by immunofluorescence was hampered by the ER association of IIGP1 and the resulting difficulty to distinguish between accidental proximity and real association with the phagosomal membrane. However, it is clear that IIGP1 does not accumulate to the same extend around latex bead containing phagosomes as around the parasitophorous vacuoles of *T. gondii*.

4.4 Domains responsible for the dynamic intracellular behaviour of LRG-47

LRG-47 is a *cis*-Golgi associated protein with a minor proportion on ER membranes. Upon phagocytosis LRG-47 is recruited to the plasma membrane and remains associated with the maturing phagosomes. To determine which domains are responsible or at least required for the differential localization several mutant forms of LRG-47 had to be expressed. Tagging of LRG-47 causes mis-localization to the recycling endosomal compartment. This is shown for the N-terminal EGFP fused protein in Figure 23. A C-terminal Flag-tagged form of LRG-47 accurately co-localized with the N-terminal EGFP fused form as determined by co-transfection (not shown). Interestingly the mis-localization of tagged LRG-47 is dependent on the integrity of the G1 motif as the S90N mutant localized very similar to the endogenous protein showing Golgi and ER association. This implies that tagging interferes at least in some cases with the nucleotide dependent regulation of LRG-47.

Due to the problems described above untagged LRG-47 was expressed in cells not induced with IFN- γ . When expressed at physiological levels transfected wild type LRG-47 accurately recapitulated the localization of the endogenous protein (Figure 11), showing that at least on light microscopically observable resolution no other IFN- γ inducible factors are required for its sub-cellular positioning. At higher expression levels LRG-47 associated exclusively with the plasma membrane. The Golgi apparatus remained intact (not shown) suggesting that no bulk-transfer of Golgi membranes to plasma membrane occurred in these cells. This plasma membrane association recalls the recruitment of LRG-47 to phagocytic cups and adjacent membrane ruffles upon phagocytosis, although during phagocytosis only a small proportion of LRG-47 is found at or near the plasma membrane. The relocalization in the LRG-47 overexpressing cells can not be explained by a simple saturation of a putative binding site on the Golgi membrane. In this case a Golgi signal would initially become increasingly intense, reach a plateau and remain constant while the plasma membrane signal would become progressively visible. The complete absence of any signal on internal membrane suggests that LRG-47 initially associates with Golgi membranes until a putative binding site is saturated or a certain concentration of LRG-47 molecules in the cytoplasm is reached. At a certain point a possibly direct interaction between LRG-47 molecules takes place which exposes a plasma membrane binding signal or masks the Golgi association motif. This process is nucleotide dependent since the S90N mutant did not localize to plasma membrane regardless of expression levels but showed Golgi

association and an increased association with ER (Figure 11). It is currently unclear whether vesicular transport or transient release into the cytosol mediates plasma membrane association. In summary, membrane association of LRG-47 is, like IGTP (93), nucleotide independent but relocalization to plasma membrane upon over expression requires an intact G1 motif.

Two different domains are responsible for the association of LRG-47 with Golgi/ER and plasma membrane, respectively (Figure 12). The isolated G-domain was not expressed in L929 cells. However, extending the G-domain to include α E and α F resulted in exclusive plasma membrane association and an additional diffuse cytosolic staining. In a hypotonic extraction the extended G-domain was about 30% membrane bound (not shown). Plasma membrane ruffles were particularly stained, again recalling the plasma membrane association of LRG-47 upon its over expression and the partial recruitment of the endogenous protein to phagocytic cups and adjacent membrane ruffles.

While the N-terminal domain itself did not associate with any membrane when fused to EGFP, the C-terminal domain accurately targeted EGFP to the Golgi apparatus and ER membranes (Figure 12) very similar to the localization of the endogenous and transfected wild type LRG-47. In contrast, the reticular diffuse pattern throughout the cell was markedly increased for the C-terminal domain which is similar to the full length S90N mutant protein. This implies that a functional G-domain is required for the exact positioning of the molecule to Golgi membranes. In summary, the Golgi and ER association is mediated by the C-terminal domain corresponding to α G- α L in the IIGP1 structure whereas the plasma membrane association is very likely to be mediated by the G-domain.

4.5 LRG-47 is targeted to Golgi by a C-terminal amphipathic helix.

No predictable motifs for membrane association in the C-terminal domain of LRG-47 were found by database searches and prediction programs. Therefore the systematic approach outlined in Figure 13 was undertaken to localize the Golgi targeting sequence in the C-terminal domain of LRG-47. Strikingly, the 25 amino acids long peptide corresponding to α K and the loop preceding α L in the IIGP1 crystal structure identified in this screen did not only mediate membrane association but also Golgi targeting. Thus, this short sequence contains a signal addressing the Golgi apparatus. (Essentially, this construct comprises a C-terminally extended version of EGFP and may even be used as

marker for the Golgi apparatus in live cell experiments). The 25 amino acids long α K peptide contains a core region which is predicted to form an α helix (149). When drawn as a helical wheel this core region forms an amphipathic helix (Figure 14). Including the two alanines and the cysteine, hydrophobic amino acids are exposed on about 75% of the surface of this predicted helix. Disturbing the amphipathic character of that helix by insertion of one or two glutamate residues resulted in loss of membrane association of the 25 amino acid long α K peptide fused to EGFP, also when inserted into the whole C-terminal domain (not shown). When introduced into the complete open reading frame of LRG-47 the resulting mutants showed loss of Golgi accumulation.

The simplest explanation for the membrane association activity of the LRG-47 α K peptide is that the hydrophobic amino acids of this amphipathic helix insert into the lipid bilayer and thereby anchor the protein in the membrane. It is of course also conceivable that the amphipathic helix mediates membrane association in other ways such as protein-protein interaction.

The mechanism conferring the striking specificity of membrane association of the α K peptide of LRG-47 remains to be uncovered. It is possible that the amphipathic helix itself harbours Golgi specificity due to preferential insertion into lipid bilayer of a specific lipid composition or that the charged amino acids on the other side of the helix confer Golgi specificity. Amino acids lying outside the amphipathic core of the α K peptide could also be involved in membrane targeting. The targeting of a protein to Golgi membranes by an amphipathic α helix is not unique to LRG-47. An N-terminal 30 amino acids long peptide of RhoGDI-3 containing an amphipathic helix has been shown to target the protein to the Golgi apparatus (200).

Mutations within the amphipathic helix abolished Golgi accumulation of full length LRG-47 but did not cause plasma membrane association (Figure 14). A second unidentified signal within LRG-47, which is not recognized by the expression of isolated domains, could be responsible for this endomembrane association. Alternatively, the interaction between the C-terminal and/or N-terminal domain and the G-domain could modify the membrane targeting property of the G-domain thereby rendering it into an endomembrane association signal.

4.6 The α K regions of all mouse GMS GTPases mediate membrane association.

When fused to EGFP in the same manner as the α K peptide of LRG-47 the corresponding regions of GTPI and IGTP targeted EGFP to membrane. The GTPI α K peptide localized EGFP accurately to the Golgi apparatus whereas the analogous IGTP fusion protein showed a more diffuse distribution including an embedded reticulum. A large proportion of the IGTP α K fusion protein appeared cytosolic. Full length IGTP localizes to the ER (93), a result which was confirmed in this study (Figure 23). Full length GTPI localized to the Golgi apparatus when expressed as an N-terminal EGFP fusion protein. Although the results obtained with fusion proteins of the p47 GTPases have to be taken with caution since LRG-47 is mis-localized at least by some tags or fusions, the EGFP fused α K peptides strikingly recapitulated the localization of full length IGTP and GTPI, respectively.

The α K region and the loop preceding α L in the IIGP1 crystal structure belong to the most divergent sequences within the p47 GTPase family and are virtually unique for each of the 6 published family members (Figure 15) (60, 149). The mechanism unravelled for LRG-47 may therefore not be directly transferred to IGTP and GTPI. The α K peptide of IGTP contains a predicted α helix which has an amphipathic character when drawn as a helical wheel (not shown). However, this amphipathic helix is considerably shorter than that of LRG-47 and showed no Golgi targeting activity but localized EGFP to a diffuse reticular pattern. The corresponding region of GTPI is not able to form an amphipathic α helix despite localizing similar to the α K peptide of LRG-47.

In order to identify the mechanism by which the α K peptide associates with membrane a BLAST search for short, nearly exact matches within the mammalian proteome was conducted. Among the best hits recovered in this search were numerous phospholipase C sequences (PLC). In fact only GTPI itself and a milk fat protein (milk fat globule-EGF factor 8 protein from *Mus musculus*) preceded phospholipase C sequences. The crystal structures of several PLCs have been determined and for rat PLC δ the crystal structure in complex with inositol-1,4,5-trisphosphate (IP₃) has been obtained (188). Strikingly, the GTPI homologous part in rat PLC δ is part of the conserved Y region of the catalytic domain which is involved in substrate binding. In particular the arginin and tyrosine of PLC δ highlighted in Figure 16 make direct contact to the bound IP₃ (188). These residues are also present in GTPI. The arginin contacts the 4-phosphate of IP₃.

Consistent with the Golgi targeting by the GTPI α K peptide, phosphatidyl inositol 4-phosphate is the most prominent phosphatidyl inositol phosphate in Golgi membranes (201-203). Moreover, since this sequence is involved in substrate binding it comes in close contact with the lipid bilayer (188, 204). In rat PLC δ a tryptophan (W555 in rat PLC δ) is proposed to be involved in membrane association (188, 204). This residue is not found in GTPI but is also absent from mouse PLC β . Both proteins have a valine instead of a threonine in rat PLC δ which may take over the function of the W555. Thus the membrane association of the GTPI α K peptide might be based on interactions that are used by PLC to bind its substrate.

The same BLAST search as described for GTPI was conducted with the IGTP α K peptide. This search uncovered significant homology to PLCs too. For the IGTP α K peptide the highest homology among the PLCs was to rabbit PLC (Figure 16). When aligned to the rat PLC δ structure it turned out that also the IGTP homologous part contacts the IP₃. Astonishingly, this part did not correspond to the GTPI homologous region but is located directly N-terminally of it, only separated by few amino acids. After closer inspection these separating amino acids also turned out to bear some homology to the IGTP α K peptide (Figure 16d). A conserved serine approaching the 4-phosphate of the bound IP₃ is located within this sequence (188, 204). This serine is an essential residue for PLC mediated catalysis. The serine is a cysteine in IGTP and it is conceivable that also the cysteine is able to interact with the same 4-phosphate of IP₃. Analogous to GTPI, also the IGTP homologous part of rat PLC δ contacts the membrane (188, 204). The leucine proposed to insert into the lipid bilayer is also found in IGTP (Figure 16a). Interestingly, the predicted amphipathic α helix of IGTP corresponds to the membrane facing helix in rat PLC δ (Figure 16b, c). Thus also IGTP may have adopted a membrane association module or sequence from PLC to bind to membrane. The IGTP and GTPI homologous structures come very close in rat PLC δ making close contact in an very suggestive manner and it is tempting to allow the two regions under some circumstances to interact with each other at the membrane to form a binding site for phosphatidyl inositol phosphates.

No PLC sequences were recovered when the same BLAST search was conducted with the LRG-47 α K peptide. However given the overall homology of the other two GMS GTPases, IGTP and GTPI, the absence of PLC sequences from the BLAST hits for LRG-47 was conspicuous. Therefore an adjacent part of the LRG-47 protein comprising

α I and α J in the IIGP1 structure was subjected to a BLAST search for short, nearly exact matches in the same unbiased manner as described for GTPI. Among other sequences human PLC-like protein ϵ (205) was identified. No PLC sequences were recovered in BLAST searches with the GTPI and IGTP α I and α J regions. The homology of the LRG-47 α I, J region and human PLC-like ϵ is significantly lower compared to GTPI and IGTP but immediately attracted the attention after the result with the other GMS GTPases (Figure 16d). Human PLC-like ϵ does not show high homology to rat PLC δ in this particular region but the regions N- and C-terminal of it show high homology to rat PLC δ . It appears that, also among PLCs, the part which is similar to LRG-47 allows more sequence divergence. Superimposed onto the structure of rat PLC δ this part forms a loop sticking out of the catalytic domain (Figure 16e) and is positioned immediately N-terminal of the IGTP homologous region. Together the GTPI, IGTP and LRG-47 homologous parts interact to form a significant part of the conserved Y region of PLC δ and comprising one half of the catalytic domain (188).

4.7 The ER protein IIGP1 shows striking differences to LRG-47

IIGP1 is among the p47 GTPases by far the best characterized member on biochemical and structural level (149, 150) In fact the crystal structure of IIGP1 served as scaffold to define the structural elements of LRG-47 and the other p47 GTPases. Therefore the membrane association properties of IIGP1 were analyzed and its properties will be compared to LRG-47.

IIGP1 localized to the endoplasmic reticulum in all cell-types analyzed (Figure 17) but about 40% of the cellular IIGP1 pool was recovered in the supernatant of a hypotonic extraction (Figure 2). This suggests that IIGP1 is not completely membrane bound but has in contrast to LRG-47 a cytosolic and a membrane bound pool. The recruitment of IIGP1 to membrane may thus be dynamic as it is for the Arf (105), Rab (44), Rho proteins (206) and dynamins (98, 102, 119). Zerrahn et al. have shown that IIGP1 localizes to the Golgi apparatus and ER (92). The Golgi localization could not be reproduced in this study. Regardless of the cell-type analyzed, no significant overlap with Golgi markers was observed. The highest degree of overlap of IIGP1 with Golgi proteins was seen in RAW 264.7 cells (Figure 17). However, also in this case co-localization was restricted to small isolated sites. In addition as giantin mainly marks the *cis*-Golgi apparatus it is possible that this overlap can be explained by IIGP1 molecules

that escaped the ER to the intermediate compartment and *cis*-Golgi and are transported back to the ER. Although numerous cell-types were analyzed and in none of these a significant Golgi association was seen it can not be excluded that the different intracellular distribution of IIGP1 observed by Zerrahn et al. (92) is cell type dependent. In their study bone marrow derived macrophages were used. In summary, IIGP1 has an intracellular localization different from LRG-47 but similar to the ER association shown for IGTP (Figure 23) (93). In contrast to IGTP, IIGP1 has a significant cytosolic pool.

Upon transfection into L929 cells IIGP1 behaved strikingly different from LRG-47 (Figure 18). When expressed at very low levels IIGP1 showed a distribution similar to the endogenous, IFN- γ induced protein. However, when expressed at levels as high as those induced by IFN- γ or higher, IIGP1 containing aggregates were formed in the transfected cells. IIGP1 forms nucleotide dependent multimers *in vitro* (150) and it appears that the cellular aggregation upon transfection involve the same mechanistic properties observed for recombinant IIGP1 *in vitro* (150). Aggregate formation is dependent on nucleotide binding as the nucleotide binding deficient G76, 81V mutant IIGP1 did not form aggregates after transfection, regardless of expression levels. A C-terminal 6xhistidine modification of IIGP1 negatively interferes with the nucleotide dependent oligomerization and consistent with the C-terminus being involved in this process, the deletion of the whole C-terminal domain (IIGP1 aa 1-287) abolished aggregation of transfected IIGP1. Therefore cellular aggregate-formation requires nucleotide binding and the C-terminal domain. In addition, IIGP1 aa 1-287 did not localize in the same pattern as the endogenous protein. The C-terminal domain thus appears to be involved in targeting of IIGP1 to membrane.

IIGP1 containing aggregates were never seen in any IFN- γ stimulated cell analysed so far. As the aggregates were also observed at physiological expression levels or or even below, over-expression alone can not explain the aggregation upon transfection. It rather appears that it is “out of context” expression of IIGP1 which causes the aberrant behaviour implying that other IFN- γ induced factors are required to prevent IIGP1 from aggregation or multimerization. The behaviour of IIGP1 after transfection is unexpectedly different from LRG-47 and the other GMS GTPases considering that they are all members of the same protein family.

IIGP1 is the only protein among the 6 published p47 GTPases, LRG-47, IGTP, GTPI, IIGP1, TGTP and IRG-47 (60) which contains a predictable lipid modification motif.

The N-terminus of IIGP1 (MGQLFSS) is predicted to be myristoylated (PSORT II prediction program, <http://psort.nibb.ac.jp/form2.html>) (207). In the Triton X-114 partitioning assay (Figure 19) about 50% of the endogenous IIGP1 partitioned in the detergent phase and this partitioning was dependent on the integrity of the myristoylation motif. The same ratio of partitioning into the aqueous and detergent phases in a series of consecutive extraction suggests that the Triton X-114 extraction procedure is only 50% efficient and that the vast majority of IIGP1 molecules are lipid modified (Figure 19). The about 40% of the IIGP1 molecules found in the supernatant after hypotonic extraction (Figure 19) are therefore not the result of a differential myristoylation of IIGP1. Myristoylation of IIGP1 is not absolutely necessary for its attachment to intracellular membranes as also the G2A had a considerable membrane bound pool although significantly smaller than the endogenous IIGP1 (Figure 2).

Consistent with the absence of any lipid modification site LRG-47, as well as IGTP, IRG-47 and TGTP, were not recovered in the detergent phase. Thus, among the analysed p47 GTPases IIGP1 is the only myristoylated protein. However among the 23 p47 GTPases in the mouse 9 are predicted to be myristoylated. To confirm the myristoylation radioactively labelled precursors of the attached myristoyl group could be applied to IFN- γ induced cells and co-precipitation of the radiolabel with IIGP1 could be analysed by autoradiography.

Compared to LRG-47 the targeting of IIGP1 to membranes showed conspicuous differences but also similarities. In contrast to LRG-47, the N-terminal domain of IIGP1 contained membrane targeting activity (Figure 20) when fused to the N-terminus of EGFP. This targeting to endomembranes was dependent on the integrity of the myristoylation motif. Since the membrane association of the full length molecule was only partly myristoyl-dependent, the N-terminal domain can not be fully responsible for the membrane association of IIGP1. The C-terminal domain of IIGP1 did not show any membrane association when fused to the C-terminus of EGFP which again contrasts the behaviour of LRG-47.

Surprisingly the isolated G-domain of IIGP1 localized exclusively to plasma membrane. In addition a diffuse cytosolic stain was apparent. This localization was undistinguishable from the localization of the LRG-47 G-domain- α F. Consistent with the same localization, the G-domain is the most homologous domain within the p47 GTPases whereas the N-terminal and C-terminal domains are rather divergent (18). The basis for the plasma membrane association of the G-domains is currently unclear.

However, in contrast to LRG-47 the isolated G-domain and the G-domain extended to include α F was expressed in L929 cells. In hypotonic extractions the extended G-domain of IIGP1 showed a higher degree of membrane association than the G-domain alone (not shown), suggesting that amino acids within the α E and α F regions stabilize the enigmatic plasma membrane association signal.

The biochemical nature and strength of membrane association of the p47 GTPases is very different. The wash-off profiles (Figure 21) of the GMS GTPases LRG-47 and IGTP were indistinguishable from that of the transmembrane protein Calnexin in this assay, only being released by detergents such as Triton X-100 or digitonin (not shown). This shows that membrane association is independent of protein-protein interactions. IIGP1 and TGTP behaved like peripheral membrane proteins being to some degree released from membrane by all buffers applied (Figure 21). In particular sodium carbonate released most of the two GKS p47 GTPases IIGP1 and TGTP from membrane. The small amount of IIGP1 which was not transferred into the supernatant by Triton X-100 might represent lipid raft associated protein (194, 195). Consistent with this, little, possibly significant co-localization of IIGP1 with Caveolin-1 was observed in TIB-75 cells (not shown) and Caveolin-1 is also found in the Triton X-100 resistant fraction (208). However, recombinant IIGP1 incubated with artificial phosphatidylserine vesicles fractionated in the Triton X-100 pellet too. Although both findings might have a different basis, it can not be excluded that also the endogenous protein aggregates to some extent during the experiment and thereby becomes Triton X-100 insoluble.

The myristoyl-group of IIGP1 did not contribute to the strength of membrane association in this assay (Figure 22). The wash off profile of the G2A mutant IIGP1 was very similar to transfected wild type IIGP1. For IIGP1 the myristoyl-group appears to play a role in targeting the protein to membrane rather than conferring strong membrane by itself which is consistent with the role of myristoylation in other proteins (107, 207). The wash off profile of IIGP1 and TGTP does not allow discriminating between a direct interaction of these proteins with lipid head groups and protein-protein interactions as basis for membrane association. *In vitro*, recombinant IIGP1 which is not myristoylated binds to synthetic phosphatidylserine vesicles (Katja Sabel, Diplomarbeit). In addition the wash off profile of recombinant IIGP1 was very similar to the endogenous IIGP1, transfected wild type IIGP1 and G2A mutant IIGP1 (Figure 22 and Katja Sabel, Diplomarbeit). Thus IIGP1 is able to bind to membrane independently of other proteins. Interestingly, the Triton X-100 insoluble fraction was elevated when the myristoyl-

group is not present on IIGP1 (Figure 22, recombinant and G2A mutant IIGP1). Assuming that this fraction reflects aggregation of IIGP1 the myristoylation may contribute to the stability of the IIGP1 protein. The GDP-bound form of the small GTPase Arf shows how the interaction of IIGP1 and its myristoyl-group might look like (106). It will therefore be informative to obtain the crystal structure of myristoylated IIGP1.

4.8 Transfection and expression of p47 GTPases in cells

In an attempt to determine the intracellular localization of the p47 GTPases for which no suitable serological reagents were available, tagged versions were expressed in L929 cells and other cell types. The results obtained with these constructs turned often out to be unexpected.

GTPI fused N-terminally to the C-terminus of EGFP, accurately localized to the Golgi apparatus defined by giantin (176) (Figure 23). In addition, a diffuse cytosolic and vesicular stain was apparent. This localization was recapitulated by the GTPI α K peptide fused to EGFP (Figure 15). GTPI is thus likely to be a Golgi localized protein. To analyze the effect of the N-terminal EGFP fusion on the localization of the p47 GTPases IGTP was modified in the same manner and the localization of this fusion protein was compared to the endogenous protein for which a suitable serological reagent was available. The localization of EGFP-IGTP and endogenous IGTP is the same confirming the published ER association (93). It therefore seemed reasonable to assume that the localization of EGFP-GTPI reflects the localization of the endogenous protein. However, as already discussed above LRG-47 was mis-localized by the same modification from the Golgi apparatus to the endosomal compartment in a nucleotide dependent manner (Figure 23). In this light, the Golgi association of EGFP-GTPI may not be directly transferred to the endogenous protein. In contrast to IIGP1 and TGTP, no visible aggregation of the GMS GTPases was observed after transfection into L929 cells.

The expression of TGTP had dramatic effects on the cellular morphology (Figure 24). Untagged wild type or C-terminally Flag tagged TGTP formed long intracellular filaments when transfected into a variety of cell types. Surprisingly, the anti-TGTP A20 antiserum used to detect untagged TGTP after transfection by immunofluorescence failed to detect the endogenous IFN- γ induced TGTP although TGTP was clearly

expressed after IFN- γ induction (Figure 1) in these cells. The TGTP containing filaments were not held in place by microtubules nor did they co-localize with F-actin. The intermediate filaments defined by Vimentin were distorted in TGTP transfected HeLa cells and co-localization of TGTP and Vimentin in these filaments can not be ruled out. The determination of the ultra structural basis of these filaments will require electron microscopy analysis. In most transfected cells the TGTP containing filaments were assembled into cage-like structures surrounding the nucleus or are positioned next to it. In many cases the complete ER and Golgi apparatus (not shown) was found within these cages. No such morphological changes were ever observed in any IFN- γ induced cell. TGTP and TGTP-Flag formed filamentous structures even when expressed at very low expression levels. The observed phenomenon may thus be caused, as for IIGP1, by the lack of an IFN- γ induced factor which controls the activity of TGTP. As already proposed for IIGP1 this factor might have an inhibitory function on TGTP. Consistently, a G1 mutant form of TGTP did not form filaments but appeared diffuse in the cytoplasm. The ER was not deformed by the expression of the TGTP G1 mutant (Figure 24). Therefore the aberrant behaviour of TGTP upon its transfection appears to be nucleotide dependent. TGTP may be controlled by the interaction with one or more inducible proteins. This putative interaction(s) may mask the binding site for the anti-TGTP A20 antiserum which was raised against a peptide mapping to the N-terminus of TGTP and may explain the ability of this serum to detect transfected TGTP but not the endogenous, IFN- γ induced protein by immunofluorescence. Alternatively it may be a modification of TGTP itself which is accidentally positioned within the A20 epitope(s) thereby preventing its binding.

Similar modifications of the cellular morphology were observed by transfection of IIGP1 and in particular IIGP1-His carrying a 6xhistidine tag at its C-terminus (Figure 25). In many transfected cells IIGP1-His localized in bag-like structures near the nucleus. Similar to TGTP the ER and Golgi (not shown) was contained within these structures and the morphology of the ER defined by Calnexin was dramatically changed. The formation of the bag-like structures but not aggregation itself was dependent on intact microtubules. Also like TGTP, the intermediate filaments were distorted in transfected HeLa cells aligning outside of the IIGP1-His containing, adnuclear aggregates. No aggregation and distortion of cellular structures was seen for the G1 mutant IIGP1-His. The appearance of the Vimentin stained intermediate filaments in the TGTP and IIGP1-His transfected cells is similar in cells containing aggresomes,

structures induced by the massive expression of mis-folded proteins (209, 210). In contrast to the Golgi and ER IIGP1-His and TGTP do not localize like the mis-folded protein in aggresomes but localize outside (209, 210). The significance of the dramatic effect of the expression of both proteins for their function *in vivo* is totally unclear. *In vitro* IIGP1-His has been shown to be defective for cooperative nucleotide GTP hydrolysis and oligomerization (150). It is unclear how these altered properties lead to the more prominent occurrence of the bag-like structures after transfection compared to wild type, untagged IIGP1.

4.9 The dynamics of p47 GTPases in infected cells

IGTP and especially IIGP1 showed a dramatically dynamic behaviour in *Toxoplasma gondii* infected primary murine astrocytes (Figure 26, 27).

T. gondii is an unicellular, obligate intracellular parasite that actively invades virtually all nucleated host cells (211-213). Invasion of host cells involves the secretion of three different kinds of vesicles and the actin cytoskeleton of the parasite but not the host (212-214). In bone marrow derived macrophages, about 20% of the parasite cells are passively taken up by phagocytosis which results in maturation of the pathogen containing vacuole along the endocytic pathway to phagolysosomes (215). Most parasites however enter the cell by a rapid process occurring within about 30 seconds that does not involve the endocytic machinery of the host cell (213, 214). During entry *T. gondii* establishes a so-called moving junction which excludes host proteins containing cytoplasmic domains from the forming parasitophorous vacuole by a yet unknown mechanism (216). In contrast, host cell proteins having only extracellular domains are found in the vacuolar membrane (216). The lipids used to form the parasitophorous vacuole are thought to be supplied by the host cell plasma membrane (170). After invasion of the cell *T. gondii* resides in a membrane bound compartment forming tight interactions with the host cell ER and mitochondria (217). The parasitophorous vacuole contains pores which allow small molecule to diffuse across the membrane (218). No fusion with the host cell exocytic and endocytic compartment occurs and molecules such as Rab5, LAMPs or mannose 6-phosphate receptors are absent from the parasitophorous vacuole (216, 219).

All three p47 GTPases (LRG-47, IGTP and IRG-47) for which knock out animals are available turned out to be required for host resistance against infections by *T. gondii* (94, 96). In astrocytes IGTP has been shown to be essential for IFN- γ mediated inhibition of

T. gondii growth (151), an effect reproduced in this study (not shown). By immunofluorescence IGTP localized near the parasites possibly staining the membrane of the parasitophorous vacuole. Although not all parasites were aligned by an enhanced IGTP signal in most cases the IGTP staining was markedly increased near the parasite compared to the surrounding signal. It is currently not clear what the basis is for the differential staining of IGTP around the parasites. *Toxoplasma* without surrounding IGTP could still be extracellular or have entered the cell by a different mechanism, e.g. by phagocytosis (215). Alternatively the differential IGTP stain might be indicative of the age of the parasitophorous vacuole, since the astrocytes had been exposed to *T. gondii* for a time window of 2h. 24h later no increased IGTP signal around the parasitophorous vacuoles, now containing numerous obviously divided parasites, was observed. There are several explanations for this seemingly transiently enhanced stain of IGTP near the parasitophorous vacuole. The ER is known to be recruited to the parasitophorous vacuole and it is described that this recruitment is transient (217). If IGTP simply follows the kinetics of ER recruitment to the vacuole other ER proteins should show similar kinetics. Another possibility is that those parasites which are surrounded by IGTP are growth inhibited or even killed by the host cell and only those parasites that somehow managed to avoid IGTP recruitment to the vacuole survive and replicate.

Even stronger than IGTP, IIGP1 accumulates dramatically around the parasitophorous vacuole in IFN- γ induced astrocytes 2h after inoculation (Figure 26). The intensity of the IIGP1 stain near the parasites is so strong that the residual diffuse ER stain becomes nearly invisible with this exposure time. As for IGTP, not all parasites were aligned by strong IIGP1 stain and the same arguments to explain the differential stain outlined for IGTP can be made for IIGP1 although the accumulation of IIGP1 appears too dramatic to be explained by ER recruitment to the vacuole. At the 2h time point, IIGP1 in most cases accumulated around only one pole of the parasite (Figure 26, magnified parasite). This stain overlapped with a dense structure in the phasecontrast image. The nature of this dense structure in the phase contrast is unclear but it is unlikely that this structure corresponds to the forming parasitophorous vacuole during invasion as this is a very rapid process (~30 seconds) and the number of parasites with adjacent polarized IIGP1 stain is considerably high (Figure 26). It is conceivable that the polarized IIGP1 stain is caused by the polarized initiation of IIGP1 oligomerization around the parasitophorous vacuole. Alternatively, in some cases not the whole parasitophorous vacuole might lie in

the plane of focus thus making the observer believe IIGP1 would have a polarized distribution. However, in particular for the parasite highlighted in Figure 26 the boundary to the strong IIGP1 staining appears too sharp to be explained by this argument. The massive recruitment of IIGP1 near the parasitophorous vacuole is unlikely to merely reflect the recruitment of ER to the vacuole because in this case also IGTP would show a similar accumulation.

After 24h only a few parasitophorous vacuoles were markedly aligned with IIGP1. In general, compared to the 2h time point the accumulation of IIGP1 was less dramatic. In a preliminary analysis, the IIGP1 positive vacuoles were smaller than those without IIGP1. It is therefore tempting to speculate that the accumulation of IIGP1 around the parasitophorous is linked to growth inhibition of *Toxoplasma gondii* and only those parasites avoiding or escaping IIGP1 accumulation are able to replicate unrestricted. In this context it will be interesting to see whether IIGP1, IGTP and possibly other p47 GTPases mark the same parasitophorous vacuoles or show a differential pattern. It is worth mentioning at this point that *Toxoplasma gondii* growth of this particular strain (Me49) is slowed down but not completely inhibited by IFN- γ in these astrocytes. Thus the parasite is at least partly able to overcome its counteraction by the p47 GTPases.

No accumulation or recruitment around vacuoles containing the mouse adapted *Salmonella typhimurium* strain SL1344 was seen for IIGP1 and IGTP in B6m29 cells. Although the biology of the intracellular lifestyle of *Salmonella typhimurium* and *Toxoplasma gondii* is radically different (97, 198, 220, 221) this difference shows at least to some degree that the recruitment of IIGP1 and IGTP is specific for the *Toxoplasma* parasitophorous vacuole, assuming that this particular strain of *Salmonella* does not actively prevent IIGP1 or IGTP recruitment. Consistent with its absence from the *Salmonella* vacuole IGTP plays no role in host resistance against *Salmonella typhimurium* (40). So far, no information is available regarding the contribution to host resistance against *S. typhimurium* or *T. gondii* is available. Considering the massive accumulation of IIGP1 around the parasitophorous vacuole *T. gondii* is a promising candidate to be targeted by IIGP1 knock.

4.10 Models for p47 GTPase function

The results presented and discussed in this study do not give an ultimate explanation how the p47 GTPases mediate cell-autonomous resistance. However they do allow, and probably even demand, outlining a few reasonable speculations about their intracellular mode of action.

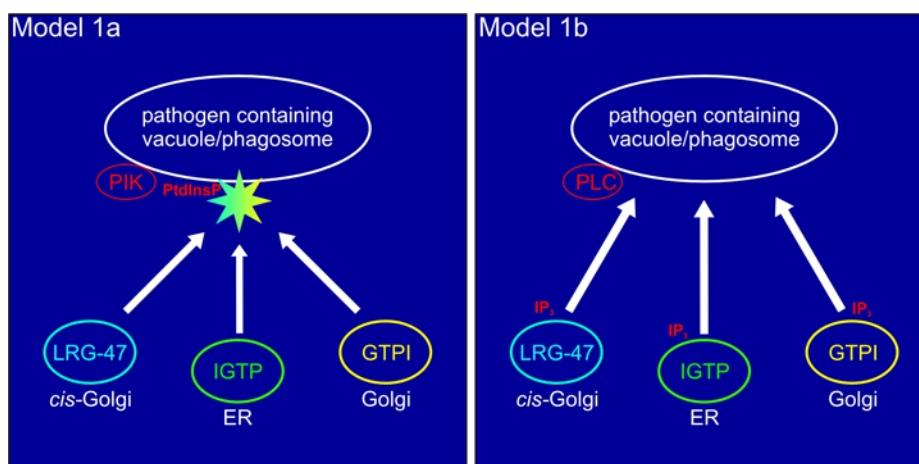
In this respect it has to be considered that the individual members of the mouse p47 GTPases turned out to have strikingly different properties. LRG-47 is completely membrane bound, IIGP1 partitions between membrane and cytosol while IRG-47 appears cytosolic under the conditions analyzed. IIGP1 uses an N-terminal myristoylation motif to associate with intracellular membranes whereas LRG-47 is targeted to the Golgi apparatus by a C-terminal amphipathic helix and although the same C-terminal regions of IGTP and GTPI bind to membranes, the mechanisms of membrane targeting are most likely very different from LRG-47. Furthermore, when transfected into cells, TGTP and IIGP1 form distinct, enigmatic presumably oligomeric, structures which have a dramatic impact on the cellular morphology. Such structures were never observed when any of the three GMS GTPases was likewise expressed. But while an N-terminal EGFP fusion mis-localizes LRG-47 it has no effect on IGTP. The different behaviours of the members of the p47 family reflect their sequence divergence in the N-terminal and C-terminal domains. Only a few family members of the mouse were investigated under a limited number of conditions and it will be fascinating to see which other unexpected properties the other p47 GTPases will display.

The recruitment of LRG-47 to plasma membrane upon phagocytosis and its subsequent association with the maturing phagosome is very intriguing. By its recruitment to the plasma membrane LRG-47 localizes to the only site which is common to all pathogens targeted by LRG-47 (40). Regardless of whether the pathogen resides in a parasitophorous vacuole, replicates in a stalled phagosome or escapes into the cytosol, all microbes have to cross the plasma membrane. LRG-47 might therefore mark the initially formed pathogen containing membrane bound compartment for maturation along the endocytic pathway to lysosomes. In fact in alveolar macrophages the deficiency of LRG-47 results in decreased acidification of phagosomes containing *Mycobacteria* (95) and it has been shown that *Mycobacterium* actively retains a host cell plasma membrane protein TACO on the phagosomal membrane. TACO has been proposed to contribute to the maturation incompetence of the *Mycobacterium* vacuole by mimicking the plasma membrane (222). In this respect it might be interesting that

LRG-47 is capable of membrane association independently of protein-protein interactions thereby rendering LRG-47 unaffected by pathogen induced modifications of the respective membrane.

It is unclear what the molecular basis for the early recruitment of LRG-47 to plasma membrane is and which signal transduction pathways are involved. Pathways emanating from active Rho GTPases are promising candidates as members of this family are not only involved in phagosome formation but also their maturation (111). Selective activation of Ras on Golgi membranes by signals emanating from plasma membrane has been recently reported (223) and it is possible that LRG-47 recruitment to plasma membrane involves similar mechanisms.

Also the generation of phosphorylated, membrane bound lipids as for example carried out PI3 kinase or PI4 kinase and/or their subsequent hydrolysis by phospholipases could induce LRG-47 recruitment to the plasma membrane and phagosomes (202). This possibility is particularly attractive because all GMS GTPases contain sequences showing homology to phospholipase C or related proteins and which are at least close to membrane. The generation of phospholipids at the pathogen containing vacuole could therefore induce the recruitment of the GMS GTPases. Because in rat PLC δ the GTPI, IGTP and LRG-47 homologous sequences interact to form the conserved Y region of the PLC catalytic domain it is conceivable that the three GMS GTPases form a complex on the vacuolar membrane on a similar basis (Model 1a). Following this argument it is even possible that this complex acquires catalytic activity in cooperation with other putative factors. In this respect it is interesting that at least the Y and X regions of PLC (188, 204) do not have to be expressed on one polypeptide chain to be catalytically active (224). Alternatively this complex or individual GMS GTPases might interfere with phospholipase C function. Consistent with the complex model IGTP and LRG-47 are non-redundant in resistance to *Toxoplasma gondii* (94, 96) although IGTP is apparently not required for host resistance against several other pathogens targeted by LRG-47 (40). The complex model (Model 1a) must thus be flexible enough to allow replacement or absence of individual p47 GTPases within this putative complex. The function of the complex at the target membrane might be to restore vesicular traffic thereby promoting maturation of the pathogen harbouring vacuole to lysosomes. To test the complex model co-immunoprecipitations and immunofluorescence experiments with *Toxoplasma gondii* infected astrocytes should be carried out in order to test physical interactions of the GMS GTPases.



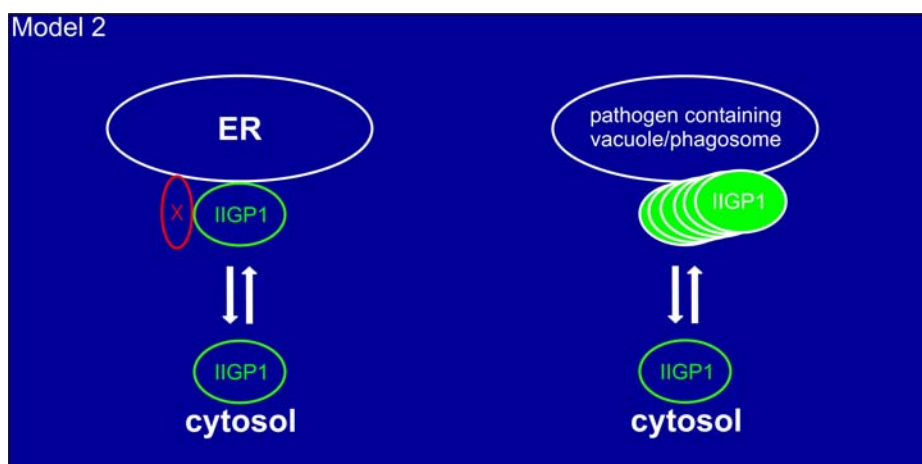
Model 1: Possible mode of function of the GMS GTPases. (1a) Complex formation model. Phosphatidyl inositol phosphates (PtdInsP) generated at the membrane of pathogen containing vacuoles or phagosomes by the action of phosphatidyl inositol kinases (PIK) induce the recruitment and complex formation of LRG-47, IGTP and GTPI. The complex is formed on the basis of the phospholipase C homologous regions of the three GMS GTPases. (1b) Release model. Phosphatidyl inositol phosphates are generated at the membrane by phosphatidyl inositol kinases and soluble inositol phosphates are formed by the subsequent action of phospholipase C (PLC). Soluble inositol phosphates such as IP₃ bind to the α K or α I, J regions of LRG-47, GTPI and IGTP leading to release of the C-terminal domain from membrane and subsequent association with the pathogen containing vacuole or phagosome.

In a second model (Model 1b) the phospholipase C homologous regions of the GMS GTPases would be involved in or mediate (GTPI and IGTP) membrane association with Golgi or ER membranes. Generation of soluble inositol phosphates generated by phospholipase C could trigger the release of the GMS α K regions from membrane and allow the association with plasma membrane or pathogen containing vacuoles possibly mediated by the G-domain. The interaction of the inositol phosphates with the α K region might lead to nucleotide exchange in the G-domain thereby exposing a plasma membrane or vacuole targeting signal. The complex formation and release models do not necessarily exclude each other.

The link between membrane bound and/or soluble phosphoinositides and the GMS GTPases could be experimentally established in lipid binding assays by incubating purified proteins with different phosphatidyl inositol phosphates using inositol phosphates as competitors.

For IIGP1 a different model will be proposed (Model 2). It is currently unclear whether IIGP1 is involved in pathogen resistance but all p47 GTPases analyzed so far turned out to be potent resistance factors against intracellular pathogens. IIGP1 will therefore be considered an intracellular resistance factor in the following model. The massive accumulation of IIGP1 around the *Toxoplasma* parasitophorous vacuole is very suggestive. IIGP1 oligomerizes in a nucleotide dependent manner *in vitro* (150) and when expressed cells which are not induced with IFN- γ , IIGP1 forms nucleotide

dependent aggregates (Figure 18). These aggregates were never observed in any IFN- γ induced mouse cell despite the massive induction of IIGP1. The activity of IIGP1 is therefore likely to be controlled by other IFN- γ inducible factors inhibiting IIGP1 from oligomerization. The control of IIGP1 might thus be based on the inhibition rather than activation of this self-activating GTPase. The cellular aggregates after transfection are likely to be membrane bound structures because transfected IIGP1 was transferred into the supernatant by detergents such Triton X-100 (Figure 22). The inhibitory factor might thus be membrane associated although molecules analogous to RabGDI are also conceivable candidates for the control of IIGP1 activity (44). The molecular composition of the parasitophorous vacuole membrane might exclude or modify this putative factor which controls IIGP1 thereby allowing oligomerization of IIGP1 at this membrane. It would thus be the absence of this factor allowing IIGP1 oligomerization and thus accumulation. In this respect it is interesting that *Toxoplasma gondii* excludes host cell proteins from the forming vacuole which puts the property of IIGP1 to associate with membrane independently of interactions with other proteins into focus. Alternatively IIGP1 might be actively recruited to the parasitophorous vacuole or active recruitment is accompanied by the absence of control. The association and accumulation of IIGP1 with the *Toxoplasma* vacuole could involve the plasma membrane targeting signal in its G-domain as the parasitophorous membrane is thought to be at least partially plasma membrane derived (170). At the vacuolar membrane IIGP1 could function as a scaffold allowing fusion with vesicles to promote maturation to lysosomes probably even in cooperation with the GMS GTPases or lead to pathogen control by other yet unknown mechanisms.



Model 2: Oligomerization model of IIGP1. IIGP1 shuttles between ER membranes and cytosol. Nucleotide dependent oligomerization of IIGP1 is prevented at the membrane by a yet unknown factor (X). X is missing from the *Toxoplasma gondii* parasitophorous vacuole allowing IIGP1 oligomerization at the vacuole.

Considering the similar behaviour after transfection in cells a similar model might be postulated for TGTP.

The analysis of IIGP1 knock out mice will show whether IIGP1 is an intracellular resistance factor against *Toxoplasma gondii* and other intracellular pathogens. Astrocytes and other cells could be isolated from these mice and stably transfected with different IIGP1 mutants to determine whether the enzymatic properties of IIGP1 established *in vitro* can be linked to the accumulation of IIGP1 at the parasitophorous vacuole of *Toxoplasma gondii*. It will be essential to determine what the function of IIGP1 at the parasitophorous vacuole is and how this contributes to host resistance. The analysis and comparison of the vesicular traffic to this vacuole in wild type and IIGP1 deficient cells will be of great interest.

5. References

1. Ehrt, S., D. Schnappinger, S. Bekiranov, J. Drenkow, S. Shi, T. R. Gingeras, T. Gaasterland, G. Schoolnik, and C. Nathan. 2001. Reprogramming of the Macrophage Transcriptome in Response to Interferon- γ and Mycobacterium tuberculosis: Signaling Roles of Nitric Oxide Synthase-2 and Phagocyte Oxidase. *J. Exp. Med.* 194:1123.
2. Relman, D. A. 2002. Genome-wide responses of a pathogenic bacterium to its host. *J. Clin. Invest.* 110:1071.
3. Scheideler, M., N. L. Schlaich, K. Fellenberg, T. Beissbarth, N. C. Hauser, M. Vingron, A. J. Slusarenko, and J. D. Hoheisel. 2002. Monitoring the Switch from Housekeeping to Pathogen Defense Metabolism in Arabidopsis thaliana Using cDNA Arrays. *J. Biol. Chem.* 277:10555.
4. Buer, J., and R. Balling. 2003. MICE, MICROBES AND MODELS OF INFECTION. *Nature Reviews Genetics* 4:195.
5. Ellis, J., P. Dodds, and T. Pryor. 2000. Structure, function and evolution of plant disease resistance genes. *Curr Opin Plant Biol* 3:278.
6. Janeway, C. A., and R. Medzhitov. 2002. INNATE IMMUNE RECOGNITION. *Annual Review of Immunology* 20:197.
7. Matzinger, P. 1994. Tolerance, Danger, and the Extended Family. *Annual Review of Immunology* 12:991.
8. Girardin, S. E., I. G. Boneca, L. A. M. Carneiro, A. Antignac, M. Jehanno, J. Viala, K. Tedin, M.-K. Taha, A. Labigne, U. Zathringer, A. J. Coyle, P. S. DiStefano, J. Bertin, P. J. Sansonetti, and D. J. Philpott. 2003. Nod1 Detects a Unique Muropeptide from Gram-Negative Bacterial Peptidoglycan. *Science* 300:1584.
9. Inohara, N., and G. Nunez. 2003. NODs: intracellular proteins involved in inflammation and apoptosis. *Nat Rev Immunol* 3.
10. Underhill, D. M., and A. Ozinsky. 2002. PHAGOCYTOSIS OF MICROBES: Complexity in Action. *Annual Review of Immunology* 20:825.
11. Williams, B. R. 1999. PKR; a sentinel kinase for cellular stress. *Oncogene* 18:6112.
12. Samuel, C. E. 2001. Antiviral Actions of Interferons. *Clin. Microbiol. Rev.* 14:778.
13. Kaufmann, S. H. E. 1993. Immunity to Intracellular Bacteria. *Annual Review of Immunology* 11:129.

14. Thomma, B. P., I. A. Penninckx, B. P. Cammue, and W. F. Broekaert. 2001. The complexity of disease signaling in Arabidopsis. *Current Opinion in Immunology* 13:63.
15. Guidotti, L. G., and F. V. Chisari. 2001. NONCYTOLYTIC CONTROL OF VIRAL INFECTIONS BY THE INNATE AND ADAPTIVE IMMUNE RESPONSE. *Annual Review of Immunology* 19:65.
16. Guidotti, L. G., and F. V. Chisari. 1999. Cytokine-induced viral purging - role in pathogenesis. *Current Opinion in Microbiology* 2:388.
17. Janeway, C., P. Travers, M. Walport, and M. Shlomchik. 2001. *Immunobiology*. Garland Publishing, New York.
18. Boehm, U., T. Klamp, M. Groot, and J. Howard. 1997. Cellular responses to interferon- γ . *Annu Rev Immunol* 15:749.
19. Stark, G. R., I. M. Kerr, R. G. Williams, R. H. Silverman, and R. D. Schreiber. 1998. How cells respond to interferons. *Annu. Rev. Biochem.* 67:227.
20. Klamp, T., U. Boehm, M. Groot, and J. C. Howard. 1997. A list of genes regulated by IFN- γ (<http://www.annurev.org/sup/material.htm>).
21. Mogensen, K. E., M. Lewerenz, J. Reboul, G. Lutfalla, and G. Uze. 1999. The type I interferon receptor: structure, function, and evolution of a family business. *J Interferon Cytokine Res* 19:1069.
22. Hauptmann, R., and P. Swetly. 1985. A novel class of human type I interferons. *Nucleic Acids Res* 13:4739.
23. LaFleur, D. W., B. Nardelli, T. Tsareva, D. Mather, P. Feng, M. Semenuk, K. Taylor, M. Buerger, D. Chinchilla, V. Roshke, G. Chen, S. M. Ruben, P. M. Pitha, T. A. Coleman, and P. A. Moore. 2001. Interferon-kappa , a Novel Type I Interferon Expressed in Human Keratinocytes. *J. Biol. Chem.* 276:39765.
24. Lefevre, F., M. Guillomot, S. D'Andrea, S. Battegay, and C. La Bonnardiere. 1998. Interferon-delta: the first member of a novel type I interferon family. *Biochimie* 80:779.
25. Sheppard, P., W. Kindsvogel, W. Xu, K. Henderson, S. Schlutsmeyer, T. E. Whitmore, R. Kuestner, U. Garrigues, C. Birks, J. Roraback, C. Ostrander, D. Dong, J. Shin, S. Presnell, B. Fox, B. Haldeman, E. Cooper, D. Taft, T. Gilbert, F. J. Grant, M. Tackett, W. Krivan, G. McKnight, C. Clegg, D. Foster, and K. M. Klucher. 2003. IL-28, IL-29 and their class II cytokine receptor IL-28R. *Nat Immunol* 4:63.
26. Kotenko, S. V., G. Gallagher, V. V. Baurin, A. Lewis-Antes, M. Shen, N. K. Shah, J. A. Langer, F. Sheikh, H. Dickensheets, and R. P. Donnelly. 2003. IFN-lambdas mediate antiviral protection through a distinct class II cytokine receptor complex. *Nat Immunol* 4:69.

27. Barchet, W., M. Cella, B. Odermatt, C. Asselin-Paturel, M. Colonna, and U. Kalinke. 2002. Virus-induced Interferon {alpha} Production by a Dendritic Cell Subset in the Absence of Feedback Signaling In Vivo. *J. Exp. Med.* 195:507.
28. Sato, M., H. Suemori, N. Hata, M. Asagiri, K. Ogasawara, K. Nakao, T. Nakaya, M. Katsuki, S. Noguchi, N. Tanaka, and T. Taniguchi. 2000. Distinct and essential roles of transcription factors IRF-3 and IRF-7 in response to viruses for IFN-alpha/beta gene induction. *Immunity* 13:539.
29. Mosmann, T. R., and R. L. Coffman. 1989. TH1 and TH2 cells: different patterns of lymphokine secretion lead to different functional properties. *Annu Rev Immunol* 7:145.
30. Sad, S., R. Marcotte, and T. R. Mosmann. 1995. Cytokine-induced differentiation of precursor mouse CD8+ T cells into cytotoxic CD8+ T cells secreting Th1 or Th2 cytokines. *Immunity* 2:271.
31. Trinchieri, G. 1995. Interleukin-12: a proinflammatory cytokine with immunoregulatory functions that bridge innate resistance and antigen-specific adaptive immunity. *Annu Rev Immunol* 13:251.
32. Munder, M., M. Mallo, K. Eichmann, and M. Modolell. 1998. Murine Macrophages Secrete Interferon gamma upon Combined Stimulation with Interleukin (IL)-12 and IL-18: A Novel Pathway of Autocrine Macrophage Activation. *J. Exp. Med.* 187:2103.
33. Decker, T., D. J. Lew, J. Mirkovitch, and J. E. Darnell, Jr. 1991. Cytoplasmic activation of GAF, an IFN-gamma-regulated DNA-binding factor. *Embo J* 10:927.
34. Decker, T., S. Stockinger, M. Karaghiosoff, M. Muller, and P. Kovarik. 2002. IFNs and STATs in innate immunity to microorganisms. *J. Clin. Invest.* 109:1271.
35. Novick, D., B. Cohen, and M. Rubinstein. 1994. The human interferon alpha/beta receptor: characterization and molecular cloning. *Cell* 77:391.
36. Leung, S., S. A. Qureshi, I. M. Kerr, J. E. Darnell, Jr., and G. R. Stark. 1995. Role of STAT2 in the alpha interferon signaling pathway. *Mol Cell Biol* 15:1312.
37. Shuai, K., G. R. Stark, I. M. Kerr, and J. E. Darnell, Jr. 1993. A single phosphotyrosine residue of Stat91 required for gene activation by interferon-gamma. *Science* 261:1744.
38. van den Broek, M., U. Muller, S. Haung, M. Aguet, and R. M. Zinkernagel. 1995. Antiviral defense in mice lacking both a/b and g Interferon Receptor. *Journal of Virology* 69:4792.

39. van den Broek, M., U. Muller, S. Huang, R. Zinkernagel, and M. Aguet. 1995. Immune defence in mice lacking type I and/or type II interferon receptors. *Immunol Rev.* 148:5.
40. Taylor, G. A., C. G. Feng, and A. Sher. 2004. p47 GTPases: Regulators of Immunity to Intracellular Pathogens. *Nature Reviews Immunology* 4:100.
41. Stremlau, M., C. M. Owens, M. J. Perron, M. Kiessling, P. Autissier, and J. Sodroski. 2004. The cytoplasmic body component TRIM5 α restricts HIV-1 infection in Old World monkeys. *Nature* 427:848.
42. Hsu, L. C., J. M. Park, K. Zhang, J. L. Luo, S. Maeda, R. J. Kaufman, L. Eckmann, D. G. Guiney, and M. Karin. 2004. The protein kinase PKR is required for macrophage apoptosis after activation of Toll-like receptor 4. *Nature* 428:341.
43. Prada-Delgado, A., E. Carrasco-Marin, G. M. Bokoch, and C. Alvarez-Dominguez. 2001. Interferon-gamma Listericidal Action Is Mediated by Novel Rab5a Functions at the Phagosomal Environment. *J. Biol. Chem.* 276:19059.
44. Zerial, M., and Heidi McBride. 2001. RAB PROTEINS AS MEMBRANE ORGANIZERS. *Nature Reviews Molecular Cell Biology* 2:107
45. Accola, M. A., B. Huang, A. Al Masri, and M. A. McNiven. 2002. The Antiviral Dynamin Family Member, MxA, Tubulates Lipids and Localizes to the Smooth Endoplasmic Reticulum. *J. Biol. Chem.* 277:21829.
46. Haller, O. 1981. Inborn resistance of mice to orthomyxo-viruses. *Curr. Top. Microbiol. Immunol.* 92:25.
47. Haller, O., and G. Kochs. 2002. Interferon-Induced Mx Proteins: Dynamin-Like GTPases with Antiviral Activity. *Traffic* 3:710.
48. Staeheli, P., O. Haller, W. Boll, J. Lindenmann, and C. Weissmann. 1986. Mx protein: constitutive expression in 3T3 cells transformed with cloned Mx cDNA confers selective resistance to influenza virus. *Cell* 44:147.
49. Chebath, J., G. Merlin, R. Metz, P. Benech, and M. Revel. 1983. Interferon-induced 56,000 Mr protein and its mRNA in human cells: molecular cloning and partial sequence of the cDNA. *Nucleic Acids Res* 11:1213.
50. Meurs, E. F., Y. Watanabe, S. Kadereit, G. N. Barber, M. G. Katze, K. Chong, B. R. Williams, and A. G. Hovanessian. 1992. Constitutive expression of human double-stranded RNA-activated p68 kinase in murine cells mediates phosphorylation of eukaryotic initiation factor 2 and partial resistance to encephalomyocarditis virus growth. *J Virol* 66:5805.
51. Lee, S. B., and M. Esteban. 1993. The interferon-induced double-stranded RNA-activated human p68 protein kinase inhibits the replication of vaccinia virus. *Virology* 193:1037.

52. Stojdl, D. F., N. Abraham, S. Knowles, R. Marius, A. Brasey, B. D. Lichty, E. G. Brown, N. Sonenberg, and J. C. Bell. 2000. The Murine Double-Stranded RNA-Dependent Protein Kinase PKR Is Required for Resistance to Vesicular Stomatitis Virus. *J. Virol.* 74:9580.
53. Yang, Y., L. Reis, J. Pavlovic, A. Aguzzi, R. Schafer, A. Kumar, B. Williams, M. Aguet, and C. Weissmann. 1995. Deficient signaling in mice devoid of double-stranded RNA-dependent protein kinase. *EMBO J.* 14:6095.
54. Jayan, G. C., and J. L. Casey. 2002. Increased RNA Editing and Inhibition of Hepatitis Delta Virus Replication by High-Level Expression of ADAR1 and ADAR2. *J. Virol.* 76:3819.
55. Wong, S. K., and D. W. Lazinski. 2002. Replicating hepatitis delta virus RNA is edited in the nucleus by the small form of ADAR1. *PNAS* 99:15118.
56. Espert, L., G. Degols, C. Gongora, D. Blondel, B. R. Williams, R. H. Silverman, and N. Mechti. 2003. ISG20, a New Interferon-induced RNase Specific for Single-stranded RNA, Defines an Alternative Antiviral Pathway against RNA Genomic Viruses. *J. Biol. Chem.* 278:16151.
57. Regad, T., Chelbi-Alix, M.K. 2001. Role and fate of PML nuclear bodies in response to interferon and viral infections. *Oncogene* 20:7274.
58. Anderson, S. L., J. M. Carton, J. Lou, L. Xing, and B. Y. Rubin. 1999. Interferon-induced Guanylate Binding Protein-1 (GBP-1) mediates an antiviral effect against Vesicular Stomatitis Virus and Encephalomyocarditis Virus. *Virology* 256:8.
59. Vestal, D. J., V. Y. Gorbacheva, and G. C. Sen. 2000. Different subcellular localizations for the related interferon-induced GTPases, MuGBP-1 and MuGBP-2: implications for different functions? *J Interferon Cytokine Res* 20:991.
60. Boehm, U., L. Guethlein, T. Klamp, K. Ozbek, A. Schaub, A. Fütterer, K. Pfeffer, and J. Howard. 1998. Two families of GTPases dominate the complex cellular response to IFN-g. *J Immunol* 161:6715.
61. Chelbi-Alix, M. K., F. Quignon, L. Pelicano, M. H. M. Koken, and H. de The. 1998. Resistance to Virus Infection Conferred by the Interferon-Induced Promyelocytic Leukemia Protein. *J. Virol.* 72:1043.
62. Regad, T., A. Saib, V. Lallemand-Breitenbach, P. P. Pandolfi, H. de The, and M. K. Chelbi-Alix. 2001. PML mediates the interferon-induced antiviral state against a complex retrovirus via its association with the viral transactivator. *EMBO J.* 20:3495.
63. Chee, A. V., P. Lopez, P. P. Pandolfi, and B. Roizman. 2003. Promyelocytic Leukemia Protein Mediates Interferon-Based Anti-Herpes Simplex Virus 1 Effects. *J. Virol.* 77:7101.

64. Gao, G., X. Guo, and S. P. Goff. 2002. Inhibition of Retroviral RNA Production by ZAP, a CCCH-Type Zinc Finger Protein. *Science* 297:1703.
65. Sheehy, A. M., N. C. Gaddis, J. D. Choi, and M. H. Malim. 2002. Isolation of a human gene that inhibits HIV-1 infection and is suppressed by the viral Vif protein. *Nature* 418:646.
66. Mangeat, B., P. Turelli, G. Caron, M. Friedli, L. Perrin, and D. Trono. 2003. Broad antiretroviral defence by human APOBEC3G through lethal editing of nascent reverse transcripts. *Nature* 424:99.
67. Mariani, R., D. Chen, B. Schrofelbauer, F. Navarro, R. Konig, B. Bollman, C. Munk, H. Nymark-McMahon, and N. R. Landau. 2003. Species-specific exclusion of APOBEC3G from HIV-1 virions by Vif. *Cell* 114:21.
68. Harris, R. S., K. N. Bishop, A. M. Sheehy, H. M. Craig, S. K. Petersen-Mahrt, I. N. Watt, M. S. Neuberger, and M. H. Malim. 2003. DNA deamination mediates innate immunity to retroviral infection. *Cell* 113:803.
69. Zhang, H. M., J. Yuan, P. Cheung, H. Luo, B. Yanagawa, D. Chau, N. S. Tozy, B. Wong, J. Zhang, J. E. Wilson, B. M. McManus, and D. Yang. 2003. Over-expression of interferon-gamma -inducible GTPase inhibits coxsackievirus B3-induced apoptosis Through the activation of the PI3-K/Akt pathway and inhibition of viral replication. *J. Biol. Chem.*:M305352200.
70. Turelli, P., B. Mangeat, S. Jost, S. Vianin, and D. Trono. 2004. Inhibition of Hepatitis B Virus Replication by APOBEC3G. *Science* 303:1829.
71. Chang, J., and J. M. Taylor. 2003. Susceptibility of human hepatitis delta virus RNAs to small interfering RNA action. *J Virol* 77:9728.
72. Jacque, J. M., K. Triques, and M. Stevenson. 2002. Modulation of HIV-1 replication by RNA interference. *Nature* 418:435.
73. Yokota, T., N. Sakamoto, N. Enomoto, Y. Tanabe, M. Miyagishi, S. Maekawa, L. Yi, M. Kurosaki, K. Taira, M. Watanabe, and H. Mizusawa. 2003. Inhibition of intracellular hepatitis C virus replication by synthetic and vector-derived small interfering RNAs. *EMBO Rep* 4:602.
74. Gitlin, L., S. Karelsky, and R. Andino. 2002. Short interfering RNA confers intracellular antiviral immunity in human cells. *Nature* 418:430.
75. Li, W.-X., H. Li, R. Lu, F. Li, M. Dus, P. Atkinson, E. W. A. Brydon, K. L. Johnson, A. Garcia-Sastre, L. A. Ball, P. Palese, and S.-W. Ding. 2004. Interferon antagonist proteins of influenza and vaccinia viruses are suppressors of RNA silencing. *PNAS* 101:1350.
76. Best, S., Le Tissier, P., Towers, G., Stoye, J.P. 1996. Positional cloning of the mouse retrovirus restriction gene Fv1. *Nature* 382:826.

77. Qi, C. F., Bonhomme, F., Buckler-White, A., Buckler, C., Orth, A., Lander, M.R., Chattopadhyay, SK., Morse, H.C. 3rd. 1998. Molecular phylogeny of Fv1. *Mamm Genome* 9:1049.
78. Goff, S. P. 1996. Operating under a Gag order: a block against incoming virus by the Fv1 gene. *Cell* 86:691.
79. Bieniasz, P. D. 2003. Restriction factors: a defense against retroviral infection. *Trends in Microbiology* 11:286.
80. Bodaghi, B., O. Goureau, D. Zipeto, L. Laurent, J.-L. Virelizier, and S. Michelson. 1999. Role of IFN- γ -Induced Indoleamine 2,3 Dioxygenase and Inducible Nitric Oxide Synthase in the Replication of Human Cytomegalovirus in Retinal Pigment Epithelial Cells. *J Immunol* 162:957.
81. Pantoja, L. G., R. D. Miller, J. A. Ramirez, R. E. Molestina, and J. T. Summersgill. 2000. Inhibition of Chlamydia pneumoniae Replication in Human Aortic Smooth Muscle Cells by Gamma Interferon-Induced Indoleamine 2,3-Dioxygenase Activity. *Infect. Immun.* 68:6478.
82. Pfefferkorn, E. R. 1984. Interferon gamma blocks the growth of Toxoplasma gondii in human fibroblasts by inducing the host cells to degrade tryptophan. *Proc Natl Acad Sci U S A* 81:908.
83. Mellor, A. L., D. B. Keskin, T. Johnson, P. Chandler, and D. H. Munn. 2002. Cells Expressing Indoleamine 2,3-Dioxygenase Inhibit T Cell Responses. *J Immunol* 168:3771.
84. Turco, J., Winkler, H.H. 1986. Gamma-interferon-induced inhibition of the growth of Rickettsia prowazekii in fibroblasts cannot be explained by the degradation of tryptophan or other amino acids. *Infect Immun* 53:38.
85. Romanska, H. M., T. S. Ikonen, A. E. Bishop, R. E. Morris, and J. M. Polak. 2000. Up-regulation of inducible nitric oxide synthase in fibroblasts parallels the onset and progression of fibrosis in an experimental model of post-transplant obliterative airway disease. *J Pathol* 191:71.
86. Kapur, S., B. Marcotte, and A. Marette. 1999. Mechanism of adipose tissue iNOS induction in endotoxemia. *Am J Physiol* 276:E635.
87. MacMicking, J. D., Q. Xie, and C. Nathan. 1997. Nitric Oxide and Macrophage Function. *Annu Rev Immunol* 15:323.
88. Jackson, S. H., J. I. Gallin, and S. M. Holland. 1995. The p47phox mouse knock-out model of chronic granulomatous disease. *J Exp Med* 182:751.
89. Vidal, S. M., D. Malo, K. Vogan, E. Skamene, and P. Gros. 1993. Natural resistance to infection with intracellular parasites: isolation of a candidate for Bcg. *Cell* 73:469.

90. Atkinson, P. G., J. M. Blackwell, and C. H. Barton. 1997. Nramp1 locus encodes a 65 kDa interferon-gamma-inducible protein in murine macrophages. *Biochem J* 325 (Pt 3):779.
91. Barton, C., T. Biggs, S. Baker, H. Bowen, and P. Atkinson. 1999. Nramp1: a link between intracellular iron transport and innate resistance to intracellular pathogens. *J Leukoc Biol* 66:757.
92. Zerrahn, J., U. E. Schaible, V. Brinkmann, U. Guhlich, and S. H. E. Kaufmann. 2002. The IFN-Inducible Golgi- and Endoplasmic Reticulum- Associated 47-kDa GTPase IIGP Is Transiently Expressed During Listeriosis. *J Immunol* 168:3428.
93. Taylor, G., R. Stauber, S. Rulong, E. Hudson, V. Pei, G. Pavlakis, J. Resau, and G. Vande Woude. 1997. The inducibly expressed GTPase localizes to the endoplasmic reticulum, independently of GTP binding. *J Biol Chem* 272:10639.
94. Taylor, G. A., C. M. Collazo, G. S. Yap, K. Nguyen, T. A. Gregorio, L. S. Taylor, B. Eagleson, L. Secrest, E. A. Southon, S. W. Reid, L. Tessarollo, M. Bray, D. W. McVicar, K. L. Komschlies, H. A. Young, C. A. Biron, A. Sher, and G. F. Vande Woude. 2000. Pathogen-specific loss of host resistance in mice lacking the IFN-gamma- inducible gene IGTP. *Proc Natl Acad Sci U S A* 97:751.
95. MacMicking, J. D., G. A. Taylor, and J. D. McKinney. 2003. Immune Control of Tuberculosis by IFN- γ -Inducible LRG-47. *Science* 302:654.
96. Collazo, C. M., G. S. Yap, G. D. Sempowski, K. C. Lusby, L. Tessarollo, G. F. V. Woude, A. Sher, and G. A. Taylor. 2001. Inactivation of LRG-47 and IRG-47 Reveals a Family of Interferon γ -inducible Genes with Essential, Pathogen-specific Roles in Resistance to Infection. *J. Exp. Med.* 194:181.
97. Knodler, L. A., Celli J., and B. Brett Finlay. 2001. Pathogenic Trickery: Deception of Host Cell Processes. *Nature Reviews Molecular Cell Biology* 2:578.
98. Praefcke, G. J. K., and H. T. McMahon. 2004. THE DYNAMIN SUPERFAMILY: UNIVERSAL MEMBRANE TUBULATION AND FISSION MOLECULES? *Nat Rev Mol Cell Biol* 5:133.
99. Bourne, H. R., D. A. Sanders, and F. McCormick. 1990. The GTPase superfamily: a conserved switch for diverse cell functions. *Nature* 348:125.
100. Bourne, H., D. Sanders, and F. McCormick. 1991. The GTPase superfamily: conserved structure and molecular mechanism. *Nature* 349:117.
101. Bourne, H. 1995. GTPases: a family of molecular switches and clocks. *Philos Trans R Soc Lond B Biol Sci* 349:283.
102. Song, B., Schmid SL. 2003. A molecular motor or a regulator? Dynamin's in a class of its own. *Biochemistry* 42:1369.

103. Kleinecke, J., and H. Söling. 1979. Subcellular Compartmentation of Guanine Nucleotides and Functional Relationships Between the Adenine and Guanine Nucleotide Systems in Isolated Hepatocytes. *FEBS Letters* 107:198.
104. Sasaki, T., A. Kikuchi, S. Araki, Y. Hata, M. Isomura, S. Kuroda, and Y. Takai. 1990. Purification and characterization from bovine brain cytosol of a protein that inhibits the dissociation of GDP from and the subsequent binding of GTP to smg p25A, a ras p21-like GTP-binding protein. *J. Biol. Chem.* 265:2333.
105. Chavrier, P., and B. Goud. 1999. The role of ARF and Rab GTPases in membrane transport. *Curr Opin Cell Biol* 11:466.
106. Goldberg, J. 1998. Structural basis for activation of ARF GTPase: mechanisms of guanine nucleotide exchange and GTP-myristoyl switching. *Cell* 95:237.
107. Bruno Antony, S. B.-D., Pierre Chardin, and Marc Chabre. 1996. N-Terminal Hydrophobic Residues of the G-Protein ADP-Ribosylation Factor-1 Insert into Membrane Phospholipids upon GDP to GTP Exchange. *Biochemistry* 36:4675
108. BurrIDGE, K., and K. Wennerberg. 2004. Rho and Rac take center stage. *Cell* 116:167.
109. Ridley, A. J., and A. Hall. 1992. The small GTP-binding protein rho regulates the assembly of focal adhesions and actin stress fibers in response to growth factors. *Cell* 70:70.
110. Ridley, A. J., H. F. Paterson, C. L. Johnston, D. Diekmann, and A. Hall. 1992. The small GTP-binding protein rac regulates growth factor-induced membrane ruffling. *Cell* 70:401.
111. Chimini, G., and P. Chavrier. 2000. Function of Rho family proteins in actin dynamics during phagocytosis and engulfment. *Nat Cell Biol* 2:E191.
112. Araki, N., M. Johnson, and J. Swanson. 1996. A role for phosphoinositide 3-kinase in the completion of macropinocytosis and phagocytosis by macrophages. *J. Cell Biol.* 135:1249.
113. Knaus, U. G., P. G. Heyworth, T. Evans, J. T. Curnutte, and G. M. Bokoch. 1991. Regulation of phagocyte oxygen radical production by the GTP-binding protein Rac 2. *Science* 254:1512.
114. May, R. C., and L. M. Machesky. 2000. Phagocytosis and the actin cytoskeleton. *J Cell Sci* 114:1061.
115. Adamson, P., C. Marshall, A. Hall, and P. Tilbrook. 1992. Post-translational modifications of p21rho proteins. *J. Biol. Chem.* 267:20033.
116. Fukumoto, Y., K. Kaibuchi, Y. Hori, H. Fujioka, S. Araki, T. Ueda, A. Kikuchi, and Y. Takai. 1990. Molecular cloning and characterization of a novel type of

- regulatory protein (GDI) for the rho proteins, ras p21-like small GTP-binding proteins. *Oncogene* 5:1321.
117. Adamson, P., H. Paterson, and A. Hall. 1992. Intracellular localization of the P21rho proteins. *J. Cell Biol.* 119:617.
 118. Bokoch, G., B. Bohl, and T. Chuang. 1994. Guanine nucleotide exchange regulates membrane translocation of Rac/Rho GTP-binding proteins. *J. Biol. Chem.* 269:31674.
 119. Hinshaw, J. E. 2000. DYNAMIN AND ITS ROLE IN MEMBRANE FISSION. *Annu Rev Cell Dev Biol* 16:483.
 120. Sever, S., A. B. Muhlberg, and S. L. Schmid. 1999. Impairment of dynamin's GAP domain stimulates receptor-mediated endocytosis. *Nature* 398:481.
 121. Stowell, M. H., B. Marks, P. Wigge, and H. T. McMahon. 1999. Nucleotide-dependent conformational changes in dynamin: evidence for a mechanochemical molecular spring. *Nat Cell Biol* 1:27.
 122. Sweitzer, S. M., and J. E. Hinshaw. 1998. Dynamin undergoes a GTP-dependent conformational change causing vesiculation. *Cell* 93:1021.
 123. Tuma, P. L., and C. A. Collins. 1994. Activation of dynamin GTPase is a result of positive cooperativity. *J Biol Chem* 269:30842.
 124. Hinshaw, J. E., and S. L. Schmid. 1995. Dynamin self-assembles into rings suggesting a mechanism for coated vesicle budding. *Nature* 374:190.
 125. Vallis, Y., P. Wigge, B. Marks, P. R. Evans, and H. T. McMahon. 1999. Importance of the pleckstrin homology domain of dynamin in clathrin-mediated endocytosis. *Curr Biol* 9:257.
 126. Lee, A., D. W. Frank, M. S. Marks, and M. A. Lemmon. 1999. Dominant-negative inhibition of receptor-mediated endocytosis by a dynamin-1 mutant with a defective pleckstrin homology domain. *Curr Biol* 9:261.
 127. Achiriloaie, M., B. Barylko, and J. P. Albanesi. 1999. Essential role of the dynamin pleckstrin homology domain in receptor-mediated endocytosis. *Mol Cell Biol* 19:1410.
 128. Kim, Y. W., D. S. Park, S. C. Park, S. H. Kim, G. W. Cheong, and I. Hwang. 2001. Arabidopsis dynamin-like 2 that binds specifically to phosphatidylinositol 4-phosphate assembles into a high-molecular weight complex in vivo and in vitro. *Plant Physiol* 127:1243.
 129. Lindenmann, J., C. A. Lane, and D. Hobson. 1963. THE RESISTANCE OF A2G MICE TO MYXOVIRUSES. *J Immunol* 90.

130. Staeheli, P., D. Pravtcheva, L. G. Lundin, M. Acklin, F. Ruddle, J. Lindenmann, and O. Haller. 1986. Interferon-regulated influenza virus resistance gene Mx is localized on mouse chromosome 16. *J Virol* 58:967.
131. Staeheli, P., and O. Haller. 1985. Interferon-induced human protein with homology to protein Mx of influenza virus-resistant mice. *Mol Cell Biol* 5:2150.
132. Haller, O., M. Acklin, and P. Staeheli. 1987. Influenza virus resistance of wild mice: wild-type and mutant Mx alleles occur at comparable frequencies. *J Interferon Res* 7:647.
133. Jin, H. K., T. Yamashita, K. Ochiai, O. Haller, and T. Watanabe. 1998. Characterization and expression of the Mx1 gene in wild mouse species. *Biochem Genet* 36:311.
134. Melen, K., T. Ronni, B. Broni, R. M. Krug, C. H. von Bonsdorff, and I. Julkunen. 1992. Interferon-induced Mx proteins form oligomers and contain a putative leucine zipper. *J Biol Chem* 267:25898.
135. Kochs, G., M. Haener, U. Aebi, and O. Haller. 2002. Self-assembly of Human MxA GTPase into Highly Ordered Dynamin-like Oligomers. *J. Biol. Chem.* 277:14172.
136. Janzen, C., G. Kochs, and O. Haller. 2000. A Monomeric GTPase-Negative MxA Mutant with Antiviral Activity. *J Virol* 74:8202.
137. Obar, R. A., C. A. Collins, J. A. Hammarback, H. S. Shpetner, and R. B. Vallee. 1990. Molecular cloning of the microtubule-associated mechanochemical enzyme dynamin reveals homology with a new family of GTP-binding proteins. *Nature* 347:256.
138. Horisberger, M. A., and H. K. Hochkeppel. 1987. IFN-alpha induced human 78 kD protein: purification and homologies with the mouse Mx protein, production of monoclonal antibodies, and potentiation effect of IFN-gamma. *J Interferon Res* 7:331.
139. Nguyen, T. T., Y. Hu, D. P. Widney, R. A. Mar, and J. B. Smith. 2002. Murine GBP-5, a new member of the murine guanylate-binding protein family, is coordinately regulated with other GBPs in vivo and in vitro. *J Interferon Cytokine Res* 22:899.
140. Gorbacheva, V. Y., D. Lindner, G. C. Sen, and D. J. Vestal. 2002. The Interferon (IFN)-induced GTPase, mGBP-2. ROLE IN IFN-gamma -INDUCED MURINE FIBROBLAST PROLIFERATION. *J. Biol. Chem.* 277:6080.
141. Guenzi, E., Topolt, Kristin, Cornali, Emmanuelle, Lubeseder-Martellato, Clara, Jorg, Anita, Matzen, Kathrin, Zietz, Christian, Kremmer, Elisabeth, Nappi, Filomena, Schwemmle, Martin, Hohenadl, Christine, Barillari, Giovanni, Tschachler, Erwin, Monini, Paolo, Ensoli, Barbara, Sturzl, Michael. 2001. The helical domain of GBP-1 mediates the inhibition of endothelial cell proliferation by inflammatory cytokines. *EMBO J.* 20:5568.

142. Guenzi, E., K. Topolt, C. Lubeseder-Martellato, A. Jorg, E. Naschberger, R. Benelli, A. Albin, and M. Sturzl. 2003. The guanylate binding protein-1 GTPase controls the invasive and angiogenic capability of endothelial cells through inhibition of MMP-1 expression. *EMBO J.* 22:3772.
143. Prakash, B., G. J. Praefke, L. Renault, A. Wittinghofer, and C. Herrmann. 2000. Structure of human guanylate-binding protein 1 representing a unique class of GTP-binding proteins. *Nature* 403:567.
144. Klamp, T., Boehm, U., Schenk, D., Pfeffer K. and Howard J.C. 2003. A giant GTPase, VLI-1, is inducible by interferons. *J Immunol* 171: 1255.
145. Carlow, D., J. Marth, I. Clark-Lewis, and H. Teh. 1995. Isolation of a gene encoding a developmentally regulated T cell-specific protein with a guanine nucleotide triphosphate-binding motif. *J Immunol* 154:1724.
146. Gilly, M., and R. Wall. 1992. The IRG-47 gene is IFN-g induced in B cells and encodes a protein with GTP-binding motifs. *J Immunol* 148:3275.
147. Taylor, G., M. Jeffers, D. Largaespada, N. Jenkins, N. Copeland, and G. Vande Woude. 1996. Identification of a novel GTPase, the inducibly expressed GTPase, that accumulates in response to interferon gamma. *J Biol Chem* 271:20399.
148. Sorace, J., R. Johnson, D. Howard, and B. Drysdale. 1995. Identification of an endotoxin and IFN-inducible cDNA: possible identification of a novel protein family. *J Leukoc Biol* 58:477.
149. Ghosh, A., U. Revathy, J. C. Howard, C. Herrmann, and E. Wolf. 2004. Crystal Structure of IIGP1: A Paradigm for Interferon Inducible p47 Resistance GTPases. *submitted*.
150. Uthaiyah, R. C., Gerrit J. K. Praefcke, Jonathan C. Howard, Christian Herrmann. 2003. IIGP1, an interferon-g inducible 47 kDa GTPase of the Mouse, showing cooperative enzymatic activity and GTP-dependent multimerisation. *J Biol Chem.* 278:29336.
151. Halonen, S. K., G. A. Taylor, and L. M. Weiss. 2001. Gamma Interferon-Induced Inhibition of *Toxoplasma gondii* in Astrocytes Is Mediated by IGTP. *Infect. Immun.* 69:5573.
152. Carlow, D. A., S. J. Teh, and H. S. Teh. 1998. Specific antiviral activity demonstrated by TGTP, a member of a new family of interferon-induced GTPases. *J Immunol* 161:2348.
153. Stossel, T. 1999. The early history of phagocytosis. G. S, ed, Stamford, p. 3.
154. Everts, V., van der Zee E, Creemers L, Beertsen W. 1996. Phagocytosis and intracellular digestion of collagen, its role in turnover and remodelling. *Histochem J* 28:229.

155. Desjardins, M. 2003. ER-MEDIATED PHAGOCYTOSIS: A NEW MEMBRANE FOR NEW FUNCTIONS. *Nature Reviews Immunology* 3:280
156. Gagnon, E., S. Duclos, C. Rondeau, E. Chevet, P. H. Cameron, O. Steele-Mortimer, J. Paiement, J. J. Bergeron, and M. Desjardins. 2002. Endoplasmic reticulum-mediated phagocytosis is a mechanism of entry into macrophages. *Cell* 110:119.
157. Desjardins, M., L. Huber, R. Parton, and G. Griffiths. 1994. Biogenesis of phagolysosomes proceeds through a sequential series of interactions with the endocytic apparatus. *J. Cell Biol.* 124:677.
158. Gruenheid, S., E. Pinner, M. Desjardins, and P. Gros. 1997. Natural Resistance to Infection with Intracellular Pathogens: The Nramp1 Protein Is Recruited to the Membrane of the Phagosome. *J. Exp. Med.* 185:717.
159. Henry, R. M., A. D. Hoppe, N. Joshi, and J. A. Swanson. 2004. The uniformity of phagosome maturation in macrophages. *J. Cell Biol.* 164:185.
160. Cox, D., P. Chang, Q. Zhang, P. G. Reddy, G. M. Bokoch, and S. Greenberg. 1997. Requirements for Both Rac1 and Cdc42 in Membrane Ruffling and Phagocytosis in Leukocytes. *J. Exp. Med.* 186:1487.
161. Radhakrishna, H., R. Klausner, and J. Donaldson. 1996. Aluminum fluoride stimulates surface protrusions in cells overexpressing the ARF6 GTPase. *J. Cell Biol.* 134:935.
162. Brown, F. D., A. L. Rozelle, H. L. Yin, T. Balla, and J. G. Donaldson. 2001. Phosphatidylinositol 4,5-bisphosphate and Arf6-regulated membrane traffic. *J. Cell Biol.* 154:1007.
163. Zhang, Q., D. Cox, C.-C. Tseng, J. G. Donaldson, and S. Greenberg. 1998. A Requirement for ARF6 in Fcγ Receptor-mediated Phagocytosis in Macrophages. *J. Biol. Chem.* 273:19977.
164. Gold, E. S., D. M. Underhill, N. S. Morrissette, J. Guo, M. A. McNiven, and A. Aderem. 1999. Dynamin 2 Is Required for Phagocytosis in Macrophages. *J. Exp. Med.* 190:1849.
165. Cox, D., D. J. Lee, B. M. Dale, J. Calafat, and S. Greenberg. 2000. A Rab11-containing rapidly recycling compartment in macrophages that promotes phagocytosis. *PNAS* 97:680.
166. Nathan, C. F., H. W. Murray, M. E. Wiebe, and B. Y. Rubin. 1983. Identification of interferon-gamma as the lymphokine that activates human macrophage oxidative metabolism and antimicrobial activity. *J Exp Med* 158:670.
167. Alvarez-Dominguez, C., and P. D. Stahl. 1998. Interferon-g selectively induces Rab5a Synthesis and Processing in Mononuclear Cells. *The Journal of Biological Chemistry* 273:33901.

168. Clemens, D. L. a. M. A. H. 1996. Characterization of the Mycobacterium tuberculosis phagosome and evidence that phagosomal maturation is inhibited. *J. Exp. Med.* 181:257.
169. Russell, D. G. 2001. Mycobacterium tuberculosis: here today, and here tomorrow. *Nat Rev Mol Cell Biol* 2:569.
170. Suss-Toby, E., J. Zimmerberg, and G. Ward. 1996. Toxoplasma invasion: the parasitophorous vacuole is formed from host cell plasma membrane and pinches off via a fission pore. *Proc Natl Acad Sci USA* 93:8413.
171. Sinai, A. P., and a. K. A. Joiner. 1997. SAFE HAVEN: The Cell Biology of Nonfusogenic Pathogen Vacuoles. *Annual Review of Microbiology* 51:415.
172. Portnoy, D. A., V. Auerbuch, and I. J. Glomski. 2002. The cell biology of Listeria monocytogenes infection: the intersection of bacterial pathogenesis and cell-mediated immunity. *J. Cell Biol.* 158:409.
173. High, N., J. mounier, M.-C. Prevost and J. P. Sansonetti. 1992. IpaB of Shigella flexineri causes entry into epithelial cells and escape from the phagocytic vacuole. *EMBO J.* 11:1991.
174. Szalay, G., J. Hess, and S. Kaufmann. 1995. Restricted replication of Listeria monocytogenes in a gamma interferon- activated murine hepatocyte line. *Infect. Immun.* 63:3187.
175. Sijts, A. J. A. M., S. Standera, R. E. M. Toes, T. Ruppert, N. J. C. M. Beekman, P. A. van Veelen, F. A. Ossendorp, C. J. M. Melief, and P. M. Kloetzel. 2000. MHC Class I Antigen Processing of an Adenovirus CTL Epitope Is Linked to the Levels of Immunoproteasomes in Infected Cells. *J Immunol* 164:4500.
176. Linstedt, A., Hauri HP. 1993. Giantin, a novel conserved Golgi membrane protein containing a cytoplasmic domain of at least 350 kDa. *Mol Biol Cell* 4:679.
177. Tanner, L., and G. Lienhard. 1989. Localization of transferrin receptors and insulin-like growth factor II receptors in vesicles from 3T3-L1 adipocytes that contain intracellular glucose transporters. *J Cell Biol.* 108:1537.
178. Goud, B., Zahraoui A, Tavitian A, Saraste J. 1990. Small GTP-binding protein associated with Golgi cisternae. *Nature* 345:553.
179. Nakamura, N., Rabouille C, Watson R, Nilsson T, Hui N, Slusarewicz P, Kreis TE, Warren G. 1995. Characterization of a cis-Golgi matrix protein, GM130. *J Cell Biol* 131:1715.
180. Burke, B., G. Griffiths, H. Reggio, D. Louvard, and G. Warren. 1982. A monoclonal antibody against a 135-K Golgi membrane protein. *Embo J* 1:1621.

181. Xu, Y., S. Martin, D. E. James, and W. Hong. 2002. GS15 Forms a SNARE Complex with Syntaxin 5, GS28, and Ykt6 and Is Implicated in Traffic in the Early Cisternae of the Golgi Apparatus. *Mol. Biol. Cell* 13:3493.
182. Moremen, K., and P. Robbins. 1991. Isolation, characterization, and expression of cDNAs encoding murine alpha-mannosidase II, a Golgi enzyme that controls conversion of high mannose to complex N-glycans. *J. Cell Biol.* 115:1521.
183. Ghosh, P., N. M. Dahms, and S. Kornfeld. 2003. Mannose 6-phosphate receptors: new twists in the tale. *Nat Rev Mol Cell Biol* 4:202.
184. Wada, I., D. Rindress, P. Cameron, W. Ou, J. Doherty, 2d, D. Louvard, A. Bell, D. Dignard, D. Thomas, and J. Bergeron. 1991. SSR alpha and associated calnexin are major calcium binding proteins of the endoplasmic reticulum membrane. *J. Biol. Chem.* 266:19599.
185. Rothenberger, S., B. J. Iacopetta, and L. C. Kuhn. 1987. Endocytosis of the transferrin receptor requires the cytoplasmic domain but not its phosphorylation site. *Cell* 49:423.
186. Ullrich, O., S. Reinsch, S. Urbe, M. Zerial, and R. Parton. 1996. Rab11 regulates recycling through the pericentriolar recycling endosome. *J. Cell Biol.* 135:913.
187. Chen, J., T. Murphy, M. Willingham, I. Pastan, and J. August. 1985. Identification of two lysosomal membrane glycoproteins. *J. Cell Biol.* 101:85.
188. Essen, L., O. Perisic, R. Cheung, M. Katan, and R. Williams. 1996. Crystal structure of a mammalian phosphoinositide-specific phospholipase C delta. *Nature* 380:595.
189. Cheng, H.-F., M.-J. Jiang, C.-L. Chen, S.-M. Liu, L.-P. Wong, J. W. Lomasney, and K. King. 1995. Cloning and Identification of Amino Acid Residues of Human Phospholipase C[IMAGE]1 Essential for Catalysis. *J. Biol. Chem.* 270:5495.
190. Lewis, M., S. Turco, and M. Green. 1985. Structure and assembly of the endoplasmic reticulum. Biosynthetic sorting of endoplasmic reticulum proteins. *J. Biol. Chem.* 260:6926.
191. Towler, D. A., J. I. Gordon, S. P. Adams, and L. Glaser. 1988. The Biology and Enzymology of Eukaryotic Protein Acylation. *Annual Review of Biochemistry* 57:69.
192. Coligan, J., B. Dunn, H. Ploegh, D. Speicher, and P. Wingfield. 2000. *Current Protocols in Protein Science*. John Wiley & Sons.
193. Kamps, M. P., J. E. Buss, and B. M. Sefton. 1985. Mutation of NH2-terminal glycine of p60src prevents both myristoylation and morphological transformation. *Proc Natl Acad Sci U S A* 82:4625.

194. Brown, D. A., and J. K. Rose. 1992. Sorting of GPI-anchored proteins to glycolipid-enriched membrane subdomains during transport to the apical cell surface. *Cell* 68:533.
195. Simons, K., and E. Ikonen. 1997. Functional rafts in cell membranes. *Nature* 387:569.
196. De Brabander, M., J. De May, M. Joniau, and G. Geuens. 1977. Ultrastructural immunocytochemical distribution of tubulin in cultured cells treated with microtubule inhibitors. *Cell Biol Int Rep* 1:177.
197. Hoff, E. F., and V. B. Carruthers. 2002. Is Toxoplasma egress the first step in invasion? *Trends in Parasitology* 18:251.
198. Meresse, S., O. Steele-Mortimer, B. B. Finlay, and J. P. Gorvel. 1999. The rab7 GTPase controls the maturation of Salmonella typhimurium-containing vacuoles in HeLa cells. *Embo J* 18:4394.
199. Sinai, A. P., and K. A. Joiner. 2001. The Toxoplasma gondii protein ROP2 mediates host organelle association with the parasitophorous vacuole membrane. *J. Cell Biol.* 154:95.
200. Brunet, N., A. Morin, and B. Olofsson. 2002. RhoGDI-3 Regulates RhoG and Targets This Protein to the Golgi Complex Through its Unique N-Terminal Domain. *Traffic* 3:342.
201. De Matteis, M., A. Godi, and D. Corda. 2002. Phosphoinositides and the Golgi complex. *Curr Opin Cell Biol* 14.
202. Simonsen, A., A. Wurmser, D. Scott, and H. Stenmark. 2001. The role of phosphoinositides in membrane transport. *Curr Opin Cell Biol* 13:485.
203. Jones, D. H., J. B. Morris, C. P. Morgan, H. Kondo, R. F. Irvine, and S. Cockcroft. 2000. Type I Phosphatidylinositol 4-Phosphate 5-Kinase Directly Interacts with ADP-ribosylation Factor 1 and Is Responsible for Phosphatidylinositol 4,5-Bisphosphate Synthesis in the Golgi Compartment. *J. Biol. Chem.* 275:13962.
204. Ellis, M. V., S. R. James, O. Perisic, C. P. Downes, R. L. Williams, and M. Katan. 1998. Catalytic Domain of Phosphoinositide-specific Phospholipase C (PLC). MUTATIONAL ANALYSIS OF RESIDUES WITHIN THE ACTIVE SITE AND HYDROPHOBIC RIDGE OF PLCdelta 1. *J. Biol. Chem.* 273:11650.
205. Kohno, T., T. Otsuka, H. Takano, T. Yamamoto, M. Hamaguchi, M. Terada, and J. Yokota. 1995. Identification of a novel phospholipase C family gene at chromosome 2q33 that is homozygously deleted in human small cell lung carcinoma. *Hum Mol Genet* 4:667.
206. Olofsson, B. 1999. Rho Guanine Dissociation Inhibitors: Pivotal Molecules in Cellular Signalling. *Cellular Signalling* 11:545.

207. Maurer-Stroh, S., M. Gouda, M. Novatchkova, A. Schleiffer, G. Schneider, F. Sirota, M. Wildpaner, N. Hayashi, and F. Eisenhaber. 2004. MYRbase: analysis of genome-wide glycine myristoylation enlarges the functional spectrum of eukaryotic myristoylated proteins. *Genome Biology* 5:R21.
208. Sargiacomo, M., M. Sudol, Z. Tang, and M. Lisanti. 1993. Signal transducing molecules and glycosyl-phosphatidylinositol-linked proteins form a caveolin-rich insoluble complex in MDCK cells. *J. Cell Biol.* 122:789.
209. Johnston, J. A., C. L. Ward, and R. R. Kopito. 1998. Aggresomes: A Cellular Response to Misfolded Proteins. *J. Cell Biol.* 143:1883.
210. Garcia-Mata, R., Z. Bebok, E. J. Sorscher, and E. S. Sztul. 1999. Characterization and Dynamics of Aggresome Formation by a Cytosolic GFP-Chimera. *J. Cell Biol.* 146:1239.
211. Sibley, L. D. 2004. Intracellular Parasite Invasion Strategies. *Science* 304:248.
212. Sibley, L. 2003. Toxoplasma gondii: Perfecting an Intracellular Life Style. *Traffic* 4:581.
213. Morisaki, J., E. Heuse, and S. LD. 1995. Invasion of Toxoplasma gondii occurs by active penetration of the host cell. *J Cell Sci* 108:2457.
214. Dobrowolski, J., and L. Sibley. 1996. Toxoplasma invasion of mammalian cells is powered by the actin cytoskeleton. *Cell* 84:933.
215. Mordue, D., and L. Sibley. 1997. Intracellular fate of vacuoles containing Toxoplasma gondii is determined at the time of formation and depends on the mechanism of entry. *J Immunol* 159:4452.
216. Mordue, D. G., N. Desai, M. Dustin, and L. D. Sibley. 1999. Invasion by Toxoplasma gondii Establishes a Moving Junction That Selectively Excludes Host Cell Plasma Membrane Proteins on the Basis of Their Membrane Anchoring. *J. Exp. Med.* 190:1783.
217. Sinai, A. P., P. Webster, and K. A. Joiner. 1997. Association of host cell endoplasmic reticulum and mitochondria with Toxoplasma gondii parasitophorous vacuole membrane: a high affinity interaction. *J. Cell Sci* 110:2117.
218. Schwab, J., C. Beckers, and J. KA. 1994. The parasitophorous vacuole membrane surrounding intracellular Toxoplasma gondii functions as a molecular sieve. *Proc Natl Acad Sci USA* 91:509.
219. Mordue, D., S. Håkansson, I. Niesman, and L. Sibley. 1999. Toxoplasma gondii resides in a vacuole that avoids fusion with host cell endocytic and exocytic vesicular trafficking pathways. *Exp Parasitol* 92:87.

-
220. Garcia-del Portillo, F., and B. Finlay. 1995. Targeting of *Salmonella typhimurium* to vesicles containing lysosomal membrane glycoproteins bypasses compartments with mannose 6-phosphate receptors. *J. Cell Biol.* 129:81.
 221. Garcia-del Portillo, F. 1996. Interaction of *Salmonella* with lysosomes of eukaryotic cells. *Microbiologia* 12:259.
 222. Ferrari, G., H. Langen, M. Naito, and J. Pieters. 1999. A Coat Protein on Phagosomes Involved in the Intracellular Survival of Mycobacteria. *Cell* 97:435–447.
 223. Bivona, T. G., Perez de Castro, I., Ahearn I. M., Grana T. M., Chiu V. K., Lockyer P. J., Cullen P. J., Pellicier A., Cox A. D. and Mark R. Philips. 2003. Phospholipase C activates Ras on the Golgi apparatus by means of RasGRP1. *Nature* 424:694
 224. Cifuentes, M., L. Honkanen, and M. Rebecchi. 1993. Proteolytic fragments of phosphoinositide-specific phospholipase C- delta 1. Catalytic and membrane binding properties. *J. Biol. Chem.* 268:11586.
 225. Kaiser, F., S. H. E. Kaufmann, and J. Zerrahn. 2004. IIGP, a member of the IFN inducible and microbial defense mediating 47 kDa GTPase family, interacts with the microtubule binding protein hook3. *J Cell Sci* 117:1747.

6. Summary

The interferon inducible p47 GTPases are a family of non-redundant mediators of cell-autonomous immunity to intracellular bacterial and protozoan pathogens in the mouse. So far 6 murine p47 GTPases have been described, LRG-47, GTPI, IGTP, TGTP, IRG-47 and IIGP1. Association with intracellular membrane compartments has been reported for some members of the p47 GTPase family and one member, LRG-47, has been implicated in the maturation of *Mycobacterium tuberculosis* containing phagosomes in macrophages. The nature and dynamics of this membrane association however is unexplored.

This study was set out to analyze the membrane association properties of two p47 GTPases, namely LRG-47 and IIGP1. The results are compared and extended to other family members (GTPI, IGTP) revealing an unexpectedly diverse cell biology of the family.

LRG-47 is completely membrane bound localizing to the Golgi apparatus in a nucleotide dependent manner. Upon phagocytosis LRG-47 is recruited to the plasma membrane and remains selectively associated with the phagosomes as they mature along the endocytic pathway. The Golgi association of LRG-47 requires an amphipathic helix in its C-terminal domain and the corresponding regions of IGTP and GTPI, the closest relatives of LRG-47 in the mouse, also mediate membrane association but possibly by different mechanisms. The plasma membrane association of LRG-47 is most likely mediated by the conserved G domain and this activity is shared by the G-domain of IIGP1.

IIGP1 partitions between cytosol and ER membranes to which it is targeted by an N-terminal myristoyl modification. IIGP1 forms nucleotide depended aggregates when expressed in mouse fibroblasts and dramatically accumulates around the parasitophorous vacuoles in *Toxoplasma gondii* infected mouse astrocytes.

Based on the presented results it is allowed to speculate that the p47 GTPases form a battery of diverse intracellular resistance factors that dynamically associate with different pathogen harbouring membrane compartments in order to gain control over these membranes to counteract intracellular microbes.

7. Zusammenfassung

Die Interferon induzierbaren p47 GTPasen sind essentiell für die Resistenz gegenüber intrazellulären Pathogenen in der Maus und vermitteln ihren Effekt auf zellautonome Weise. Bis jetzt wurden 6 p47 GTPasen in der Maus beschrieben, LRG-47, GTPI, IGTP, TGTP, IRG-47 und IIGP1. Für einige Mitglieder dieser Proteinfamilie wurde die Assoziation mit intrazellulären Membranen beschrieben und ein Familienmitglied, LRG-47, wurde in Makrophagen mit der Reifung von Phagosomen nach der Phagozytose von *Mycobacterium tuberculosis* in Verbindung gebracht. Über den Mechanismus und die Dynamik der Membranassoziation ist jedoch nichts bekannt.

Die hier vorgestellten Untersuchungen wurden durchgeführt, um die Membranassoziationseigenschaften von LRG-47 und IIGP1, zwei Mitgliedern der p47 GTPasen, näher zu untersuchen. Die biochemischen und zellbiologischen Eigenschaften der beiden Proteine wurden hinsichtlich ihrer Membranbindung verglichen und auf GTPI und IGTP übertragen. Dabei zeigte sich, dass die biochemischen und zellbiologischen Charakteristika der p47 GTPasen, zumindest im Hinblick auf die untersuchten Eigenschaften, bemerkenswert unterschiedlich sind.

LRG-47 ist vollständig membrangebunden und in Nukleotid unabhängiger Weise an den Golgi Apparat gebunden. Während eines Phagozytoseprozesses wird LRG-47 an die Plasmamembran rekrutiert und bleibt dann mit den Phagosomen assoziiert, während diese zu Phagolysosomen reifen. Die Bindung an die Plasmamembran wird sehr wahrscheinlich durch die konservierte G-Domäne vermittelt, während die Bindung an den Golgi Apparat von einer amphipatischen Helix (α K) in der C-terminalen Domäne von LRG-47 abhängig ist. Auch die α K Regionen von IGTP und GTPI vermitteln Membranassoziation, jedoch vermutlich über einen Mechanismus, der auch von der katalytischen Domäne der Phospholipase C verwendet wird.

IIGP1 ist zytosolisch sowie membrangebunden und die Membranbindung wird durch eine N-terminale Myristolierung gefördert. IIGP1 bildet nach der Expression in Mausfibroblasten nukleotidabhängige Aggregate und akkumuliert sehr stark um parasitophore Vakuolen in *Toxoplasma gondii* infizierten Astrozyten.

Die Ergebnisse dieser Arbeit erlauben die Annahme, dass die p47 GTPasen einen Verbund zellautonomer Resistenzfaktoren bilden und einzelne Mitglieder dynamisch und auf unterschiedliche Weise mit Pathogen umgebenen Kompartimenten assoziieren. Diese Assoziation dient vermutlich der Kontrolle des weiteren intrazellulären Schicksals dieser Kompartimente und damit der darin enthaltenen Pathogene.

8. Danksagungen

Diese Arbeit wurde am Institut für Genetik der Universität zu Köln unter der Anleitung von Prof. Dr. Jonathan C. Howard durchgeführt. Jonathan Howard danke ich für das in mich gesetzte Vertrauen und die ständige Diskussionsbereitschaft.

Prof. Dr. Thomas Langer danke ich für die Übernahme des Zweitgutachtens.

Priv. Doz. Dr. Gaby Reichmann danke ich für die großartige Zusammenarbeit im Hinblick auf die Toxoplasmaexperimente, die Hilfe und die ständige Diskussionsbereitschaft.

Priv. Doz. Dr. Michael Knittler danke ich für die geduldige Hilfe und Beantwortung von Fragen während der gesamten Doktorarbeit.

Dr. Eva Wolf danke ich für ihre Diskussionsbereitschaft und Zusammenarbeit.

Dr. Matthias Cramer danke ich die stets vorhandene Hilfsbereitschaft.

Rita Lange danke ich für die jahrelange exzellente Zusammenarbeit und Hilfe, ohne die diese Arbeit so nicht möglich gewesen wäre.

Katja Sabel danke ich für die zur Verfügungsstellung von Daten.

Revathy Uthaiyah danke ich für die großartige jahrelange Zusammenarbeit.

Cemali Bekpen danke ich für die anregenden Diskussionen.

Steffi Könen-Waismann danke ich für das Korrekturlesen dieser Arbeit.

Dem ganzen Labor für „Zellgenetik“ danke ich für die Hilfe, Zusammenarbeit, Diskussionsbereitschaft und schöne Zeit, die ich während meiner Arbeit dort hatte.

9. Erklärung

Ich versichere, dass ich die von mir vorgelegte Dissertation selbständig angefertigt, die benutzten Quellen und Hilfsmittel vollständig angegeben und die Stellen der Arbeit – einschließlich Tabellen, Karten und Abbildungen-, die anderen Werken im Wortlaut oder dem Sinn nach entnommen sind, in jedem Einzelfall als Entlehnung kenntlich gemacht habe; dass diese Dissertation noch keiner anderen Fakultät oder Universität zur Prüfung vorgelegen hat; dass sie abgesehen von den unten angegebenen Teilpublikationen noch nicht veröffentlicht worden ist, sowie, dass ich eine solche Veröffentlichung vor Abschluss des Promotionsverfahrens nicht vornehmen werde.

Die von mir vorgelegte Dissertation ist von Prof. Dr. Jonathan C. Howard betreut worden.

Köln, im Mai 2004

Sascha Martens, Katja Sabel, Rita Lange, Revathy Uthaiiah, Eva Wolf and Jonathan C. Howard, 2004

Mechanisms regulating the positioning of mouse p47 resistance GTPases LRG-47 and IIGP1 on cellular membranes; retargeting to plasma membrane induced by phagocytosis
J Immunol 173:2594

Sascha Martens, Studien an Interferon- γ induzierten GTPasen in der Maus, Diplomarbeit, 2000

10. Lebenslauf

Name: Sascha Martens
Geburtsdatum: 23.09.1974
Geburtsort: Berlin
Staatsangehörigkeit: deutsch
Familienstand: ledig

Ausbildung

1981-1985 Besuch der Grundschule „Schwerfelstrasse“
in Bergisch Gladbach
1985-1994 Besuch des „Otto-Hahn-Gymnasiums“
in Bergisch Gladbach
1994 Allgemeine Hochschulreife
1994-1995 Zivildienst
WS 1995/1996 Immatrikulation an der
Mathematisch-Naturwissenschaftlichen Fakultät
der Universität zu Köln. Diplomstudiengang: Biologie
1995-1999 Studium der Biologie an der Universität zu Köln
1999-2000 Diplomarbeit Biologie (Fachrichtung Genetik)
am Institut für Genetik, Universität zu Köln,
Abteilung von Prof. Dr. Jonathan C. Howard
ab WS 2000/2001 Promotionsstudiengang Biologie (Fachrichtung Genetik)
am Institut für Genetik, Universität zu Köln,
Abteilung von Prof. Dr. Jonathan C. Howard